Loss of heterozygosity in acute myeloid leukaemia with normal karyotype

A dissertation submitted to the

Technical University of Dresden

For the degree of

Doctor rerum naturalium

In Biology

Presented by

Sofia Traikov

Institute of Microbiology, Technical University of Dresden

Allelverlust bei Patienten mit akuter myeloischer Leukämie und normalem Karyotyp

DISSERTATION

Zur Erlangung des akademischen Grades
Doktor der Naturwissenschaften
(Dr. rer. nat.)

eingereicht an
der Fakultät Mathematik und Naturwissenschaften
der Technischen Universität Dresden

von
Diplom-Biologin Sofia Traikov
geboren am 30.01.1976 in Sofia, Bulgarien

Tag der Verteidigung: 02.11.2009

Gutachter:
Prof. Dr. Gerold Barth
Prof. Dr. Rolf Jessberger

Datum der Einreichung: 20.07.2009

Abstract

Loss of heterozygosity (LOH) is detectable in many forms of cancer including leukaemia. It contributes to tumorigenesis through the loss of one of the two alleles of one tumor suppressor gene at a given locus, caused by deletion or uniparental disomy (UPD). UPD can only be the result of homologous recombination. Little is known about the mechanisms of UPD and what connection this aberration has with the outcome of this disease.

In this study, 146 patients with primary AML were analysed using a novel technique based on single nucleotide polymorphisms (SNPs). Leukaemic cells and healthy T-cells from each patient were obtained using FACS-Vantage cell sorting. In cases with very few sorted cells whole genome preamplification was done. Genome-wide SNP analysis was carried out according to the standard GeneChip Mapping Assay protocol (Affymetrix, USA) using the Human Mapping 10K Arrays. Moreover, the impact of the FLT3-ITD mutation on the homologous recombination using pmHPRT-DRGFP /pCbASce vectors system and yHA2x assay was investigated.

Of 146 patients with normal karyotype LOH was found in 30 cases. The potential LOH regions, were confirmed by microsatellite analysis of short tandem repeat (STR) markers. In 21 of these cases STR-analysis of T-cells, representing the corresponding tumor-free material, confirmed the regions of partial UPD. This aberration affected different chromosomes, but most commonly chr. 2, 6, 11, 21, 13, and 7, and covered between 11.5 and 88 Mb. Interestingly, in 6 LOH cases, long stretches of homozygosity present at the same positions as in the healthy cells and in the blasts were found. The impact of this phenomenon is unknown. Additionally, chromosome losses were detected in 3 patients classified with normal karyotype according to current methods. These 9 cases were not included in the UPD positive group.

No differences were observed regarding any clinical factors including age, WBC-counts and sex. The FAB M1 subtype was observed in 47.6% of the UPD positive patients, compared to only 19.2% of the UPD negative patients ($P=0.04$, $n=146$). In addition, no correlation between FLT3-ITD, MLL-PTD and NPM1 mutations in the UPD patients was found, but the data indicate that patients with UPD have a higher rate of treatment failure.

Moreover, in this study the relationship between UPD and gene aberrations was able to be confirmed. In some cases, UPD found on chromosomes 21, 19 and 11 was correlated with mutations in the RUNX1, CEBPA and WT genes, respectively. Furthermore, AML cases with and without UPD showed different but specific gene expression profiles, revealing different expression levels for genes involved in double strand break repairs.

Furthermore, it was found that different mutations could be responsible for the increase in efficiency of HR, such as FLT3-ITD or BCR-ABL. Moreover, cells with a FLT3-ITD mutation (without wt expression) rapidly increased the HR efficiency compared with heterozygous (FLT3-ITD/wt) cells. Preliminary results showed that the high repair efficiency was mainly dependent on the translocation of RAD51.

In conclusion, SNP array technology allow the identification and mapping of LOH in AML patients with normal karyotype. The obtained data also point out the necessity of analysing tumour-free material to confirm the somatic origin of the alteration. Furthermore, the available results indicate that compared to patients without UPD, patients with UPD have a higher relapse rate, which might be used as a prognostic marker in the future. Also, it could be hypothesized that downregulation of RAD51 (for example by FLT3 inhibition) might be beneficial DNA damage occurs through the genotoxic agent by reducing the relapse risk of AML.

Contents

Abbreviations

ALL	Acute lymphoblastic leukaemia
AML	Acute myeloid leukaemia
AML1/RUNX1	Runt-related transcription factor
AML1-ETO	Fusion protein encoded by the translocation t(8;21)
BCR-ABL	Breakpoint cluster region - C-abl oncogene 1, receptor tyrosine kinase t(9;22)
BER	Base Excision Repair
Bo TMR	Fluorescence dye visualized with black colour (Abs/Em = 535/574 nm)
BSA	Bovinserumalbumin
CEBPA	CCAAT/enhancer binding protein
CBFB-MYH11	Core-binding factor, beta subunit - myosin, heavy chain 11, smooth muscle (inv(16))
c-KIT	Stem cell factor receptor
CLL	Chronic lymphocytic lymphoma
cM	Genetic distance
CML	Chronic myelogenous leukaemia
CNAT	Chromosome copy number analysis tool
CPA_pVal	Continuous point analysis of the significance value
CR	Complete remission
CSF1	Colony stimulating factor 1
DMSO	Dimethylsulfoxid
DNA	Deoxyribonucleic acid
dNTP	Desoxynucleosidtriphosphat
DSB	Double-Strand Break
DSIL	Deutsche Studieninitiative Leukämie
DTT	Dithiothreitol
EB	Ethidium bromide
EDTA	Ethylenediaminetetraacetic acid
EPO	Erythropoietin
FAB	The French-American-British
FACS	Fluorescence activated cell sorting
FAM	Blue fluorescence dye (Abs/Em = 494/521 nm)
FBS	Fetal Bovine Serum
FEN1	Flap-endonuclease
FISH	Fluorescence in situ hybridization
FL	FLT3-Ligand
FLK-2	Fetal liver kinase 2

FLT3	Fms-like tyrosine kinase-3 gene
G-CSF	Granulocyte colony stimulating factor
GFP	Green fluorescent protein
GG-NER	Global genome repair
GM-CSF	Granulocyte-macrophage colony stimulating factor
GTP	Guanosintriphosphat
H2Ax	H2A histone family, member X
HCL	Hairy-cell leukaemia
Hex	Green fluorescence dye (Abs/Em = 533/550 nm)
HR	Homologous Recombination
HSDNA	Herring Sperm DNA
ITD	Internal tandem duplication
KD	Kinase domain
K-RAS	v-Ki-ras2 Kirsten rat sarcoma viral oncogene homolog
LB	Luria Bertani
LCRs	Lowcopy repeats
LM	Length mutations
LOH	Loss of heterozygosity
MAPK	Mitogen-activated protein kinase
MDS	Myelodysplastisches Syndrom
MLL-PTD	The mixed lineage leukaemia gene
MMR	Mismatch repair
NAHR	Non-allelic homologous recombination
NED	Fluorescence dye visualized with black colour.
NER	Nucleotide Excision Repair
NHR	Non-Homologous End Joining
NPM1	Nucleophosmin gene
N-RAS	Neuroblastoma *RAS* viral oncogene homolog
OS	Over Survival
PBS	Phosphate Buffer Saline
PBS	Phosphat buffer saline
PCR	Polymerase chain reaction
PDGF-R	Platelet-derived growth factor
PI3K/AKT	Phosphatidylinositol 3 kinase signalway
PML/RARα	Promyelocytic leukemia/ retinoic acid receptor, alpha t(15;17)
PML-RARA	Fusion protein encoded by the translocation t(15;17)
RNA	Ribonucleic acid
RT	Raumtemperatur
RTK	Receptor tyrosine kinase
SCF	Stem Cell Factor

SDS	Sodiumdodecylsulfat
SKY	Spectral karyotyping
SNPs)	Single nucleotide polymorphisms
SPA_CN	Single point analysis of the copy number estimate
SPA_pVal	Single point analysis of the copy number variation significance
SS RT	Super script reverse transcriptase
SSA	Single strand annealing
STAT5	Signal transducer and activator of transcription 5
STK-1	Human stem cell kinase 1
STR	Short tandem repeat analyses
TCR-NER	Transcription-coupled repair
TKD	Tyrosine kinase domain
TMACL	Tetramethyl Ammonium Chloride
TPO	Thrombopoietin
U	Unit
UPD	Uni-parental disomy
UV	Ultraviolett
WBC	White Blood Cell counts
WHO	World Health Organisation
WT	Wild type
WT1	Wilms tumor

1. Introduction

In 1845 the British pathologist John Hughes Bennett and the German pathologist Rudolf Virchow described leukaemia as a lethal disease characterized by enlargement of the spleen, and an excess of cells in the blood. Both claimed to have been the first who described leukaemia, but actually one year earlier the French physician Alfred Donné had published the first description of this disease in his book "*Complimentary course on microscopy for medical studies".* He was the first who believed that the excess of white blood cells is due to an arrested maturation of blood and it should be the result of an arrested development of intermediate cells.

Today we know that Donné was right. Leukaemia (Greek for "white blood") is a type of cancer that is characterized by uncontrolled immaturation of blood cells in the bone marrow. The bone marrow is normally responsible for haematopoiesis – formation of new blood cells. This (haematopoiesis) is a highly organized and balanced process of cell proliferation, differentiation, maturation and survival. In cases of leukaemia, malignant cells replace the population of healthy blood cells. This results in anaemia, internal bleeding and increased susceptibility to infection. Ultimately, leukaemic cells enter the peripheral blood circulation and infiltrate other organs such as spleen, liver, and kidneys. Untreated, leukaemia is a lethal disease.

Leukaemia is a collective name for over a dozen of different blood malignancies. Recent progress in the molecular biologic methods has allowed the characterisation of different leukaemia subtypes. Depending on the lineage of the cell in which the leukaemia originates, this disease can be divided into *lymphoid (or lymphocytic)* and *non-lymphoid (or myeloid)* leukaemia. Both lymphoid and myeloid leukaemias can be further classified into *acute* and *chronic*. *Acute leukaemias* progress rapidly involving highly immature haematopoietic progenitors that are only limitedly differentiated. In contrast, *chronic leukaemias* involve well-differentiated (but immunologically incompetent) cells and usually develop more slowly.

In this project I focus on adult patients with acute myeloid leukaemia (AML). It has been found that this disease is genetically very heterogeneous and is associated with diverse cytogenetic abnormalities such as chromosomal deletions, translocations and duplications. The diagnosis of the karyotype is one of the most important factors to determine patient outcome. The development of new methods of diagnosis and the

classification of different genetic aberrations present in leukaemia is very important for the treatment of this disease

1.2 Haematopoiesis

Haematopoiesis is the development of blood cells. Postnatally, haematopoiesis occurs mainly in the bone marrow. All mature blood cells are generated from a relatively small number of pluripotent haematopoietic stem cells (Till and McCulloch, 1961). They generate the various haematopoietic lineages through a successive series of intermediate progenitors (Dzierzak *et al.,* 2005; Lemischka *et al.,* 2001; Weissman *et al.,* 2000). The initial differentiation of pluripotent stem cells will follow one of two major pathways, lymphoid or myeloid. Stem cells then become progenitor cells for each type of mature blood cell. These cells have lost the capacity for self-renewal and are committed to a given cell lineage: T- and B- progenitors (Kondo *et al*., 1997) and progenitor cells for erythrocytes, neutrophils, eosinophils, basophils, monocytes, mast cells and platelets (Akashi *et al*., 2000) (Fig.1.1)

Haematopoiesis is a continuous process throughout adulthood. Production of mature blood cells equals their loss. Cell division and differentiation during haematopoiesis are balanced by apoptosis – there must be maintenance of a stable state.

Haematopoietic cells grow and mature on a meshwork of non-haematopoietic stromal cells. The accumulation, maturation, differentiation and survival of the haematopoietic cells are caused by certain growth factors – small molecules with a biologically active concentration lower than 10^{-12} M, that are mainly provided by the stromal cells.

The first differentiation step to myeloid or to lymphoid progenitor cells is caused by the Stem Cell Factor (SCF). Under the impact of other growth factors like Interleukin-3 (IL-3), Erythropoietin (EPO), Granulocyte-macrophage colony stimulating factor (GM-CSF), Granulocyte colony stimulating factor (G-CSF) and Thrombopoietin (TPO), erythrocytes, macrophages, granulocytes and thrombocytes maturate for about 10 days. When this process is completed, the blood cells migrate to the bloodstream and to different body tissues.

The differentiation of the lymphoid stem cells into B- and T- lymphocytes is caused by different interleukins. (Reya *et al*., 2001; Speck and Gilliland, 2002).

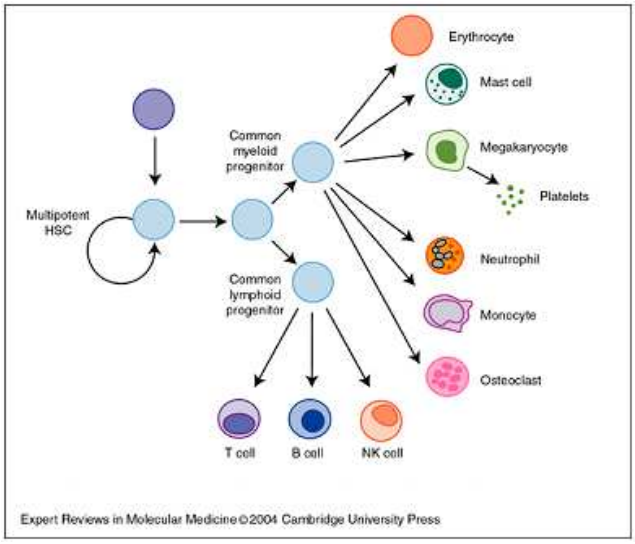

Fig.1.1 Normal haematopoiesis.

1.3 Acute myeloid leukaemia

Acute myeloid leukaemia (AML) is the most common acute leukaemia affecting adults, with an age-dependent mortality of 2.7 to nearly 18 per 100,000 people (Deschler and Lübbert, 2006). The median age of patients with AML is 65 to 70 years. The risk factors for acquiring AML include exposure to ionising radiation, benzene, and cytotoxic chemotherapy.

Acute myeloid leukaemia represents a heterogeneous group of early stem cell disorders. They are characterized by an uncontrolled expansion of malignant cells ("blasts") which are blocked at certain stages of myeloid differentiation. (Ailles *et al.*, 1997; Haase *et al.*, 1995; Mehrotra *et al.*, 1995). In absence of treatment this leads to fatal infection, bleeding, or organ infiltration typically within one year of diagnosis. The outcome for patients with AML depends greatly on the age of the patient and leukaemic cell karyotype (Grimwade *et al.*, 1998). For this reason the diagnoses and the classification of different abnormalities is very important for the treatment.

1.3.1 Classification

There are two systems for routine classification of AML. The first is the French-American-British (FAB) system, based on morphologic histochemic and immunologic analysis (Table 1.1) (Bennett *et al*., 1976). The second is the World Health Organisation (WHO) system (Harris *et al*., 1999). A basic principle of the WHO system is that the classification of haematopoietic and lymphoid neoplasm should utilize not only morphologic findings but also all available information, including genetic, immunophenotypic, biologic, and clinical features to define specific disease properties (Table 1.2).

Table 1.1 FAB classification (Bennett *et al*., 1976).

French-American-British (FAB) Classification of acute myeloid leukaemia

M0 Undifferentiated AML

M1 Myeloblastic, without maturation

M2 Myeloblastic, with maturation and with or without t(8;21) (Tenen, 2003).

M3 Promyelocytic, or acute promyelocytic leukaemia (APL) with t(15;17)(q22;q12)

M4 Myelomonocytic

$M4_{eo}$ Myelomonocytic together with bone marrow eosinophilia

$M5_a$ Monoblastic leukaemia

$M5_b$ Monocytic leukaemia

M6 Erythrocytic or erythroleukaemia

M7 Megakatyoblastic

Table 1.2 WHO classification (2008).

World Health Organisation (WHO) Classification of AML
Acute myeloid leukaemia with recurrent genetic abnormalities
AML with t(8;21)(q22;q22);(*RUNX1-RUNX1T1*)
AML with inv(16)(p13.1q22) or t(16;16)(p13.1;q22);(*CBFB-MYH11*)
APL with t(15;17)(q22;q12);(*PML-RARA*)
AML with t(9;11)(p22;q23);(*MLLT3-MLL*)
AML with t(6;9)(p23;q34);(*DEK-NUP214*)
AML with inv(3)(q21q26.2) or t(3;3)(q21;q26.2);(*RPN1-EVI1*)
AML (megakaryoblastic) with t(1;22)(p13;q13);(*RBM15-MKL1*)
Provisional entity: AML with mutated *NPM1*
Provisional entity: AML with mutated *CEBPA*
AML with myelodysplasia-related changes
Prior history of myelodysplastic syndrome (MDS)
MDS-related cytogenetic abnormality
Multilineage dysplasia
Therapy-related myeloid neoplasms
Acute myeloid leukemia, not otherwise specified
AML with minimal differentiation
AML without maturation
AML with maturation
Acute myelomonocytic leukemia
Acute monoblastic/monocytic leukemia
Acute erythroid leukemia
Acute megakaryoblastic leukemia
Acute basophilic leukemia
Acute panmyelosis with myelofibrosis

1.3.2 Genetic variations

Acute myeloid leukaemia is a clinically and genetically very heterogeneous disease (Estay and Döhner, 2006). Numerous cytogenetic studies have described more than 200 different structural and numerical aberrations (Mrózek *et al.*, 2001). Little is known about the mechanisms leading to the development of chromosome aberrations in cancer. Therefore, the cytogenetic diagnosis is a very important factor for the achievement of complete remission (CR), a low relapse risk and survival (Bloomfield *et al.*, 1984; Grimwade *et al.*, 1998, 2001; Slovak *et al.*, 2000; Mrózek *et al.*, 2001, 2004; Byrd *et al.*, 2002; Schoch *et al.*, 2004; Farag *et al.*, 2006).
Clonal chromosome aberrations are observed by current techniques in approximately 55% of patients with de novo acute myeloid leukaemia (AML). There are two general types: the balanced and the unbalanced aberrations. In the remaining group of about 45% of the patients, a normal karyotype is detected. According to cytogenetics and dependent on the prognosis, AML patients are currently classified into three groups – with favourable, intermediate and adverse prognosis (Grimwade *et al.*, 1998; Schoch *et al.*, Oncology Reports 2002; Bloomfield *et al.*, 1997; Mrozek *et al.*, 1997).

1.3.2.1 Balanced chromosome abnormality

The primary balanced translocations occur in 20-25% of AML cases. These abnormalities are characterized by primary reciprocal translocations or inversions, with rearrangements but without visible gains or loses of chromosomal material. For each of the balanced aberrations the break points are highly conserved from case to case. These kinds of aberrations tend to be found in younger patients. Biologically, several AMLs with balanced aberrations involve the deregulation of transcription factors resulting in an impairment of cell differentiation and proliferation (Melnick *et al.,* 1999; Goger *et al.,* 1999).
The most common balanced abnormalities in this group predict a favourable prognosis are AML1-ETO t(8;21), occurring in 12-15% of the AML cases; CBFB-MYH11 - inv(16) (p13;q22) that accounts for 8-10% of the cases of AML and PML-RARA t(15;17) (Grimwade *et al.*, 1998; Moorman *et al.,* 2001). 11q23 translocations

are also balanced aberrations but are associated with an unfavourable prognosis (Schoch *et al.*, 2003).

1.3.2.2 Unbalanced aberrations

35-40% of the AML cases have an unbalanced (complex) karyotype characterised by visible gains or losses of rather larger regions of the genomes. One complex karyotype is defined by detection of >3 abnormalities in one clone (excluding those with recurrent balanced rearrangements) (Grimwade *et al.,* 1998; Schoch *et al.,* 2002; Schoch *et al.*, 2001; Swansbury *et al.,* 1994). The chromosomal brake points often show major variations from case to case. Furthermore these aberrations are mostly characterized by a loss of genetic material resulting in an alteration of cell cycle control and DNA repair. AMLs with non-balanced aberrations have a poor prognosis with only 10-15 % long-term survivors.

Two of the most common unbalanced cytogenetic changes in therapy- and chemically-related leukaemia are the loss and the deletion of the long (q) arm of chromosomes 5 and 7 (Pedersen-Bjergaard *et al.*, 1995). These specific chromosome aberrations are also common among leukaemia patients with previous exposure to chemical solvents, including chronic exposure to benzene, insecticides, petroleum, etc. (Mitelman *et al.*, 1981; Crane *et al.*, 1996)

1.3.2.3 Normal karyotype

At diagnosis, about half (45%) of all AML patients have a normal karyotype, which puts them at an intermediate risk of recurrence (Grimwade *et al.*, 1998, 2001; Slovak *et al.*, 2000; Byrd *et al.*, 2002). Only about 30% of karyotypically normal patients are long term survivors (Farag *et al.*, 2005). Thus, the identification of other molecular markers should help improve the precision of prognostic stratification of the patients in this group. By the use of molecular genetic techniques, such as reverse transcription polymerase chain reaction (RT-PCR), fluorescence in situ hybridization (FISH), direct sequencing and spectral karyotyping (SKY), some molecular alternations with important prognostic impact were identified (Mrózek *et al.*, 2007).

One of the frequently detected abnormalities in AML patients with normal karyotype is the internal tandem duplication (ITD) in the fms-like tyrosine kinase-3 gene (FLT3), a haematopoietic growth factor receptor (Thiede *et al.*, 2002; Nakao *et al.*, 1996; Kottaridis *et al.*, 2001; Whitman *et al.*, 2001; Fröhling *et al.*, 2002; Kainz *et al.*, 2002; Schnittger *et al.*, 2002; Beran *et al.*, 2004). FLT3-ITD mutation is detected in 25% to 30% of the cases and is associated with poor treatment outcome. A second type of mutation in the tyrosine kinase (TKD) domain of the FLT3 receptor is present in approximately 5% to 7% of AML patients. The impact of FLT3-ITD mutation on other mutations and on some cell mechanisms like DNA repair mechanism is an important topic in this project. Therefore the formation and the function of FLT3 are described in more detail below. Another molecular abnormality also associated with worse prognosis is the presence of a partial tandem duplication of the mixed lineage leukaemia gene (MLL-PTD) in approximately 8% of the cases (Schichman *et al.*, 1994; Caligiuri *et al.*, 1998; Schnittger *et al.*, 2000; Döhner *et al.,* 2002; Shiah *et al.*, 2002; Munoz *et al.*, 2003). Furthermore, some mutations were found in one of the most important haematopoietic transcription factors - AML1/RUNX1. These aberrations are common in adult haematologic malignancies, especially acute myeloid leukaemia (AML)-M0 or leukaemia with acquired trisomy 21, and familial platelet disorder with a predisposition toward AML. However, the prognostic implication of RUNX1 mutations is limited.

Associated with a good clinical outcome are mutations in either the gene coding for the transcription factor CEBPA (approximately 7% of the cases) (Pabst *et al.*, 2001; Preudhomme *et al.*, 2002; Fröhling *et al.*, 2004) or the most common somatic gene mutation of the nucleophosmin (NPM1) gene (in approximately 35% of the cases).

Other examples of genetic aberrations found in AML with a normal karyotype are mutations in the tyrosine kinase receptor c-KIT and the GTPases N-RAS and K-RAS. However, c-KIT as well as RAS mutations do not show any correlation with clinical outcome in AML (Care *et al.*, 2003; Kiyoi *et al.*, 1999; Neubauer *et al.*, 1994).

Unfortunately, not all mutations in this group could be detected by conventional cytogenetic methods. For this reason, the development of new molecular methods is important for the classification of different chromosomal aberrations and for better understanding of the pathogenesis of this disease and development of innovative therapeutic strategies.

1.3.3 FMS-like tyrosine kinase 3 (FLT3) and Loss of heterozygosity (LOH)

FLT3 (Fms-like tyrosine kinase 3) also known as FLK-2 (fetal liver kinase 2) and STK-1 (human stem cell kinase 1) is a type III receptor tyrosine kinase plays a key role in haematopoiesis (Gilliland and Griffin, 2002a; Kottaridis *et al.*, 2003; Stirewalt and Radich, 2003). FLT3 expression occurs primarily in immature myeloid and lymphoid progenitors, including CD34+ cells with high levels of CD117 (c-KIT) expression (Rasko *et al.*, 1995; Rosnet *et al.*, 1996). Furthermore FLT3 is also expressed at high levels in a spectrum of haematologic malignancies, including 70-100% of AML of all FAB subtypes, B-precursor cell acute lymphoblastic leukaemia (ALL), a fraction of T-cell ALL, and chronic myelogenous leukaemia (CML) in lymphoid blast crisis. However, the recent data indicate that FLT3 expression could be involved in the survival, proliferation and differentiation of primitive hemopoietic progenitor cells (Carow *et al.,* 1996; Drexler, 1996).

FLT3 gene is localised on the chromosome 13q12 (Gilliland and Griffin, 2002b). FLT3 receptor contains five extracellular Ig-like domains, a transmembrane domain, a juxtamembrane domain and two tyrosine-kinase domains that are linked through the tyrosine-kinase insert (Small *et al.,* 1994) The extracellular part is responsible for the ligand binding. (van der Geer *et al.*, 1994). After the binding of FLT3-Ligand (FL) conformational changes in FLT3 promote dimerization, phosphorylation and adaptor-protein docking, transmitting signals to downstream effectors (Fig.1.2). This results in subsequent activation of several signalling pathways involved in the cell growth and proliferation.

Constitutively activating mutations of FLT3 are one of the most common genetic abnormalities in AML. FLT3 mutations cause ligand-independent receptor dimerisation and constitutive activation (Kiyoi *et al.*, 1998). The mutations involve more often an internal tandem duplication (ITD) of the juxtamembrane domain and the result is an activation of STAT5 (Zhang *et al.*, 2000), Ras/mitogen-activated protein kinase (MAPK) and phosphatidylinositol 3 kinase (PI3K)/AKT pathways (Hayakawa *et al.*, 2000; Mizuki *et al.*, 2000).

A FLT3-ITD mutation within the juxtamembrane domain of FLT3 was found in about 25 - 30% of AML patients (Nakao *et al.,* 1996). The presence of the FLT3-ITD mutation is generally associated with a statistically significant poor clinical outcome

compared with patients not harbouring this aberration. In fact, three distinct genotypes have been identified in AML patients: normal $FLT3^{WT/WT}$, heterozygous $FLT3^{ITD/WT}$, and hemizygous $FLT3^{ITD/-}$ - FLT3-ITD-positive that also lacked the FLT3 wt allele. The loss of the WT allele is also known as Loss of heterozygosity (LOH). LOH is a form of allelic imbalance that can arise via several pathways, including deletion, gene conversion, mitotic recombination and chromosome loss. If $FLT3^{ITD/-}$ genotype is detected in patients with normal karyotype, the two copies of chromosome 13 indicate that the loss of the wt FLT3 allele is not a result of a monosomy 13, or a cytogenetically detectable deletion involving band 13q12 also. Results of LOH studies suggest that there are two possible explanations of the $FLT3^{ITD/-}$ genotype in the patients with normal karyotype. The first one is, that submicroscopic deletion of 13q12 is responsible for the observed wt FLT3 allele loss. The second is that the whole chromosome 13 with a wt allele could have been initially lost and later replaced by a duplicated copy of the chromosome 13 containing the FLT3-ITD allele (thus generating a $FLT3^{ITD/ITD}$ genotype). This process is known as uni-parental disomy (UPD). In UPD, one allele or an entire chromosome from one parent are missing leading to the reduplication of the other parental allele (uni-parental = from one parent, disomy = duplicated).

Recent studies have reported that the $FLT3^{ITD/-}$ patients have a significantly shortened survival compared with $FLT3^{WT/WT}$ and/or $FLT3^{ITD/WT}$ patients. It has been suggested that FLT3-ITD arises via a slippage-repair mechanism (Kiyoi *et al.,* 1998), but the mechanism leading to the loss of the wt FLT3 allele is currently unknown.

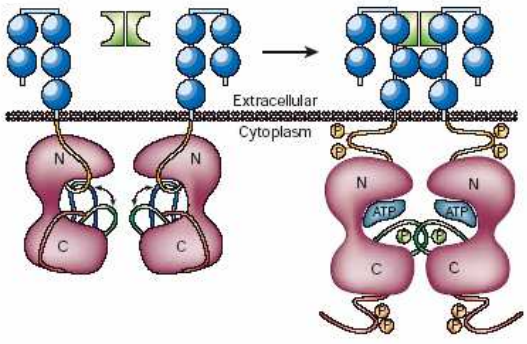

Fig 1.2 Mechanism of FLT3 activation (Blume-Jensen and Hunter, 2001).

Left: inactive Form; **Right:** Ligand-dependent dimerisation and autophosphorylation.

Not only chromosome 13 can be affected by LOH. This mechanism commonly occurs in cancer and is associated with the absence of a functional tumor suppressor gene in the lost region. Despite this, many people remain healthy with such a loss, because there is still one functional gene left on the other chromosome of the chromosome pair. However, the remaining copy of the tumor suppressor gene can be inactivated by a point mutation, leaving no tumor suppressor gene with protection function. Subsequently this mutation can be duplicated -UPD. Recently it has been speculated that UPD found in the AML patients is associated with the up regulation of some genes´ coding proteins involved in the DNA repair process. Loss of heterozygosity and UPD respectively can be identified using polymorphic markers, such as single nucleotide polymorphisms, explained in more details below.

1.3.4 "Two hits" model of leukaemogenesis

A majority of authors defend the theory that AML cannot be induced by just one mutation (Fenske *et al*., 2004; Kelly *et al*., 2002; Yuan *et al*., 2001). They agree that for AML development the co-operation of a minimum of two mutations is necessary. These mutations are subdivided in two classes. One class of mutations (class I) (FLT3 or c-KIT) confers a proliferative or survival advantage to cells, and a second class of mutations (class II) (AML1-ETO or PML/RARα) serves primarily to interfere with haematopoietic differentiation and subsequent apoptosis of cells. This model predicts that only one mutation in each class would be required for AML development. Together, both transformations induce disruption in the proliferation and differentiation of both stem- and progenitors cells, and are thus responsible for the development of AML (Fig 1.3).

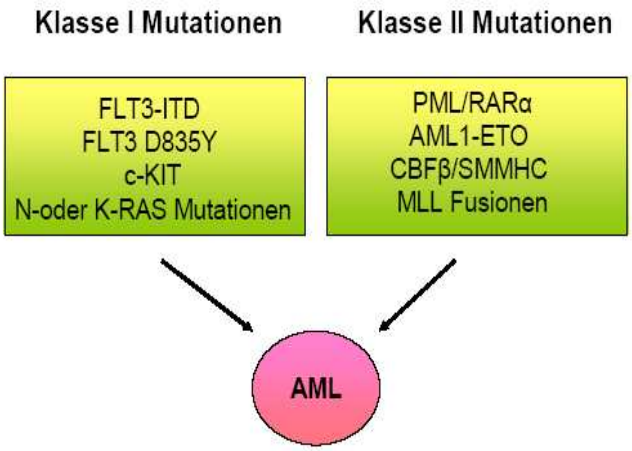

Fig.1.3 Model of the two classes of mutations responsible for the development of AML (Gilliland and Griffin, 2002a).

1.4 Genome instability and repair

DNA is subjected to spontaneous instability and decay. In addition to spontaneous damage, cellular DNA is under constant attack from reactive chemicals that the cell itself generates as by-products of metabolism. Moreover, the integrity of cellular DNA is assaulted by such environmental threats as X-rays, ultraviolet radiation from the sun, and many chemical agents, some of which are products of our industrialised society.

Approximately 10^4 spontaneous molecular lesions are known to occur in every human cell every day, mostly by oxidation, hydrolysis, alkylation, radiation, or toxic chemicals (Fortini *et al.*, 2003). The result can be gene mutations that are further transferred to the gene product (protein). If these mutations are in genes that normally control cell proliferation or suppress tumour growth, the cells may start to grow uncontrollably. Cells have therefore developed mechanisms to repair DNA damage. Individuals with inherited disorders of DNA repair display increased levels of chromosomal aberration and mutation in somatic cells, and a predisposition to cancer (Karran *et al.*, 2003). The rate of DNA repair is dependent on many factors, including the cell type age, and the extracellular environment. There are four mechanisms leading to error free repair of DNA damage: Base Excision Repair

(BER), Nucleotide Excision Repair (NER), Mismatch repair (MM) and Homologous Recombination (HR).
Other mechanisms of repair are Non-Homologous End Joining (NHR) and Single strand annealing (SSA). However, NHR and SSA often lead to the loss of genetic information resulting in DNA damage.
Excision repair, explained in more details below, removes lesions that affect only one DNA strand. It involves excision of the lesion and subsequent use of the complementary strand to fill the gap.

1.4.1 Base Excision Repair (BER)

DNA's bases may be modified by deamination or alkylation as a result of oxidative processes (e.g. ionizing radiation). These mutations are repaired by BER. The position of the modified (damaged) base is called the "abasic site" or "AP site". The repair process starts with the enzymatic removal of the AP site and of neighbouring nucleotides by DNA glycosylases, that can recognize the AP site. The BER mechanism can proceed through two different subpathways: the short-patch BER and the long-patch BER. The short-patch BER sub-pathway is characterized by the insertion of a single base at the lesion site by DNA polymerase ß (Pol ß). The long-patch Pol ß or the replicative Pol δ/ε re-synthesize an oligonucleotide by 2-7 nucleotides. The long patch also requires PCNA, which is a loading clamp for the replicative polymerases, and a flap-endonuclease, FEN1, that recognises and cleaves at the base of the flap structure. The gap is filled by DNA polymerase I and DNA ligase (Fortini *et al.*, 2003; Hung *et al.*, 2005; Hung *et al.*, 2005). No human disorders have been related directly to inherited BER deficiencies, and knockout mice that lack core BER proteins die as embryos, attesting to the important role of the BER process (Fortini *et al.*, 2003) (Fig.1.4)

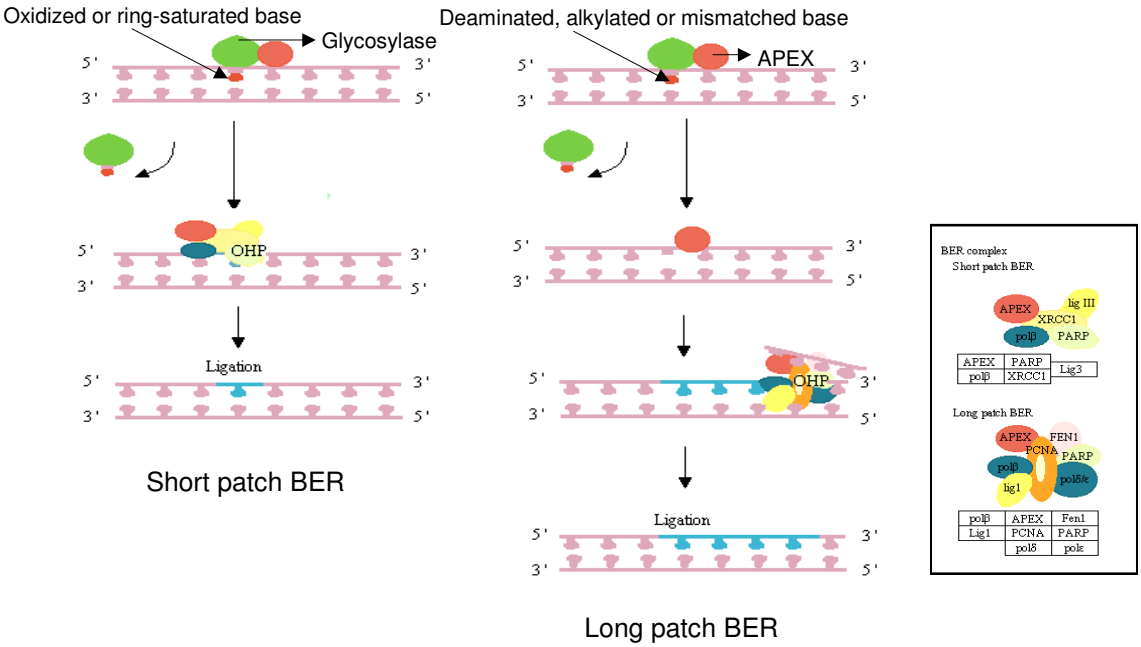

Fig.1.4 Base Excision Repair (BER) and the short and long patch sub-pathways. Modified from Minoru Kanehisa (Kanehisa Laboratories).

1.4.2 Nucleotide Excision Repair (NER)

Nucleotide excision repair recognizes a wide range of substrates, including damage caused by UV irradiation (pyrimidine dimers and 6-4 photoproducts) and chemicals (intrastrand cross-links and bulky adducts). This process consists of recognition of the damaged DNA, excision of an oligonucleotide of 24 – 32 residues containing the damaged DNA. The gap is then filled by DNA polymerase I and DNA ligase (Costa *et al.*, 2003; Batty, and Wood, 2000; de Laat *et al.*, 1999; Friedberg, 2001). nucleotide excision repair can be categorized into two classes, global genome NER (GG-NER) and Transcription Coupled NER (TCR-NER)

The GG-NER surveys the entire genome for lesions which distort the DNA. In this sub-pathway the DNA disorder is recognised by the XPC-hHR23B Complex (Fig.1.5). The TCR-NER focuses on DNA lesions that block the activity of RNA polymerases and the overall transcriptional activity, and rapidly repairs damage on the transcribed strand of active genes (Fig.1.5) (Costa *et al.*, 2003; Hoeijmakers 2001; Benhamou and Sarasin, 2000). In this sub-pathway, stalled RNA polymerase II acts as a marker for lesion recognition by CSA/CSB. In both pathways a nine-subunit complex (TFIIH)

of helicases carry out DNA unwinding. The RPA stabilizes the unwound DNA, and XPA assembles DNA repair factors. The damaged DNA is then removed by XPG and the XPF-ERCC1 complex, which make 3´ and 5´ incisions. The gap is filled by DNA polymerase δ/ε and sealed by DNA ligase (Fig.1.5)

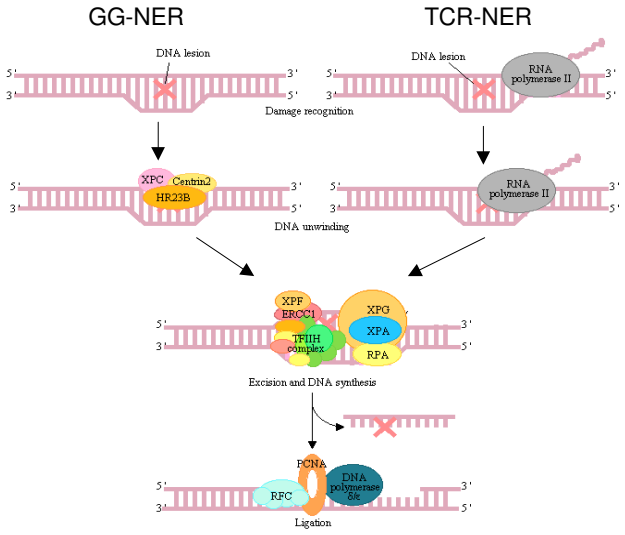

Fig.1.5 Nucleotide excision repair of a bulky adduct. Modified from Minoru Kanehisa (Kanehisa Laboratories).

1.4.3 Mismatch repair (MMR)

The DNA mismatch repair (MMR) pathway has been evolved to correct errors made by DNA polymerase during DNA replication. Such errors fall into two broad categories: base substitutions and insertions/deletions. A base substitution error occurs when the DNA polymerase inserts an incorrect (noncomplementary) nucleotide opposite the template base. Often, DNA polymerase will make a base substitution error when copying a base that has been damaged by alkylation. An insertion error occurs when the DNA polymerase adds one or more extra nucleotides to a sequence. A deletion error is made when one or more nucleotides are omitted from a sequence.

The process of MMR, like the BER and NER pathways, comprises damage recognition, damage excision, DNA repair synthesis, and DNA ligation. Mismatch repair is a highly conserved process from prokaryotes to eukaryotes. The first

evidence for mismatch repair was obtained from *S. pneumoniae*. Subsequent work on *E. coli* has identified a number of genes wich gene products are therefore called the "Mut" proteins, and are the major active components of the mismatch repair system. Three of these proteins are essential in detecting the mismatch and directing repair machinery to it; MutS, MutH and MutL. The human MMR protein family members responsible for recognition of mispaired DNA are termed hMSH, for human MutS Homologs. MutS heterodimer recognises a mismatch (Fig.1.6.1) and MutL heterodimer is recruited (Fig.1.6.2). The MutS sliding DNA clamps can migrate in either direction. MutL works as a matchmaker, displacing the PCNA/DNA polymerase complex when encountered (i.e. when the DNA clamp moves in 5´>3` direction) (Fig.1.6.3). The MutL complex in humans is a heterodimer consisting of hMLH1 and hPMS2 proteins.

MutH is a very weak endonuclease that is activated once bound to MutL (which itself is bound to MutS). MutH has no eukaryotic homolog. Its endonuclease function is taken up by MutL homologs, which have some specialized 5'-3' exonuclease activity. MutL recruits exonuclease 1 (Exo I) that excises up to a kilobase of DNA at the site of the mismatch (Fig.1.6.4). The error is corrected by re-synthesis.

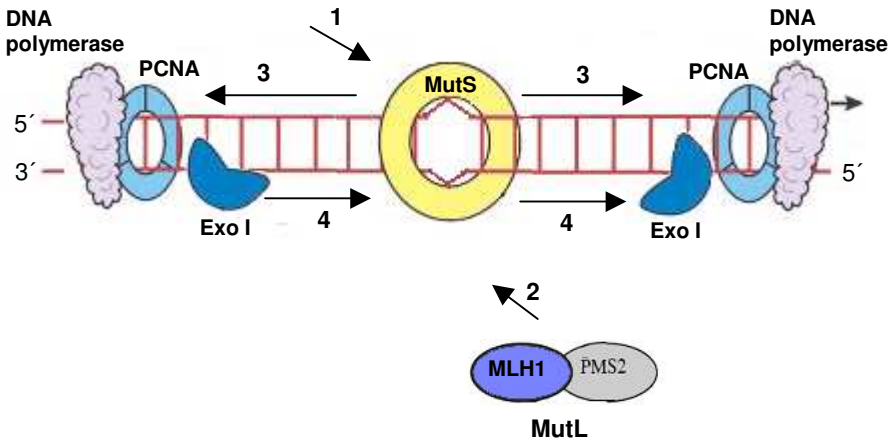

Fig.1.6 Repair of a single nucleotide mismatch. Modified from Jascur and Boland, 2006.

1.5 Double-Strand Break (DSB)

DSBs are the most serious form of DNA damage because they pose problems for transcription, replication, and chromosome segregation. DSBs affect both strands of the DNA duplex and therefore prevent the use of the complementary strand as a

template for repair. Cells have evolved two major pathways of DSB repair: HR (Homologous Recombination) and NHEJ (Non-Homologous End Joining). When two repeated sequences are very close to each other, SSA (Single Strand Annealing) is another possible mechanism of repair.
In this project I concentrated on DSB repair. For this reason, the repair processes involved in this mechanism will be explained in more details below.
When DSBs are generated, independent of the repair mechanism (HR NHEJ or SSA), ATM is activated and relocated through an interaction with the RAD50/MRE11/NBS1 complex. In the next step, ATM phosphorylates histone H2Ax in the chromatin micro-environment surrounding a DNA double-strand break (DSB). Afterwards, different signalling pathways are involved in these three repair mechanisms.

1.5.1 Non-Homologous End Joining (NHEJ)

NHEJ seems to be the primary mechanism of DSBs repair in mammalian cells (Jeggo *et al.,* 1998). Conceptually, the mechanism of NHEJ is simple—the broken ends are brought together and then joined. If the cell incurs more than one DSB, then previously unlinked DNA molecules may be joined, resulting in gross chromosomal rearrangements. The binding of specific protein factors to the broken ends is the first step in NHEJ. This serves to limit nucleolytic degradation, which would result in the loss of genetic information. Using genetic studies of mammalian cell lines, several proteins involved in the DSB repair process were identified (Jeggo *et al.,* 1991; Lees-Miller *et al.,* 1995; Gu *et al.,* 1997; Riballo *et al.,* 1999).
One of the most important proteins in NHEJ in mammalian cells is the Ku complex, which is a heterodimer of Ku70 and Ku86 (also known as Ku80) and is the major DNA end binding factor in mammalian cells. The Ku complex recruits DNA-PKcs (DNA-dependent protein kinase catalytic subunit) to the DSBs, activating its kinase function (Weaver *et al.,* 1996; Chu *et al.,* 1997; Critchlow & Jackson, 1998). It has been proposed that DNA-PKcs has an impact on the XRCC4/DNA and ligase IV heterodimer, factors that are also important for NHEJ (Critchlow *et al.,* 1997; Grawunder *et al.,* 1997; 1998). However, the precise roles of these proteins in the repair process are unknown. Three possible steps have been suggested for the

repair of DSBs by NHEJ: 1. end-binding and bridging, 2. terminal processing, and 3. ligation.

The Ku heterodimer initiates NHEJ by binding to the free DNA ends, thus protecting from degradation and recruiting other NHEJ factors such as DNA-PK, XRCC4, and DNA Ligase-IV (Cary *et al.,* 1997; Pang *et al.,* 1997; Yaneva *et al.,* 1997; Feldmann *et al.,* 2000). DNA-PK becomes activated upon DNA binding, and phosohorylates a number of substrates including p53, Ku, and XRCC4. (Mahajan *et al*., 2002). The phosphorylation of these factors further facilitates the repair process. Because the ends of most DSBs generated by genotoxic agents are damaged and are unable to be directly ligated, they often have to undergo limited processing by nucleases and/or polymerases before NHEJ can proceed. This process includes the MRE11-RAD50-NBS1 complex, that has exonuclease and helicase activities (Paull *et al.,* 1998; Khanna *et al.,* 2001). RAD50, MRE11 (Meiotic Recombination-11) and NBS1 (Nijmegan Breakage Syndrome-1) function particularly if the DNA ends require processing before ligation. The final step in NHEJ repair involves ligation of the DNA ends by Ligase-IV in a complex that also includes XRCC4 and Ku. (Junop *et al.,* 2000; Lee *et al.,* 2000; Sibanda *et al.,* 2001) (Fig.1.7).

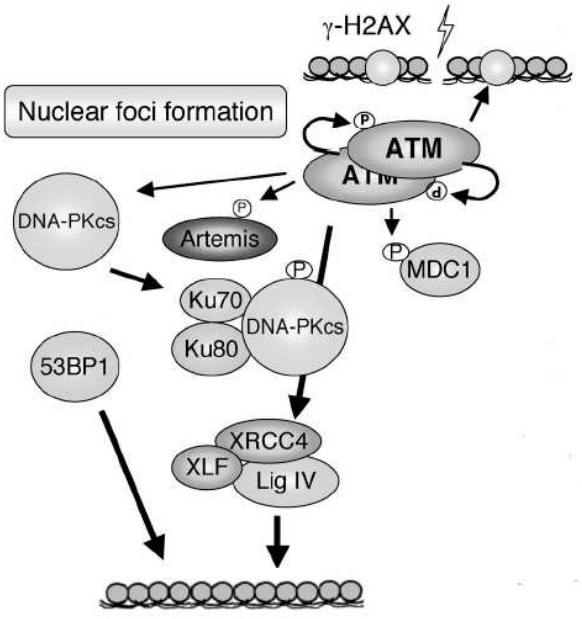

Fig.1.7 Repair of DNA double strand breaks by non-homologous end joining. Adapted from Kobayashi *et al.,* 2004.

1.5.2 Single strand annealing (SSA)

Single strand annealing (SSA) is a process initiated when a double strand break is made between two repeated sequences oriented in the same direction. Single stranded regions are created adjacent to the break, and they extend along the repeated sequences, so that the complementary strands can anneal to each other. This annealed intermediate part can be processed by digesting away the single stranded tails and filling in the gaps.

SSA requires several gene products that are also necessary for other types of recombination assays. RAD52, for example, is important for most if not all types of recombination processes that include SSA. RAD52 is a DNA binding protein that can anneal ssDNA in vitro (Mortensen *et al.,* 1996, Shinohara *et al.,* 1998). A homolog of RAD52, RAD59 is also required for SSA and has DNA binding properties and strand annealing activity.

Another pair of proteins that exhibit homologous sequence length dependence during SSA comprises MSH2 and MSH3 (Sugawara *et al.,* 1997). These proteins, along with the RAD1-RAD10 excision endonuclease protein complex (Fishman-Lobell and Haber 1992), are involved in removing nonhomologous 39-ended DNA tails from annealed intermediates. However, whereas RAD1 and RAD10 are required to clip off the tails regardless of the length of the annealed homologous regions, the requirement for MSH2 and MSH3 decreases dramatically as the annealed regions increase from 205 bp to 1.17 kb. Interestingly, MSH2 and MSH3 are also needed for the removal of nonhomologous sequences from the ends of the invading strands during DSB-induced gene conversion, even when the length of homologous sequence shared by the donor and recipient is 2 kb (Paˆques and Haber 1997). They presumably act in a similar manner, by binding to the junctions between single-stranded DNA and double-stranded DNA and promoting the RAD1- RAD10 - mediated cleavage of the single-stranded nonhomologous tail, so that the 39 end of the invading DNA strand can be used as a primer to initiate new DNA synthesis. The need for MSH2 and MSH3 in gene conversion, even with long homologous regions adjacent to the nonhomologous ends, presumably reflects the difference between the instability of a strand invasion structure (involving an invading single strand and a duplex template) and the more stable intertwining of two complementary single strands during SSA (Fig.1.8).

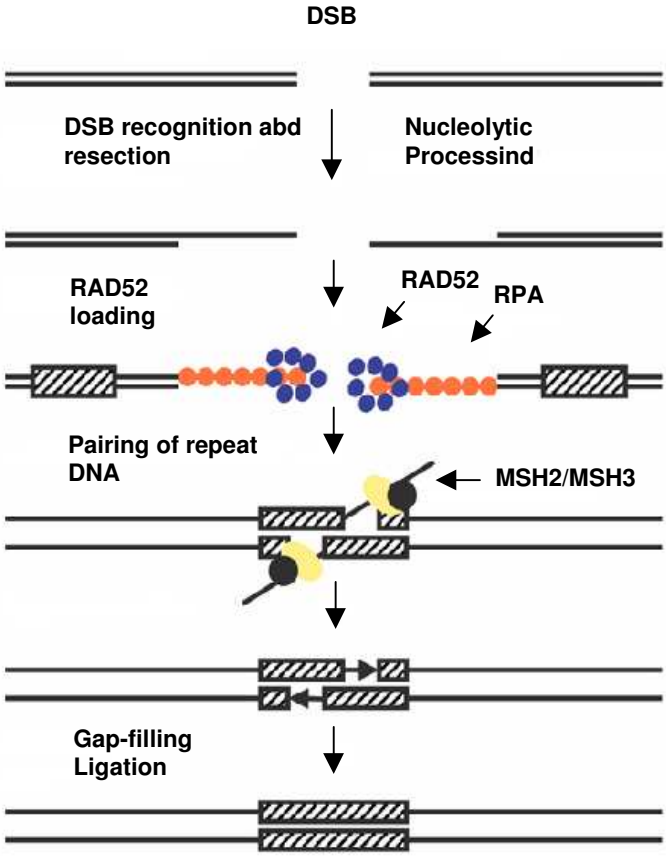

Fig.1.8 Repair of DNA double strand breaks by single strand annealing. Adapted from Kristoffer and Lawrence 2003.

1.5.3 Homologous Recombination (HR)

In the process of HR, a DSB is repaired by copying the missing information from the sister chromatid or homologous chromosome, resulting in the exact restoration of the DNA. HR is the main pathway for postreplicative repair during the late S/G2-phase.
One of the earliest events in HR-dependent repair is converting the DSB ends to a recombination competent structure. This step involves degradation of single strands by the eukaryotic MRE11/RAD50/NBS1 (MRN) complex leaving a 3' protruding end, which is hundreds of bases long (Fig.1.9B) (Krogh and Symington, 2004). The resulting 3´ ssDNA tails are bound by RPA (1.9C), which is replaced with RAD51 in a reaction mediated by RAD52 and RAD51 paralogues (1.9D) (Sung 1997; Shinohara and Ogawa 1998). Subsequently, this nucleoprotein filament invades the intact DNA duplex, and forms a structure called the "D-loop". Strand displacement and branch

migration are complicated tasks and involve many energy-dependent processes, such as breaking internal hydrogen bonds, unwinding the DNA, and competing with other DNA binding proteins (Fig.1.9E). Hence, many proteins play roles during these processes, including RAD51, and all five RAD51-like proteins, namely XRCC2, XRCC3, RAD51B (or RAD51L1), RAD51C (RAD51L2) and RAD51D (RAD51L3) (Albala *et al*., 1997; Rice *et al.,* 1997; Cartwright *et al.,* 1998; Dosanjh *et al.,* 1998; Liu *et al.,* 1998; Pittman *et al.,* 1998; French *et al.,* 2002). These RAD51 paralogues form four different complexes, XRCC2-RAD51D, RAD51B-RAD51C, XRCC3-RAD51C and RAD51B-RAD51C-RAD51D-XRCC2, that stimulate the activity of RAD51 in various aspects (Braybrooke *et al.,* 2000; Kurumizaka *et al,* 2001; Sigurdsson *et al.,* 2001; Henry-Mowatt *et al.,* 2003; Yokoyama *et al.,* 2003). Other relevant proteins include: RAD54, RAD54 paralogues, and the breast cancer associated proteins BRCA1/2 (Jasin 2002). RAD54 likely has a dual function both in enabling strand exchange and in facilitating branch migration. It can stabilize RAD51 nucleofilament and enhance D-loop formation by introducing negative supercoils (1.9 D-F) (Sigurdsson *et al.,* 2002; Mazin *et al.,* 2003). Normal basepairing follows after the dissociation of RAD51 from ssDNA of the invading and complementary donor strands and subsequent strand extension by DNA polymerase. The extended strand can dissociate and anneal with the processed end of the non-invading strand on the opposite side of the DSB in a process called synthesis- dependent strand annealing. Alternately, both ends may invade, producing a double-holiday junction that is resolved to yield crossover or non-crossover recombination. Once intermediates are resolved, possibly by the action of XRCC3/RAD51C complex (Fig.1.9G) (Brenneman *et al.,* 2002; French *et al.,* 2002; Liu *et al.,* 2004), the remaining ssDNA gaps and nicks are repaired by DNA polymerase and DNA ligase.

Crossovers are associated with a fraction of HR events and can have a stabilizing or destabilizing effect on the genome. In meiosis, crossovers are highly regulated such that at least one crossover occurs between each pair of homologous chromosomes to ensure proper chromosome segregation, while excess crossovers are suppressed (Champion *et al*., 2002). In mitosis, crossover poses serious risks of large-scale genome alterations: half of the G2 phase crossovers between homologous result in loss of heterozygosity from the point of the crossover to the telomere, and crossover between repeated regions on non-homologous chromosomes, the same

chromosome, or sister chromatides can result in translocations, inversions, deletions, and UPD (Nickoloff 2002). All these increase genome instability

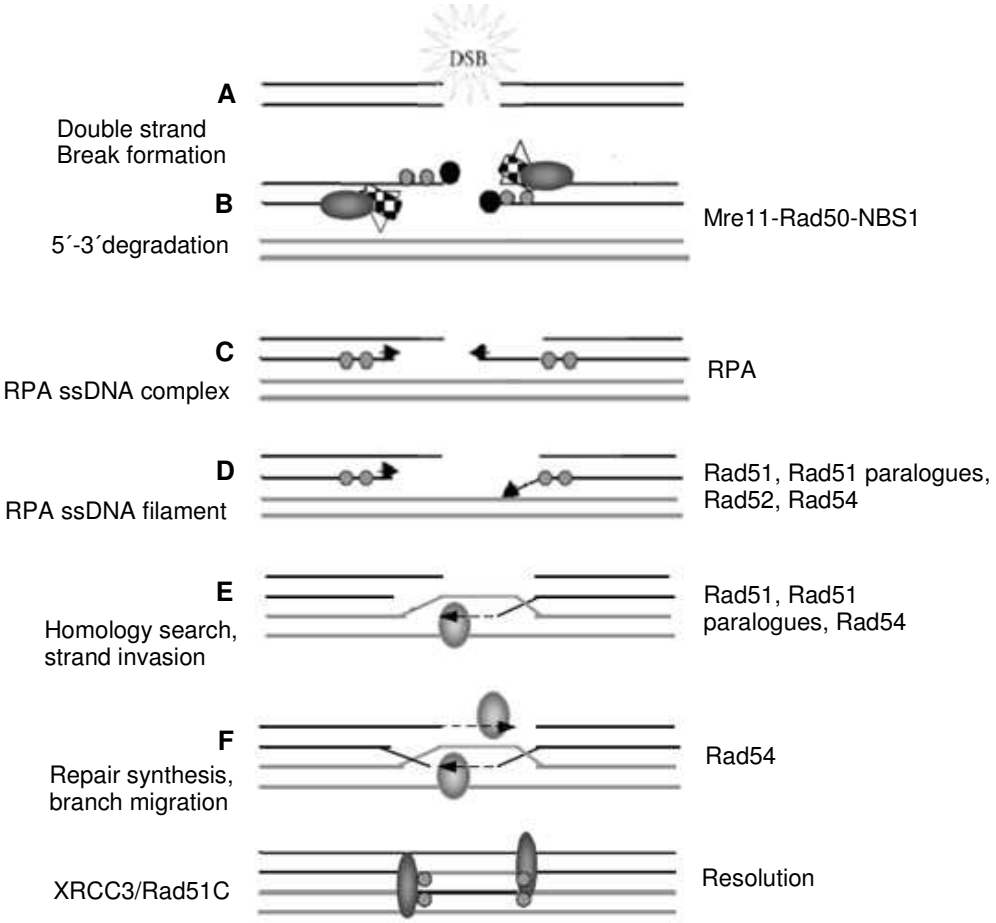

Fig.1.9 Repair of DNA double strand breaks by Homologous Recombination. Modified from Jackson 2001; 2002.

1.6 Polymorphism

A polymorphism is a geremline variation in the base sequence of the genetic code, defined by inheritable variations present at an allele frequency higher than 1% in the general population. At lower frequencies it is termed a germline mutation (Strachan and Read 1996). Polymorphisms are not associated with diseases, unlike mutations. The polymorphisms can remain and spread within a population, either because they have no major effect or because they are associated with beneficial effects for individuals. Some mutations tend to be selected against by evolution, even if they do not disappear completely, and they may arise spontaneously in new

generations. Also, some deleterious mutations persist in populations because they are associated with a selective advantage under certain environmental conditions. Polymorphisms and germline mutations are present in the genetic code of every cell of an individual. Furthermore, non-inheritable alterations acquired during the lifetime of an individual are present in the genetic code. These are known as somatic mutations and are present within the affected tissue only. Thus, somatic mutations can proliferate by clonal expansion of the mutated cell, but cannot be transmitted to the offspring of the affected individual.

The most common type of polymorphisms in the human genome are single nucleotide polymorphisms (SNPs). Previous estimates suggest that there may be ~ 5 million SNPs with minor allele frequencies of at least 10%, possibly as many as ~ 10 million with major allele frequencies of at least 1% (Kruglyak and Nickerson 2001). The Human Genome Project has provided a windfall of sequence polymorphism data, and because of collaborative SNP discovery initiatives such as the SNP Consortium (TSC), millions of human SNPs have been catalogued. The mapping of these SNPs is an excellent genotypic marker for research. Recently, SNP arrays were developed to analyse polymorphisms and to study the whole genome within a population. A very important application of SNP array is in determining disease susceptibility and consequently, in pharmacogenomics, by measuring the efficacy of drug therapies specifically for each individual. As a result, drugs can be personally designed for more efficiency on a group of individuals who share a common allele, or even for a single individual.

Furthermore, a SNP array can be used for studying the loss of heterozygosity (LOH), which includes not only genomic gains or deletions, but can also detect copy number neutral LOH due to uniparental disomy (UPD). The use of a high density SNP array for LOH detection allows the identification of pattern of allelic imbalance with potential prognostic and diagnostic utilities. This has a huge potential in cancer diagnosis, as LOH is a prominent characteristic of most human cancers. Recent studies based on the SNP array technology have shown that not only solid tumours (e.g. gastric cancer, liver cancer etc) but also haematological malignancies (ALL, AML, MDS, CML etc) have a high rate of LOH due to either genomic deletions or UPD and genomic gains. The results of these studies may help to gain insights into mechanisms of these diseases and to create targeted drugs.

1.7 Aim of the project

Acute myeloid leukaemia is a very heterogenous disease which is associated with diverse cytogenetic abnormalities like chromosomal deletions, translocations and duplications. The diagnosis of the karyotype is one of the most important factors to determine the outcome of this disease, but only in 50% of patients the genetic background of cancer development could be found. In the remaining group normal karyotype has been detected. With current methods it is very difficult to understand the mechanisms of AML progression in this group. However, some genetic aberrations were reported like point mutations in FLT3 gene, inactivating mutations in transcriptionfactors CEBPA and one of the most common mutations in the NPM1-gene. Recently it was also reported about UPD (uniparental disomy) in connection with AML. Little is known about the mechanisms of UPD and what connection this aberration has with the outcome of this disease. In particular, in this project the following tasks were proposed:

1. Screening of larger panels of patients for LOH

2. Identification of chromosomal location of UPD

3. Identification of genes affected by this mutation

4. Identification of links between LOH and disease outcome

5. Explore the mechanism of UPD

2. Materials and Methods

2.1. Laboratory equipment

Laboratory Centrifuges 4-15 C	Qiagen, Hilden, Germany
Centrifuge 5810R	Eppendorf, Germany
Centrifuge 5417C	Eppendorf, Germany
BioRobot 8000	Qiagen, Hilden, Germany
Vortex REAX top	Heidolph, Schwabach, Germany
Thermoblock	Eppendorf, Germany
Thermoblock	Liebisch Labortechnik, Bielefeld, Germany
Laborpipetts:	Gilson, Middleton, USA
Anthos htII spectrometer	Anthos Labtec Instruments, Wals, Australia
NanoDrop™ 1000 Spectrophotometer	Thermo scientific, Germany
GeneAmp PCR System 9700	Applied Biosystem, Foster City, USA
GeneAmp PCR System 2400	Perkin Elmer, Germany
Mastercycler epgradients	Eppendorf, Germany
Vortex REAX 2000	Heidolph, Schwabach, Germany
Minicentrifuge	Fischer Scientific, Schwerte, Germany
Facs Calibur	Becton Dickinson, Heidelberg, Germany
FacsVantage SE	Becton Dickinson, Heidelberg, Germany
FACSAria	Beckton Dickinson, Heidelberg, Germany
CO_2 water – Jacketed Incubator US AUTO FLOW	Nuaire, Plymouth, USA
Inkubator 1000	Heidolph, Schwabach, Germany
G.F.L. Shaking Incubator 3033	Progen Scientific Ltd, Mexborough,UK
Biometra TI 3	Polaroid, Germany
Horizon 11-14 gel electrophoresis apparatus	GIBCO BRL, Karlsruhe, Germany
Electrophoresis power supply ST 606 T	Gibco BRL, Karlsruhe, Germany
ABI 377	Applied Biosystems, Darmstadt, Dermany

ABI PRISM *3130X/ Genetic* Analyzer	Applied Biosystems, Darmstadt, Dermany
GloMax™ 96 Plate Luminometer	Promega GmbH, Germany
GeneChip® Fluidics Station 450	Affymetrix, Germany
GeneChip® Hybridization Oven	Affymetrix, Germany
GeneChip® Scanner 3000	Affymetrix, Germany
PH-Meter	WTW, Weilhem, Germany
Epifluorescence microscope Nikon Eclipse TS100	Nikon, New York, USA
Light microscope Nikon eclipse TS 100	Nikon, New York, USA
Leica SP5 inverse confocal microscope	Leica Microsystems, Wetzlar, Germany
XE-2100 Sorter	Sysmex, Germany GMBH
7500 Real Time PCR System	Applied Biosystems, Darmstadt, Dermany
Anthos htII spectrometer	Anthos Labtec Instruments, Wals, Australia

2.2 Chemicals and reagents

2.2.1 Fine chemicals

Ethanol	Prolabors, Georgsmarienhütte, Germany
Methanol	Merck, Darmstadt, Germany
Isopropanol	Merck, Darmstadt, Germany
Acrylamid	Sigma, München, Germany
Ethidiumbromid	Roth, Karlsruhe, Germany
37% formaldehyde solution	Merck, Darmstadt, Germany
Acetic acid	Merck, Darmstadt, Germany
Ampicillin	Gibco BRL, Karlsruhe, Germany
Kanamycin	Gibco BRL, Karlsruhe, Germany
Puromycin	Gibco BRL, Karlsruhe, Germany
Zeocyn	Invitrogene, Karlsruhe, Germany
Agarose	Gibco BRL, Karlsruhe, Germany
Sephadex	Gibco BRL, Karlsruhe, Germany
Bacto™-Tryptone	Becto Dickinson, sparks, USA
Bacto™- yeast extract	Becto Dickinson, sparks, USA

Loading buffer	Promega GmbH, Germany
Penicillin/Streptomycin	PAA, Pasching, Australia
FBS (Fetal Bovine Serum)	Gibco BRL, Karlsruhe, Germany
RPMI 1640	Gibco BRL, Karlsruhe, Germany
DMSO	Sigma, München, Germany,
Phosphate Buffer Saline (PBS)	PAA, Pasching, Australia
BSA (Bovine Serum Albumin):	New England Biolab, Ipswich, MA
dNTP	Invitrogene, Karlsruhe, Germany
Dextran Blue	Fluka, Buchs, Switzerland
5M TMACL (Tetramethyl Ammonium Chloride)	Sigma, München, Germany
Tween-20	SERVA, Heidelberg, Germany
MES hydrate	Sigma, München, Germany
MES Sodium Salt	Sigma, München, Germany
R-Phycoerythrin Streptavidin	Molecular Probes
Denhardt's Solution	Sigma, München, Germany
HSDNA (Herring Sperm DNA)	Promega GmbH, Germany
Human Cot-1	Invitrogen, Karlsruhe, Germany
20X SSPE (3M NaCl, 0.2M NaH2PO4, 0.02 M EDTA)	BioWhittaker, Maine, USA
5M NaCl, RNase-free, DNase-free	Ambion, Austin, USA
5X 1st Strand Reaction MixL	Invitrogen, Karlsruhe, Germany
5X 2nd Strand Reaction Mix	Invitrogen, Karlsruhe, Germany
DTT, 0.1M	Invitrogen, Karlsruhe, Germany
Formamid	Sigma, München, Germany
Glycerol	Sigma, München, Germany
Sephadex^{TM}C50 Fine	Amersham, Uppsala, Sweden
SOC medium	Invitrogen, Karlsruhe, Germany
Tris	Roth, Karlsruhe, Germany

2.2.2 Enzymes and PCR reagents

Eco RI	New England Biolabs, Ipswich, MA
SacI	New England Biolabs, Ipswich, MA
HindIII	New England Biolabs, Ipswich, MA
AmpliTaq gold DNA polymerase	Applied Biosystem, Darmstadt, Dermany
10xPufer with $MgCl_2$	New England Biolab, Ipswich, MA
MgCl2	Applied Biosystems, Darmstadt, Dermany
SS RT	Promega GmbH, Germany
Xba I (20,000 U/mL)::	New England Biolab, Ipswich, MA
T4 DNA Ligase:	New England Biolab, Ipswich, MA
SuperScript II	Invitrogen, Karlsruhe, Germany
E. coli DNA ligase	Invitrogen, Karlsruhe, Germany
E. coli DNA Polymerase I	Invitrogen, Karlsruhe, Germany
RNase H Invitrogen	Invitrogen, Karlsruhe, Germany
T4 DNA Polymerase	Invitrogen, Karlsruhe, Germany

2.3 Kits

HiSpeed Plasmid Maxi kit (25)	Qiagen, Hilden, Germany
QIAprep Spin Miniprep kit (250)	Qiagen, Hilden, Germany
Dye Ex 2.0 Spin kit	Qiagen, Hilden, Germany
QIAquick PCR Purification kit	Qiagen, Hilden, Germany
TOP10 Chemically Competent E. coli	Invitrogen, Karlsruhe, Germany
One Shot® TOP10 *E. coli*	Invitrogen, Karlsruhe, Germany
DH5α™ Cells	Invitrogen, Karlsruhe, Germany
TOPO TA Cloning®	Invitrogen, Karlsruhe, Germany
QIAamp DNA Blood Midi Kit	Qiagen, Hilden, Germany
QIAamp RNA Blood Mini Kit	Qiagen, Hilden, Germany
H2A.X Phosphorylation Assay Kit	Upstate; Millipore, Schwalbach/Ts, Germany
REPLI-g Kit	Qiagen, Hilden, Germany
Genomiphi DNA Amplification kit	Amersham; Uppsala, Sweden
CD3 MicroBeads	Miltenyi biotec, Bergisch Gladbach,

	Germany
Humantype Chimera PCR Amplification kit	Biotype, Dresden, Germany
GeneChip® Human Mapping 10K Xba 131 Array	Affymetrtix, Germany
GeneChip® Human Mapping 10K Xba 142 Array	Affymetrix, Germany
GeneChip® Human Mapping 10K Xba 131 Kit	Affymertix, Germany
GeneChip® Human Mapping 10K Xba 142 Kit	Affymetrix, Germany
GeneChip® Human Genome U133A Array	Affymetrix, Germany
MinElute 96 UF PCR Purification Kit:	Qiagen, Hilden, Germany
Each T7-Oligo(dT) Promoter Primer Kit	Affymetrix, Germany
BioArray™ HighYield™ RNA Transcript Labeling Kit (T7)	ENZO, Farmingdale, NY
GeneChip® Sample Cleanup Module	Affymetrix, Germany
GeneChip Eukaryotic Hybridization Control Kit	Affymetrix, Germany
Power SYBR® Green PCR Master Mix	Applied Biosystem, Foster City, CA, USA
Big Dye Terminator v 3.1 cycle sequencing kit	Applied Biosystem, Foster City, CA, USA

2.4 Antibodies

Antibodies used in this work were diluted and stored according to supplier's information.

Primary antibodies

RAD51 antibody (Mouse)	GeneTex, Hiddenhausen, Germany

Secondary antibodies

Goat anti-mouse IgG/HRP	Dako Cytomation, Glostrup, Denemark
Anti-streptavidin antibody (goat), biotinylated,	Vector Laboratories, Burlingame, CA

2.5 Nucleic acids

2.5.1 Acquired plasmids

Table 2.1 An overview of the reporter plasmids used in this work.

Restriction map of the plasmids can be found in the results section (chapter 3.2.6.1).

Plasmid	Genetic markers	Description	Reference
pmHPRT-DRGFP	Amp^r	Contains DR-GFP repotrer with I-Sce I cleavage site	Generous gift of Maria Jasin, Sloan-Kettering Cancer Center (New York USA)
pCbASce	Amp^r	Contains I-Sce I endonuclease	Generous gift of Maria Jasin, Sloan-Kettering Cancer Center (New York USA)

2.5.2 Synthetic oligonucleotides

The tables above represent a list of synthetic oligonucleotides used in this work.

All oligonucleotides were purchased from TiB MolBiol (Berlin).

Table 2.2 Primer using for STR analyses to confirm LOH

Chromosome	Name	Forward primer	Reverse primer	Physical Position
Chr.1	D1S2724	TGTGAAGCCACATTTTCCAA	TGTTCTGCTTGGCACTTTTG	47353920-47354196
Chr.1	D1S2843	GGGCTGGGCATTACACAAC	ATCAAATTGGCTTCTCACCG	18756299-18756477
Chr.1	D1S2644	TGCAACCCACCTGAATGA	TACGTGAAGTGCCAGCACA	17272558-17272774
Chr.1	D1S238	TCATGTCTAGATCCTGTGCC	TGGAGGCAGTTTAGATTGTG	159380623-159380922
Chr.1	D1S1660	TGCTATCCTCTCACCAGTGA	GTCTGAAGTTCATGGGAACG	169778575-169778814
Chr.2	D2S2153	CCTCAGGGACTTGGTTTAACAG	CCTTTGGGAAATGCTGATTG	54440636-54440786
Chr.2	D2S378	TGTGGGCTGGTCAGATATTC	CGCTAGGATCACTATGTTTTGC	57039502-57039616
Chr.2	D2S2352	TCACGCTGCTGGACTC	GGGCAAAATTCGACTCATTA	53610256-53610529
Chr.2	D2S285	TGTAGAAATCACAGGGCAGG	CACCACTGCACATGGCTAAT	67384252-67384450
Chr.2	D2S139	AGCTCAAAGCAAATGCATGC	AAATTGCGAAACTGTGGCTT	79499062-79499211
Chr.2	D2S387	AGCTCACTTTTGGCCTC	TGGATCTTGGATGTTCATTC	19099786-19100000
Chr.3	D3S3695	TTGATTTTGGACTTTTCAGC	TGGCACCTGTATGTATGAGA	106495856-106496064
Chr.3	D3S3045	ACCAAATGAGACAGTGGCAT	ATGAGGACGGTTGACATCTG	104364610-104364808
Chr.3	D3S3655	GCATTCATACTATGCTAGTTGAGAG	ATAATGTTTGCCCACTGGAG	100097895-100098090

Chromosome	Name	Forward primer	Reverse primer	Physical Position
Chr.3	D3S1591	TGGAGTCTTCAGCATTTTT	TGACATCTATTTACAGATATTAACC	102700083-102700325
Chr.3	D3S2459	CTGGTTTGGGTCTGTTATGG	AGGGACTTAGAAAGATAGCAGG	100570538-100570730
Chr.6	D6S1617	TGCAAAACAGGCACACATAC	TTAATCAATTTTCTGCAAAGATAAA	4088927-4089040
Chr.6	D6S263	CTTAAGGCAAAATTCTTTTCAACAC	CTCAAAGTAAGACCATAAAATACCA	8427239-8427346
Chr.7	D7S2555	AGTTAGCCCATGCCAC	GCCAATCAGTTTCAATCTC	80200584-80200707
Chr.7	D7S513	AGTGTTTTGAAGGTTGTAGGTTAAT	ATATCTTTCAGGGGAGCAGG	11509549-11509733
Chr.7	D7S820	TGTCATAGTTTAGAACGAACTAACG	CTGAGGTATCAAAAACTCAGAGG	78397881-78398094
Chr.8	D8S1477	AGCAAACTTCATCCACTTGG	TTCCTGTCCTCTAATGTAACTTACC	30612326-30612495
Chr.8	D8S505	AGCCTGCTATTTGTAGATAATGTTT	AGTGCTAAGTCCCAGACCA	32984444-32984650
Chr.8	D8S1694	TGACCAGCACACCACTAAAT	TGCTTCAAAATTCTCATTCC	113670715-113670962
Chr.8	D8S1122	GGTGACAGAATCAGACCCTG	TGCTCAAATCTGCAATTTCA	105749182-105749310
Chr.11	D11S968	GGCTCTTGTAGTTTCTTATCTCCT	AAGGCGGATGCTGGAC	129772991-129773137
Chr.11	D11S976	TCAGTTCAAGTTGCAGAAGAA	CAACTTGGTGACAGCCTTTC	113849631-113849750
Chr.11	D11S4107	TCATTCTACAAGACTAGCATTACC	GCTTGATCATGGTGTATTATCTT	116989733-116989930
Chr.11	D11S937	CTAATAAACAAATCCCTCTACCTCC	TAGTCAGTCAGGGACCCAAGT	74152079-74152342
Chr.13	D13S279	TGGTTTGTTGCAGAAAGCACAC	TTGGGCCTTGTCAACCTTCATA	52497146-52497396
Chr.13	D13S1244	TCAACAAGTGGATTAAGAAACTGTG	CTGTTTATGGCTGAGAAGTATGC	27144977-27145072
Chr.13	D13S173	CCCTGTTCCAGTAATGATGACC	GTCTCTGGCTGCTCTCAAGACTAT	106604948-106605119
Chr.13	D13S1283	AAGTTCACAGTTTTTTAGAGAAACA	AGGTTAGGTGAGGGTTGTCT	68615741-68615916
Chr.13	D13S1254	AAATTACTTCATCTTGACGATAACA	CTATTGGGGACTGCAGAGAG	26416434-26416657
Chr.19	D19S425	CCACAGGTGTGCATAAAAG	GCCATGTGACTGTAGCAGA	32002284-32002550
Chr.19	D19S571	ATTGAGCCACTGAACTCCA	TTAGCCAAACTTGACAGCA	49625061-49625282
Chr.20	D20S471	GGGATGCAGAAATTGCAGTA	TTTTCTCTTTGCCACTGACC	19779543-19779862
Chr.20	D20S170	TTCTCAGGCTCCTGGC	GGGGGCTTCCATGAGT	37052492-37052735
Chr.20	D20S107	CTACATGATGCCTCTTGGGA	TCAGACAATGGCAAATTCCT	35593077-35593344
Chr.20	D20S910	AATGATGGAAATAATTCATGTCA	CTCTCCACATTGTCGGAT	15097071-15097159
Chr.20	D20S871	GTGAGCCGAGATTATGCC	TGCACACTAGAATCCCTTGG	23283573-23283756
Chr.21	D21S265	TTAAAGCAATCAATCATGG	GGGTTCTGTGAATATGGG	12102891-12103141
Chr.21	D21S1909	CTGTGATTGTGTTTTCCATTTAGCA	TTCCACACTGAGTCAAGAGCAGG	17716281-17716520
Chr.21	D21S2055	AACAGAACCAATAGGCTATCTATC	TACAGTAAATCACTTGGTAGGAGA	26388901-26389065
Chr.22	D22S446	CCGGAACTTTGGAAGG	CCACTTGGGTAACCACTG	20349158-20349359
Chr.22	D22S1169	GCACACACATGCACATAATC	AACAACTTCCAGCAGACG	32346136-32346259

Table 2.3 Primer using for measurment of the expression level of RAD51.

Name	Forward primer	Reverse primer
Rad51-s	GAGGTGAAGGAAAGGCCATGT	
Rad51-as		GGGTCTGGTGGTCTGTGTTGA

Table 2.4 Primer using for detection of HR, NHR and SSA.

Name	Forward primer	Reverse primer	Dye	Description
HPRTGFP_1	TTCAGATCCGCCGCCACTAT		BoTMR	Fragment in the mutated GFP region
HPRTGFP_2		TTGCCGTAGGTATTACCCTGTTAT	Fam	Fragment in the intact GFP region
HPRTGFP_3	CTCTCCTGACTACTCCCAGT			
HPRTGFP_4		AGGTGGCATCGCCCTCG	Hex	
HPRT-NHR		TCGTGCTGCTTCATGTGGTC		Primer for the detection of NHR
HPRT-SSA-F1	CTCCTGGGCAACGTGCTGGTT		Fam	
HPRT-SSA-R2		GCTATGACCATGATTACGCCAAGC		Primer for the detection of SSA
SSA_R		TGACCATGATTACGCCAAGC		

2.6 Patients

146 newly diagnosed *de novo* AML cases with normal karyotype, the majority of patients treated according to the AML-96 Deutsche Studieninitiative Leukämie protocol (DSIL).

2.7 Cell lines

MV_{4-11} - AML M5 isolated from Patient 10-year-old male;

Karyotype: 48(46-48)<2n>XY, +8, +18, +19, -21, t(4;11)(q21;q23);

Specifics: t(4;11)(q21;q23); *MLL-AF4* fusion gene;

Gene alteration: FLT3 ITD (homozygous)

Molm13 - MDS (RAEB) → AML M5a isolated from 20-year-old male

Karyotype: hyperdiploid with 4% polyploidy; 51(48-52)<2n>XY, +8, +8, +8, +13, del(8)(p1?p2?),ins(11;9)(q23;p22p23)

Specifics: ins(11;9)(q23;p22p23); *MLL-AF9* fusion gene (2 different transcripts)

Gene alteration: *FLT3* ITD (hererozygoty), *P15INK4B* deletion, *P16INK4A* deletion

K562 - CML isolated from 53-year-old female

Karyotype: 61-68<3n>XX, -X, -3, +7, -13, -18, +3mar, del(9)(p11/13), der(14)t(14;?)(p11;?), der(17)t(17;?)(p11/13;?), der(?18)t(15;?18)(q21;?q12), del(X)(p22)

Specifics: Ph+ t(9;22)(q34;q11); *BCR-ABL1* b3-a2 fusion gene

Gene alteration*: ABL* amplification, *P15INK4B* deletion, *P16INK4A* deletion, *P53* mutation

THP1 - AML M5 isolated from 1-year-old male

***Karyotype**:* 94(88-96)<4n>XY/XXY, -Y, +1, +3, +6, +6, -8, -13, -19, -22, -22, +2mar, add(1)(p11), del(1)(q42.2), i(2q), del(6)(p21)x2-4, i(7p), der(9)t(9;11)(p22;q23)i(9) (p10)x2, der(11)t(9;11)(p22; q23)x2, add(12)(q24)x1-2, der(13)t(8;13)(p11;p12), add(?18)(q21)

***Specifics**:* t(9;11)(p21;q23); *MLL-AF9* fusion gene

***Gene alteration**: NRAS* mutation, *P15INK4B* deletion, *P16INK4A* deletion, *P53* mutation, *RB1* rearrangement

2.8 Growth media

All media for cultivation of microorganisms were prepared as described below. For solid media, agar was added to the final concentration of 20 g/l.

LB medium (Luria-Bertani medium)

	Final concentration
Pepton	1 % (w/v)
Yeast extract	0.5 % (w/v)
NaCl	1 % (w/v)

Complete media for the cellculture

	Final concentration
RPMI-1640	
FCS (Fetal Bovine Serum)	10%
Penicillin/Streptomycin	1%

2.9 Cell sorting of CD3 (T-cells) and CD33; CD34 and CD117 (Blasts)

Max puffer: 500ml PBS
16ml 20% Albumine
55ml Citrate Solution

The frozen cells (–80^{0}C) were warmed briefly and carefully added to 10ml Max. Buffer, followed by centrifugation at 300xg for 10 min. The cells were resuspended in a buffer and magnetically labelled with 20 µl CD3 MicroBeads. Then the cell suspension was loaded onto a MACS® Column which was placed in the magnetic field of a MACS Separator. The magnetically labelled CD3+ cells were retained on the column. The unlabeled cells were run through and this cell fraction was depleted of CD3+ cells. After removal of the column from the magnetic field, the magnetically retained CD3+ cells could be eluted as the positive cells. Additionally the eluted CD3+ cells were stained with CD4, CD8, CD3 and sorted by Facs. The remaining fraction with the cells without CD3+ was stained with CD34FITC, 33PE and 117 PC5 dyes, and the cell fraction CD33, CD34 and CD117 were isolated.

2.10 DNA-techniques

2.10.1 DNA isolation, using QIAamp DNA Blood Midi Kit (Qiagen)

The cell suspension (1x10^7) was centrifuged and the pellet was mixed with 180 µl of Buffer ATL. 20 µl Proteinase K, were added and mixed by vortexing followed by incubation at 56°C for 10 min. Briefly the 1.5 ml microcentrifuge tube was centrifuged to remove drops from the inside of the lid. 200 µl Buffer AL were added to the sample, and mixed by pulse-vortexing for 15 sec., and incubated at 70°C for 10 min. Briefly the 1.5 ml microcentrifuge tube was centrifuged. 200 µl ethanol (96–100%) were add to the sample, and mixed for 15 sec. After mixing, briefly the 1.5 ml microcentrifuge tube was centrifuged. The mixture was transferred to the QIAamp spin column (in a 2 ml collection tube) and centrifuged at 6000 x *g* (8000 rpm) for 1 min. The QIAamp spin column was place in a clean 2 ml collection tube. 500 µl Buffer AW1 was added followed by centrifugation at 6000 x *g* (8000 rpm) for 1 min. The QIAamp spin column was placed in a clean 2 ml collection tube. 500 µl Buffer AW2 was added and centrifuged at full speed (20,000 x *g*; 14,000 rpm) for 3 min. The QIAamp spin column was placed in a clean 1,5 ml collection tube and 30-50 µl prewarmed TE buffer was pipetted directly to the QIAamp spin column followed by centrifugation at 8000 xg for 1 min.

2.10.2 Whole genome preamplification

2.10.2.1 REPLI-g Kit (Qiagen)

Solution A: 0.4 ml 5M KOH; 0,1 ml 0,5M EDTA pH 8.0 and 5,5 ml H_2O

Denaturation solution: 5 µl solution A and 35 µl H_2O

Neutralisation Solution: 3 µl solution B(Kit) and 27 µl H_2O

2.5 µl Denat. solution was added to 2,5 µl DNA (5-10 ng) and incubated for 3 min at RT. The reaction was stopped with 5 µl Neutral solution. Next, a mix – 27 µl H_2O; 12,5 µl 4xMix; 2,75 µl DNA-polymerase - was added to each reaction and incubated at 30^0C for 16h and at 65^0C for 3 min.

2.10.2.3 GenomiPhi DNA Amplification (Amersham)

To be amplified 1 µl of a template (5-10 ng) is added to 9 µl of sample buffer and is heated to 95^0C for 3 min to denature the template DNA. The sample is cooled and mixed with 9 µl of reaction buffer and 1 µl of enzyme mix, and incubated at 30^0C overnight (16-18h). After amplification, Phi29 DNA polymerase is heat-inactivated during a 10 min incubation at 65^0C

2.10.3 PCR assays for monitoring of chimerism by STR analyses

STR analysis refers to 'short tandem repeat.' This type of DNA analysis works to examine individual areas in DNA. The differences for certain DNA regions in one person versus another can allow for distinguishing between individuals. Despite the fact that humans share the overwhelming majority of the same DNA, the tiny fraction of a percent that varies can be exploited to create a profile of the individual.

The method is based on amplification with one reaction of twelve highly polymorphic autosomal loci and the sex specific Amelogenin- Locus. One of the two corresponding primers is labelled with fluorescence dye: 6-FAM, Hex or NED.

The recommended amount of DNA is 0.2-2.0 ng. Additionally: 5 µl Reactionmix D (kit); 2.5 µl Primermix (kit); 0.4 µl TaqDNA Polymerase (hot start, 2.5 U/µl) and to 25µl volum Nuclease free water were added.

The following cycling conditions were generally used:

Initial denaturation		95℃, 4 min
35 cycles	*Denaturation*	95℃, 30 sec
	Annealing	60℃, 120 sec
	Elongation	72℃, 30 sec
Final elongation		*68℃, 60 min*

The electrophorese was done using ABI PRISM *3130XL Genetic* Analyzer (Applied Biosystems, Darmstadt, Germany), or ABI 377.

2.10.4 Amplification of DNA by PCR

Polymerase Chain Reaction (PCR) is a general method to amplify in vitro a specific nucleotide sequence from a matrix molecule, called template. In this work, PCR amplification was used to obtain specific DNA fragments from human. Generally AmpliTaq gold DNA polymerase was used (*see 2.2.2*).

Components of a typical PCR reaction were as follows:

- DNA template (5-30 ng)
- downstream and upstream primers (both 30 pmol)
- dNTPs mix (dATP, dCTP, dGTP and dTTP in the final concentration of 800 µM) -
- 10 x reaction buffer with $MgCl_2$ (in the final concentration of 1x)
- 2 U of the DNA polymerase

The following cycling conditions were generally used:

Initial denaturation		*95 ℃, 11 min*
30-35 cycles	*Denaturation*	*94 ℃, 30 sec*
	Annealing	*Tm - 6 ℃, 30 sec – 2 min*
	Elongation	*72 ℃, 30sec*
Final elongation		*60 ℃, 45 min*

Melting temperature of the primers was determined from the following equation:
Tm = 63.9 + 0.42 (G + C) – 650/n, where *Tm* is a melting temperature, in ºC, *(G + C)* – a GC content of the primer, and *n* – a primer length. The composition of reaction

mix and cycling conditions were slightly modified depending on the expected product length as well as enzyme and template used. PCR products were then purified by means of QIAquick PCR Purification kit (*see 2.2.3*) in accordance with manufacture's instructions and if necessary sequenced as described below *(see 2.10.11)*.

2.10.5 Agarose gel electrophoresis

Solutions:

50 x TAE buffer : 242 g Tris base
57.1 ml glacial acetic acid
100 ml 0.5 M EDTA (pH 8.0)

EB-stock solution: 10 mg/ml

6 x gel-loading buffer: 10 mM Tris-HCl (pH 7.6)
60 % (v/v) glycerol
60 mM EDTA (pH 8.0)
0.03 % bromphenol blue

For visualisation and separation of DNA fragments, a standard horizontal agarose gel electrophoresis was used. The electrophoresis was performed in 1 x TAE buffer at 8-10 V/cm at room temperature. Gel percentage was determined according to the size range of the DNA fragments and was typically 1.5-3% (w/v) of agarose. Ethidium bromide was added to gels to the final concentration of 0.4 µg/ml. The DNA samples were mixed with 1/4 volume of 6 x gel-loading buffer and loaded into the sample wells. After electrophoresis, the EB-DNA complexes were visualized directly under UV light.

2.10.6 Cloning of DNA fragments

Fresh PCR product (0.5 to 4 µl) was mixed with upto 5 µl water and 1 µl Topo vector to a final volume of 6 µl and incubated for 5 min at room temperature. The TOPO® Cloning reaction could be stored at -20°C overnight or immediately used for to the transformation of competent cells

2.10.7 Transformation of competent E. coli

The cells were thawed on ice and 100µl of the cells were transferred to a 2 ml collection tube. After that 1-50ng DNA (0.1-5 µl) was added. The mix was incubated

on ice for 30min and then for 30 sec in a 42℃ water bath. The vial(s) was placed on ice for 2 min. After the addition of 900 µl of S.O.C medium to each vial, (sterile techniques must be practised to avoid contamination) the tubes were incubated at 37^0C for one hour at 225 rpm in a shaking incubator. After incubation 150 µl of the cells were spread on a LB plate with appropriate antibiotics and the plates were incubated at 37℃ overnight. The remaining transformation mix could be stored at +4℃ and plated out the next day, if desired. Selected colonies were analysed by plasmid isolation, PCR, or sequencing.

2.10.8 Mini-preparation

(QIAprep Spin Miniprep Kit Protocol)

This protocol was designed for purification of up to 20µl of high-copy plasmid DNA from 2-5 ml overnight cultures of E. coli in LB (Luria-Bretani) medium. Pelleted bacterial cells were resuspended in 250µl of Buffer P1 and transferred to a microfuge tube. 250 µl of Buffer P2 was added. 350 µl of Buffer N3 was added and tubes were centrifuged for 10 min. The supernatants were applied to the QIAprep column by pipetting and centrifuged for 30 sec. QIAprep spin column was washed by adding 0.75 ml of Buffer PE and centrifuged for 30 sec and then for an additional 1 min to remove residual wash buffer. Further QIAprep spin column was placed in a clean 1.5-ml microfuge tube. To elute DNA, 50µl of dH_20 was added and centrifuged for 1 min. EB (10mM Tris-Cl, pH 8.5)

2.10.9 Maxi-preparation

(using the HiSpeed® Plasmid Purification Handbook)

A single colony was picked from a freshly streaked selective plate and incubated first in 2-5 ml LB medium containing the appropriate selective antibiotic for 8 hours at 37^0C at 225 rpm in a shaking incubator and then in 250 ml for an additional 12-16 hours at 37^0C with vigorous shaking (225rpm). After that the bacterial cells were harvested by centrifugation at 6000xg for 15 min at 4℃ and resuspended in 10 ml Buffer P1. Then 10 ml Buffer P2 was added and incubated at room temperature for 5 min. After that 10 ml of chilled Buffer P3 was added to the lysate and the whole mix was poured into the barrel of the QIAfilter Maxi Cartridge and filtrated into the HiSpeed Maxi Tip after the equalibrated by applying 10 ml Buffer QBT. The HiSpeed Maxi Tip was washed with 60 ml QC buffer and the DNA elution was performed with

15 ml Buffer QF. The DNA was precipitated by adding 10.5 ml room-temperature isopropanol and bound to QIAGEN membrane. DNA was washed with room-temperature 70% ethanol and eluted with 1ml dH_20.

2.10.10 Digestion of DNA with restriction endonucleases

Restriction enzyme digestions were generally performed by incubating of DNA molecules with an appropriate amount of a restriction enzyme under proper conditions. For analytical digestion, 500 ng of DNA were mixed with 2 U of enzyme and a corresponding buffer in a volume of 20 µl and incubated at 37 ºC for 2 h. Digestion of plasmid DNA (40 µg) was carried out in a volume of 40-60 µl overnight with 40-50U of enzyme. In the case of double digestion with two different endonucleases, a buffer providing a maximal activity for both enzymes was selected.

2.10.11 DNA sequencing

DNA sequencing was performed by the modified dideoxy-mediated chain termination method (Sanger *et al.*, 1977). For sequencing reactions, the Big Dye Terminator v 3.1 cycle sequencing kit from Applied Biosystem (Foster City, CA, USA) (*see 2.2.3*) was used as described by the manufacturer. 100-200ng DNA were mixed with 7 µl primer (0,47 µM) and 2 µl Big Dye Terminator v3.1 sequencing buffer. The following PCR conditions were performed:

35 cycles	95 ℃, 10 sec
	55 ℃, 5 sec
	60 ℃, 4 sec

The sample were purified using centrifugation at 730 x g for 2min. through 600 µl Sephadex G50 (2.4 g diluted in 28.8 ml aqua dest).
Sequencing itself was done with ABI PRISM *3130X Genetic* Analyzer Applied Biosystems, Darmstadt, Germany *(see 2.1)*.

2.11 HG 10K SNPArrays Hybridization

2.11.1 Buffers

12 X MES Stock
For 1000 mL:
- MES Hydrate - 70.4 g
- MES Sodium Salt - 193.3 g
- Molecular Biology Grade water - 800 ml

Mix and adjust volume to 1,000 mL.
The pH should be between 6.5 and 6.7.
Filter through a 0.2 µM filter.

Wash A: Non-Stringent Wash Buffer
For 1000 ml:
- 20X SSPE - 300 ml
- 10% Tween-20 – 1.0 ml
- water - 699 ml

Filter through a 0.2 µm filter.
Store at room temperature.

Wash B: Stringent Wash Buffer
For 1000 mL:
- 20X SSPE - 30 ml
- 10% Tween-20 – 1.0 ml
- water - 969 ml

Filter through a 0.2 µm filter.
Store at room temperature.

1X Array Holding Buffer
For 100 mL:
- 12X MES Stock Buffer - 8.3 ml
- 5M NaCl - 18.5 ml
- 10% Tween-20 – 0.1 ml
- water - 73.1 ml

Store at 2℃ to 8℃, and shield from light

Stain Buffer for HG 131 Xbal
For 3 stains:
- SSPE – 450 µl
- Tween 20 (3%) – 5 µl
- Denhardt´s (50) – 30 µl

Stain Buffer for HG 142 Xbal
For 2 stains
- H_2O - 666.7 µl
- SSPE (20X) - 300 µl
- Tween-20 (3%) - 3.3 µl
- Denhardt's (50X) – 20 µl

2.11.2 Digestion and ligation procedure

To digest the DNA, follow mix was prepared: NE buffer 2 (10X) 2 µL; BSA (10X (1 mg/mL)) 2 µL and Xba I (20 U/µL) 0.5 µL 250 µg DNA and H_2O to 20 µl and incubated at 37ºC for 120 minutes and at 70ºC for 20 minutes. Than to the digested DNA was added Adaptor Xba (5 µM) 1.25 µL; T4 DNA Ligase buffer (10X) 2.5 µL and T4 DNA Ligase 1.25 µL to a total volume of 25 µl and incubated at 16ºC - 120 minutes and at 70ºC - 20 minutes.

2.11.3 PCR reaction

To the ligated DNA (25 µl) was added 75 µL dH_2O and afterwards PCR MM was prepared: PCR buffer (10X) 10 µL; dNTP (2.5 mM each) 10 µL; $MgCl_2$ (25 mM) 10 µL; PCR Primer Xba (10 µM) 7.5 µL; AmpliTaq Gold® (5 U/µL) 2 µL; H2O 50.5 µL.

To this MM (90 µl) 10 µl from the diluted ligated DNA was added. From each probe 4 PCR reactions were prepared. The following cycle was chosen:

Initial denaturation		95°C, 3 min
35 cycles	*Denaturation*	95°C, 30 sec
	Annealing	59°C, 30 sec
	Elongation	72°C, 30 sec
Final elongation		72°C, 7 min

The reaction was controlled by Gel electrophoresis: 3 µL of each PCR product were mixed with 3 µL 2X Gel Loading Dye and run on 2% TBE gel at 120V for 1 hour.

2.11.4 PCR Purification Fragmentation and Labelling

The PCR product was cleaned using the MinElute 96 UF PCR Purification Kit (Qiagen, Hilden, Germany). The cleaning procedure is described in the Mapping 10K 2.0 Assay Manual. The purified DNA was eluted with 40 µl EB buffer.Purified PCR product (20 µg in EB buffer) 45 µL was mixed with 5 µL 10X Fragmentation Buffer to a total volume 50 µL. The following MM was prepared: Fragmentation Reagent 3 µL; 10X Fragmentation Buffer 12.5 µL and H2O 109.5 µL. 5 µl from this MM was mixed with 50 µL Fragmentation Mix and incubated at 37ºC for 30 minutes and at 95ºC for 15 minutes. The fragmentation was controlled by Gel electrophoresis: 4 µL of fragmented PCR product was mixed with 4 µL gel loading dye and run on 4% TBE gel at 120V for 30 minutes to 1 hour.

To label the fragmented DNA: 5X TdT Buffer 14 µL; GeneChip DNA Labeling Reagent (5 mM) 2 µL was added; and TdT (30 U/µL) 3.4 µL and incubated at 37ºC for 2 hours and at 95ºC for 15 minutes

2.11.5 Hybridization, Wash and Stain procedures

The hybridization wash and stain procedures were performed as described in genetic Mapping 10K 2.0 Assay Manual. The hybridization mix also contains control nucleotides. After the hybridization of the Arrays at 48°C for 16 to 18 hours at 60 rpm, they were stained with Streptavidin phycoerythrin conjugat and finally washed. The scanning procedure was performed using *GeneChip Scanner 3000.*

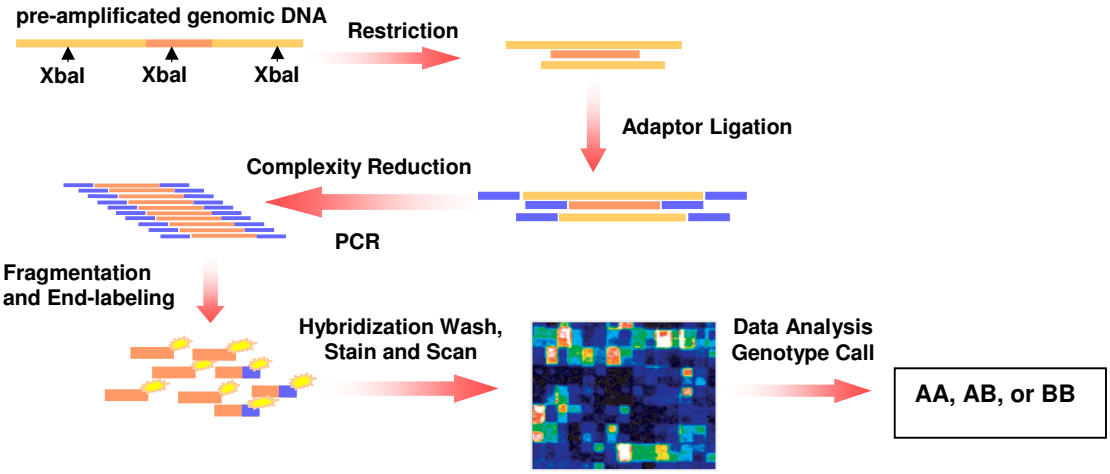

Fig.2.1 GeneChip Mapping Assay

2.12 RNA-techniques

2.12.1 RNA isolation, using QIAamp RNA Blood Mini Kit (Qiagen)

The cell suspension ($1x10^7$) was centrifuged and the pellet was mixed with 200 µl EL buffer followed by centrifugation for 10 min at 400 x*g* and 4 °C. 350 µl Buffer RTL were added and the suspension was mixed by vortex. The mixture was transferred to the QIAshredder spin column (in a 2 ml collection tube) and centrifuged at maximum speed for 2 min. The QIAshredder spin column was removed and to the mixture 350µl 70% ethanol were added. The mixture were transferred to the QIAamp spin column (in a 2 ml collection tube) and centrifuged for 15 sec. at ≥ 8000 xg. The QIAamp spin column was placed in a clean 2 ml collection tube. 700 µl Buffer RW1 were added followed by centrifugation at 8000 xg for 15 sec. The QIAamp spin column was placed in a clean 2 ml collection tube. 500 µl Buffer RPE were added followed by centrifugation at 8000 x g for 15sec. 500 µl RPE Buffer were added again and centrifuged at max speed for 3min. The QIAamp spin column was placed in a clean 1,5 ml collection tube and 30-50 µl RNAse free water were pipetted directly to the QIAamp spin column followed by centrifugation at 8000 x g for 1 min.

2.12.2 Reverse transcription RNA to cDNA and Real Time quantitative PCR

The following mix was prepared: 1.5 µl dNTP (25 µM), 4.0 µl 5xRT Puffer, 1 µl $pd(N)_6$ and added to 1 µg RNA followed by incubation of 65^0C for 10 min. After the

incubation of ice for 10 min. 1 µl RNAse Inhibitor and 1 µl Superskript (Promega) were added and incubated at 37 ^{0}C for 2h followed by incubation of 90^{0}C for 10 min. cDNA is stored at –20^{0}C.

The Real Time quantitative PCR reaction was performed using the Power SYBR® Green PCR Master Mix and Real Time quantitative PCR protocol from Applied Biosystem. 25 µl Master Mix (kit) and 0.5-3 µl primer were added to 1 µl of the cDNA and diluted to 50 µl with aqua dest. The following PCR condition were performed:

HOLD	*95 ℃, 10 min*
40 cycles	*94 ℃, 15 sec*
	60 ℃, 1 min

2.12.3 RNA Precipitation

For concentration of RNA samples, a standard procedure of alcohol precipitation was used. 1/10 volume 3M NaOAc, pH 5.2, and 2.5 volumes 100% ethanol were added to the RNA sample and incubated at -20℃ for at least 1 hour. After centrifugation at ≥ 12,000 x g in a microcentrifuge for 20 minutes at 4℃, the RNA pellet was washed with cold 80 % ethanol solution, followed by air drying and dissolved in DEPC-treated H_2O.

2.13. Gene expression procedure using GeneChip® Human Genome U133A arrays from Affymetrix

For One-Cycle Eukaryotic Target Labelling Assay experimental outline total RNA (1 µg to 15 µg) is first reverse transcribed using a T7-Oligo(dT) Promoter Primer in the first-strand cDNA synthesis reaction. Following RNase H-mediated second-strand cDNA synthesis, the double-stranded cDNA is purified and serves as a template in the subsequent *in vitro* transcription (IVT) reaction. The IVT reaction is carried out in the presence of T7 RNA Polymerase and a biotinylated nucleotide analog/ribonucleotide mix for complementary RNA (cRNA) amplification and biotin labelling. The biotinylated cRNA targets are then cleaned up, fragmented, and hybridized to GeneChip expression arrays.

2.13.1 Buffers

12 X MES Stock
For 1000 mL:
MES Hydrate – 64.61 g
MES Sodium Salt - 193.3 g
Molecular Biology Grade water - 800 ml
Mix and adjust volume to 1,000 mL.
The pH should be between 6.5 and 6.7.
Filter through a 0.2 µM filter.

Wash A: Non-Stringent Wash Buffer
For 1000 ml:
20X SSPE - 300 ml
10% Tween-20 – 1.0 ml
water - 699 ml
Filter through a 0.2 µm filter.
Store at room temperature.

Wash B: Stringent Wash Buffer
For 1000 mL:
12x MES Stok Buffer – 83.3ml
5M NaCl – 5.2ml
20X SSPE - 30 ml
10% Tween-20 – 1.0 ml
water – 910.5 ml
Filter through a 0.2 µm filter.
Store at room temperature.

2X Hybridization Buffer
For 50 mL:
12X MES Stock Buffer - 8.3 mL
5M NaCl - 17.7 mL
0.5M EDTA - 4.0 mL
10% Tween-20- 0.1 mL
water - 19.9 mL
Store at 2℃ to 8℃, and shield from light

2X Stain Buffer
For 250 mL
12X MES Stock Buffer - 41.7 ml
5M NaCl - 92.5 ml
10% Tween-20 - 2.5 ml
water - 113.3 ml
Filter through a 0.2 µm filter
Store at 2℃ to 8℃ and shield from light

SAPE –Solution mix
For 2 stains
2X Stain Buffer 600.0 µL
50 mg/mL BSA 48.0 µL
1 mg/mL Streptavidin Phycoerythrin 12.0 µL
DI H20 - 540.0 µL
Total Volume 1200 µL

Antibody Solution mix
For 1 stain
2X Stain Buffer 300.0 µL
50 mg/mL BSA 24.0 µL
10 mg/mL Goat IgG Stock 6.0 µL
0.5 mg/mL biotinylated antibody 3.6 µL
DI H20 266.4 µL
Total Volume 600 µL

2.13.2 The first strand synthesis

RNA should be of good quality.

First 5-8 µg RNA was mixed with 2 µl T7-dT24-Primer (50 pmol/µl) and to a final volume of 20 µl dH_2O and incubated at 70^0C for 10 min. 4 µl 5xFirst strand cDNA buffer, 2 µl 0.1M DTT and 1 µl 10 mM dNTP were added and incubated for 2 min at

42 ^{0}C. Then 1 µl Super Script II RT (200 U/µl) was added and incubated for 1 hour at 42 ^{0}C.

2.13.3 Second strand reaction

The following mix was be prepare and added to the first strand reaction:
91 µl Water-DEPC treated, 30 µl 5x 2th Strand Reaction Buffer, 3 µl 10 mM dNTP mix, 1 µl 10 U/µl E. coli DNA Ligase, 4 µl 10 U/µl E. coli DNA Polymerase I and 1 µl 2U/µl E. coli Rnase H.
The mix was incubated for 2 hours at 16 ^{0}C. Than 2 µl 10 U T4 Polymerase was added followed by incubation for 5 min at 16 ^{0}C and the reaction was stopped with 10µl 0.5M EDTA.

2.13.4 Cleanup of double – stranded cDNA

To the double – stranded cDNA was added 600 µl cDNA binding buffer and then this mixture was applied to the spin column and centrifuged for 1 min at 8000 xg. The spin column was washed with 750 µl cDNA wash buffer and centrifuged 1 min at 8000xg. The spin column was dried for 5 min at max speed and the cDNA was eluted with 14 µl cDNA Elution buffer.

2.13.5 Synthesis of biotin – labelled cDNA

the following Master mix was added to the cleaning cDNA. :

Water	10 µl
10 HY reaction buffer (vial 1)	4 µl
10x Biotin labelled Ribonucleotides (vial 2)	4 µl
10x DTT (vial 3)	4 µl
10x Rnase Inhibitor Mix (vial 4)	4 µl
20x T7 RNA Polymerase (vial 5)	2 µl

12 µl Template cDNA was added and incubated at 37^{0}C for 5 hours

2.13.6 Cleanup of biotin – labelled cRNA

60 µl Rnase – free water were added to the cRNA, 350 µl IVT cRNA binding Buffer and 250 µl ethanol (100%). The samples was applied to the IVT cRNA Cleanup Spin Column, and was centrifuged for 15 sec at 8000 xg. The Spin Column was washed with cRNA Wash Buffer (15 sec at 8000 xg). 500 µl 80% ethanol was added,

centrifuged by 8000 xg and the membrane was dried for 5 min at max speed. The cRNA was eluted with 30 µl RNAse free water.

2.13.7 Quantification from the IVT Product

Adjusted cRNA yield = RNAm – (total RNA_i) (y)

RNA_m = amount of cRNA measured after IVT (µg)

Y = Fraction of cDNA reaction used in ITV

2.13.8 Fragmenting the cRNA for Target Preparation

The following mix: 20 µg cDNA, 8 µl 5x Fragmentation Buffer and water to 40 µl was incubated for 35 min at 94^0C.

2.13.9 Hybridization, Wash and Stain procedures

The hybridization, wash and stain procedures were performed as described in GeneChip® Expression Analysis Technical Manual. The hybridization mix also contains different control oligonucleotides. After the hybridized of the Arrays at 45^0C for 16 hours at 60 rpm, they were stained with Streptavidin phycoerythrin conjugate and finally washed. The scanning procedure was performed using *GeneChip Scanner 3000.*

2.14 Cell culture methods

2.14.1 Cell culture techniques

The mammalian cells, which were used in this work, were grown in suspension in plastic flasks. The plastic was obtained in sterile wraps from commercial suppliers and is specially prepared for use in cell culture. All these tissue culture flasks have caps with filters which permit gaseous exchange, allowing maintenance of correct pH (which is monitored by the colour of the phenol red present in the medium) and the right percentage of CO_2 (5%). The optimal atmosphere conditions are maintained by a CO_2 incubator, which automatically controls temperature and pCO_2. The incubator temperatures are set at 37°C and regularly checked. The relative humidity was ~ 95%. The use of plastic pipettes and special medium (very low endotoxin) was necessary to work in endotoxin-free conditions. The cell lines used in this project

were acquired from DSMZ - the German Collection of Microorganisms and Cell Cultures (Braunschweg, Germany). The cells were seeded every 3 days in fresh medium with $1x10^6$ cell/ml density. When necessary zeocin in a concentration of 4mg/ml was added.

2.14.2 Cell quantification and evaluation of viability

An efficient way of counting cells and at same time evaluating the percentage of viable cells is the technique of "dye exclusion". This test is based on the concept that viable cells do not absorb some dyes, whereas dead cells are permeable to these dyes. Trypan blue is the most commonly used dye, but has the disadvantage of staining soluble proteins. In the cell culture however some situations such as recent trypsinization and freezing and thawing in the presence of dymethylsulphoxide (DMSO) may lead to membrane leakness. From each suspension cell an aliquot of 10 µl was harvested, mixed with 10 µl of Tryplan Blue (ratio cells:trypan blue=1:1) and counted on a counting slide under the microscope. The mean of at least three counts of viable cells (not stained with trypan blue) pro quadrant was calculated and multiplied to the magnitude (10^4) and the dilution factor.
Cell quantification was also done using XE –2100 Sorter (Sysmex). The Cells in RPMI medium were measured directly.

2.14.3 Storage of cells

In order to minimise the cellular injury induced by freezing and thawing procedures (intracellular ice crystals and osmotic effects), a cryoprotective agents such as dimethyl sulphoxide (DMSO) were added. A variable number of suspension cells between 2-10 x 10^6 were spun down and resuspended in a 500 µl freezing medium (10% DMSO, 20% fetal calf serum amd 20% RPMI medium).
The cell culture freezing medium was thawed and mixed well by a gently swirling bottle. The medium could be kept on ice during use. Before to be frozen the cells should be in late log phase growth. While short-term preservation of cell lines using mechanical freezers (-80°C) is possible, storage in liquid nitrogen (-196°C) or its vapour (-120°C) is much preferred. Rapid thawing of cell suspension is essential for optimal recovery.

2.14.4 Determining of Cell Drug Sensitivity

In this project **pmHPRT-DRGFP** vector with selective drug puromycin was used. It was necessary to determine for each cell line what level of drug selection will kill nonresistant cells. 500 000 cell/ml were seeded in a fresh medium and puromycin with a final concentration of 0, 0.5, 1, 1.7, 2.8, 3.5 µg/ml was added. The cells were incubated at 37^0C in a humidified incubator with 5% CO_2 for 5 days. The minimal concentration of puromycin that was necessary to kill all the cells was applied Table 2.5.

Table 2.5 The minimal concentration of puromycin needed to kill all nonresistent cells.

Cell lines	Puromycin µg/ml
MV_{4-11}	1.7
Molm13	1.7
K562	2.8
THP1	2.8

2.14.5 Transfection of the cells

2-4x10^7 Cells in the log phase were washed and resuspended in 300 µl of PBS or RPMI without phenol red. 40 µg of the plasmid DNA were added and mixed by pipetting up and down. Than the cell suspension was added to a 0.4 sm. electroporation cuvet and incubated for 10 min on ice. The DNA/cell suspension was electroporated with appropriate voltage and capacitance. The mixture was left for 10-15 min at room temperature and then resuspended in 10 ml RPMI medium (1% P/S and 10% FCS) prewarmed to 37^0C.

2.15 Chemiluminescence Detection of H2A.X Phosphorylation

2.15.1 Buffers:

1X TBS:
50ml 20X TBS with 950ml sterile water were mixed to create a
working solution of 1X TBS. Store at room temperature.

1X TBS/T (Wash Buffer):
1.5ml 20% Tween®-20 (v/v) was deluded in 600ml 1X TBS to create a working solution of 1XTBS with 0.05% Tween®-20 (v/v). Store at room temperature.

Blocking Buffer:
12 ml 10% BSA were diluted in 28 ml of 1X TBS to make a working solution of 3% BSA in TBS. This solution is stable for several days at 4°C.

1% Formaldehyde in TBS:
405.5µl 37% formaldehyde solution (formalin) was diluted in 15ml 1X TBS. This solution must be prepared fresh.

95% EtOH/5% Acetic Acid:
750µl acetic acid was diluted in 14.25ml of ethanol. This solution must be prepared fresh.

Primary Antibody Solution:
75µl anti-phospho histone H2A.X was diluted in 10ml Blocking Buffer. Store at 4°C.

Detection Antibody Solution:
10µl Goat Anti-Mouse HRP was diluted in 10ml Blocking Buffer. Store at 4°C.

2.15.2 Fixing Cells to 96-Well Cell Culture Plates

The media from the wells was aspirated and approximately 10µl of media were left. 125µl/well of 95% EtOH 5% acetic acid fixing agent was added Immediately and incubated for 7 minutes at room temperature. The fixing agent from the wells was removed and the plate was tapped gently onto absorbent paper to remove any excess fixing agent still within the wells. 150µl/well of 1% formaldehyde in TBS was added and incubated for 5 minutes at room temperature. Formaldehyde solution from the wells was removed and the plate was tapped gently onto absorbent paper to remove any excess liquid. 150µl/well Wash Buffer (1X TBS/T) was added and incubated for 1 minute at room temperature. The wash buffer was removed and the plate was once again tapped gently onto absorbent paper. 150µl/well Blocking Agent (3% BSA in TBS) was added and incubated for 1 hour at 37℃ or overnight at 4℃.

2.15.3 Addition of Primary and Secondary Antibodies

The blocking agent was removed and the wells were rinsed once with 300µl/well of Wash Buffer. The Wash Buffer was removed and the plate was tapped gently onto absorbent paper. 100 µl/well of Primary Antibody Solution was added and incubated for 1 hour at 37℃. After the incubation the Primary Antibody were removed and the wells were rinsed once with 300 µl/well of Wash Buffer. After that the Wash Buffer was removed and the plate was taped gently onto absorbent paper. The cells were washed 3-5 times with 150 µl/well Wash Buffer for ~3 minutes each with gentle agitation. 100 µl/well of the Detection Antibody were added and incubated for 1 hour at room temperature.

2.15.4 Luminescence Detection

The Detection Antibody was removed and the wells were rinsed once with 300µl/well Wash Buffer. The wells were washed 3-5 times with 150µl/well Wash Buffer for ~3 minutes. During the last wash, LumiGLO™ substrate was prepared. For each plate, 8ml of 1:1 (v/v) mixture of LumiGLO™ Chemiluminescent Substrate Reagent A and LumiGLO™ Chemiluminescent Substrate Reagent B were prepared. After the last wash with Wash Buffer, the wells were rinsed once with 300µl/well 1X TBS and the plate was taped gently onto absorbent paper.

75µl/well of prepared LumiGLO™ substrate was added. The plate was read on 96-well microplate luminometer between 10 and 20 minutes after the addition of LumiGLO™ substrate.

2.16 Immunofluorescence staining of suspension cells

Indirect immunofluorescence staining is used to visualise the subcellular distribution of biomolecules of interest. In this project combination of one antibody with a chemical fluorescence dye (DAPI for nuclei) and protein specific monoclonal antibody from a mouse was used (*see 2.2.4*). Subsequently, an antimouse secondary, dye-coupled (Cy3) antibody was introduced that recognised the primary antibody.
Briefly, the cells were fixed with 4% PFA for 20 min. at room temperature (RT). and washed. The cells were incubated for 10 min at RT and washed again twice with PBS. The permeabilisation of the cells was done with 0.2% Triton for 5 min at RT followed by blocking with 10%FCS in PBS for 1h at RT. The cells were washed again twice with PBS. 20 µl of the primary antibody in Blocking buffer (1:50) was added and incubated for 1h at RT and washed with PBS. 20 µl of the fluorescently labelled secondary antibody in blocking buffer (1:100) was added and incubated for 30 min. at RT follow by PBS wash. Additionally the nuclei were visualised with DAPI. For the visualisation of the stained biomolecule.

2.17 Statistical methods

2.17.1 Chi-square test

A chi-square test is any statistical hypothesis test in which the sampling distribution of the test statistic is a chi-square distribution when the null hypothesis is true, or any in which this is asymptotically true, meaning that the sampling distribution (if the null hypothesis is true) can be made to approximate a chi-square distribution as closely as desired by making the sample size large enough.

2.17.2 logrank test

The logrank test is a hypothesis test to compare the survival distributions of two samples. It is a nonparametric test and appropriate to use when the data are right censored (technically, the censoring must be non-informative). It is widely used in clinical trials to establish the efficacy of new drugs compared to a control group when the measurement is the time to event.

2.17.3 Kaplan–Meier estimator

The Kaplan–Meier estimator estimates the survival function from life-time data. In medical research, it is used to measure the fraction of patients living for a certain amount of time after treatment.

A plot of the Kaplan–Meier estimate of the survival function is a series of horizontal steps of declining magnitude which, when a large enough sample is taken, approaches the true survival function for that population. The value of the survival function between successive distinct sampled observations ("clicks") is assumed to be constant.

3. Results

3.1 Detection of loss of haetherozygosity (LOH) in AML patients with normal karyotype using GeneChip Mapping 10K Array

Chromosome abnormalities are associated with a wide range of clinical problems including cancer. The identification and characterisation of chromosome abnormalities represent the basis of cytogenetic analysis and are crucial for accurate diagnosis and prognosis. Current methods used for assessing chromosomal integrity and copy number focus on microscopy of metaphase chromosome spreads and interphase nuclear preparation. These techniques include karyotyping and fluorescence in situ hybridization (FISH). Despite the great diagnostic and prognostic benefits provided by these methods, they have some disadvantages such as limited resolution. Furthermore they are not well suited for identifying regions of the genome that have undergone LOH (Loss of Hetherozygosity) as in the case of a single allele present without a reduction in copy number. With the completion of the human genome, single nucleotide polymorphisms (SNPs), the most common sequence variation among individuals, are emerging as the marker of choice in large-scale genetic studies due to their abundance, stability and relative ease of scoring. These characteristics make SNPs powerful markers for LOH studies. High-density DNA array technology has been applied to Affymetrix for the identification of genomic alterations in tumour cells, most notably LOH. Recently a method termed “whole genome sampling analysis” was developed for large-scale SNP genotyping of complex DNA. The SNPs on the GeneChip Mapping 10K Array were selected from Affymetrix through a stringent and iterative process which utilised genotype clustering patterns, genotype calls, accuracy, reproducibility, heterozygosity, and genome coverage as the selection criteria. Extensive testing and validation of 11,555 SNPs on the Mapping 10K Array demonstrated that they consistently generate correct call rates and are reliable and informative across several ethnic populations. The physical and genetic maps show that coverage of the SNPs on the Mapping 10K Array is comprehensive, with a median physical distance between SNPs of approximately 105 kb and an average distance of 210 kb. The median genetic distance between SNPs is approximately 0.10 cM (genetic distance) and the average distance is approximately 0.31 cM. This ensures the sufficient coverage and significant statistical

power of the Mapping Array making this method ideally suited for linkage analysis and other genetic research (Fig.3.1).

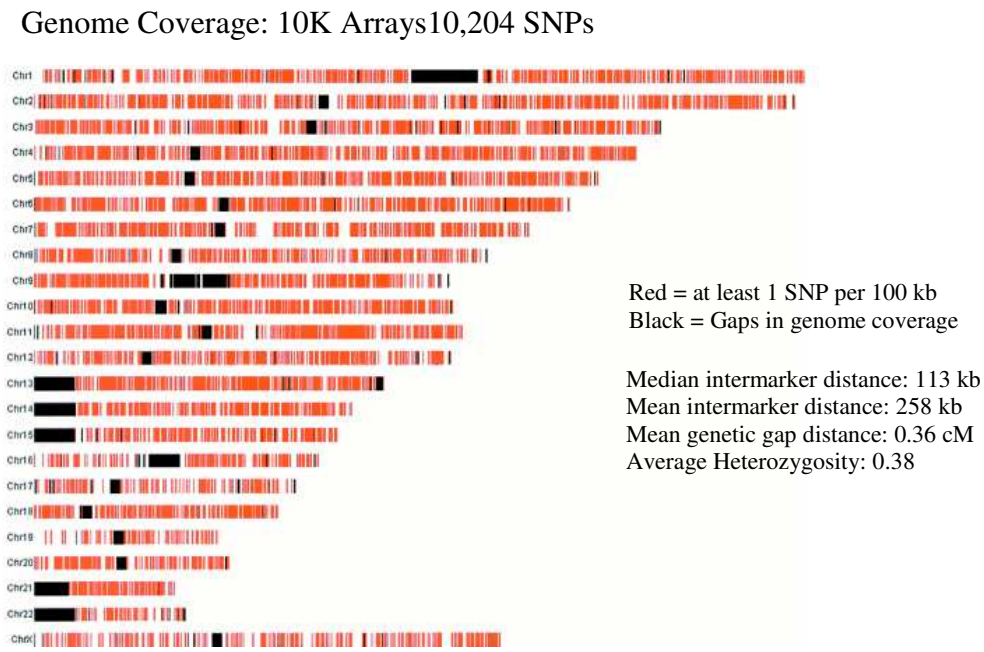

Fig.3.1 Distribution of SNPs across the genome.

Red vertical bars represent the presence of at least one SNP in 100-kb regions. Black vertical bars represent large counting gaps that are 100,000 nucleotides or longer.

In this study bone marrow or blood samples from 146 adult patients with newly diagnosed and untreated AML were analysed for LOH changes using Affymetrix SNPs Arrays. All patients were diagnosed as having AML according to the standard French-American-British (FAB) and WHO criteria. The median age in this group was 55 years, 50% were male and 50% female and the patients had different OS after the induction chemotherapy. The screening was started with the sorting of the blasts (CD33, CD34 and CD117) and the T-cells (CD3). The T-cells were used as a disease free control, as a conformation of the somatic nature of SNPs-detected lesions. In the AML patients, the T-cell count is often very low so the amount of the isolated DNA in some samples was minor. In these cases whole genome preamplification was performed using Repli-g kit from Quiagene recommended by Affymetrix. To be sure that no genetic information was lost, the quality of the DNA after preamplification was controlled using Humantype Chimera PCR amplification kit (this method is described

in the materials and methods section). With this analysis it could be shown that some loci after preampliffication were lost (data not shown). This loss of genetic information had a subsequent impact on the technical values after the array hybridization. The quality of the hybridization was analysed with the GTYPE software from Affymetrix and is very important to the correct analysis of the copy number changes. Two kinds of 10K Arrays were used: Macro Array *Xba*1 131 Assay and Macro Array *Xba*1 142 Assay. Macro Array *Xba*1 142 contains fewer SNPs (10,200 SNPs) then Array *Xba*1 131 (11,555 SNPs) because the SNPs with lower quality were removed. In the Table 3.1 the technical results from some samples are present.

Table 3.1 Technical values after hybridization.

The quality of the hybridization was analysed with GTYPE software. SNP Call and Signal Detection show the hybridization quality. AA Call AB Call and BB Call show the distribution of the A and B allele in percent.

Mapping Array Report							
Report File Name - C:\Program Files\Affymetrix\GeneChip\Affy_Data\Data\Gr3_SNP_2479_06.RPT							
Date:	07/16/08 12:32:13						
Total number of SNPs:	10204						
Total number of QC Probes:	4						
Probe array type:	Mapping10K_Xba142						
SNP Performance							
CEL Data	Gender	Called Gender	SNP Call	Signal Detection	AA Call	AB Call	BB Call
Gr3_SNP_2479_06	Unknown	F	99.01%	99.96%	33.07%	34.57%	32.36%
Gr3_SNP_2662_06	Unknown	M	94.98%	99.15%	33.68%	33.14%	33.18%
Gr3_SNP_2664_06	Unknown	F	98.09%	99.90%	31.57%	35.63%	32.80%
Gr3_SNP_2988_99	Unknown	M	97.13%	99.60%	33.03%	34.60%	32.37%

However, the technical values of the preamplificated DNA after the hybridization were lower compared with the values of the primary DNA. To improve the quality of the preamplificated DNA I compared Repli-g kit with Genomy-Phi kit from Amersham and confirmed that the loss of the loci with the GenomyPhi was rare (Fig.3.2) and the quality of the DNA was higher. Thus, with GenomyPhi, it was possible to increase the technical values after hybridization. In Table 3.2 the differences in the technical data after hybridization between the primary DNA and the amplificated DNA are shown.

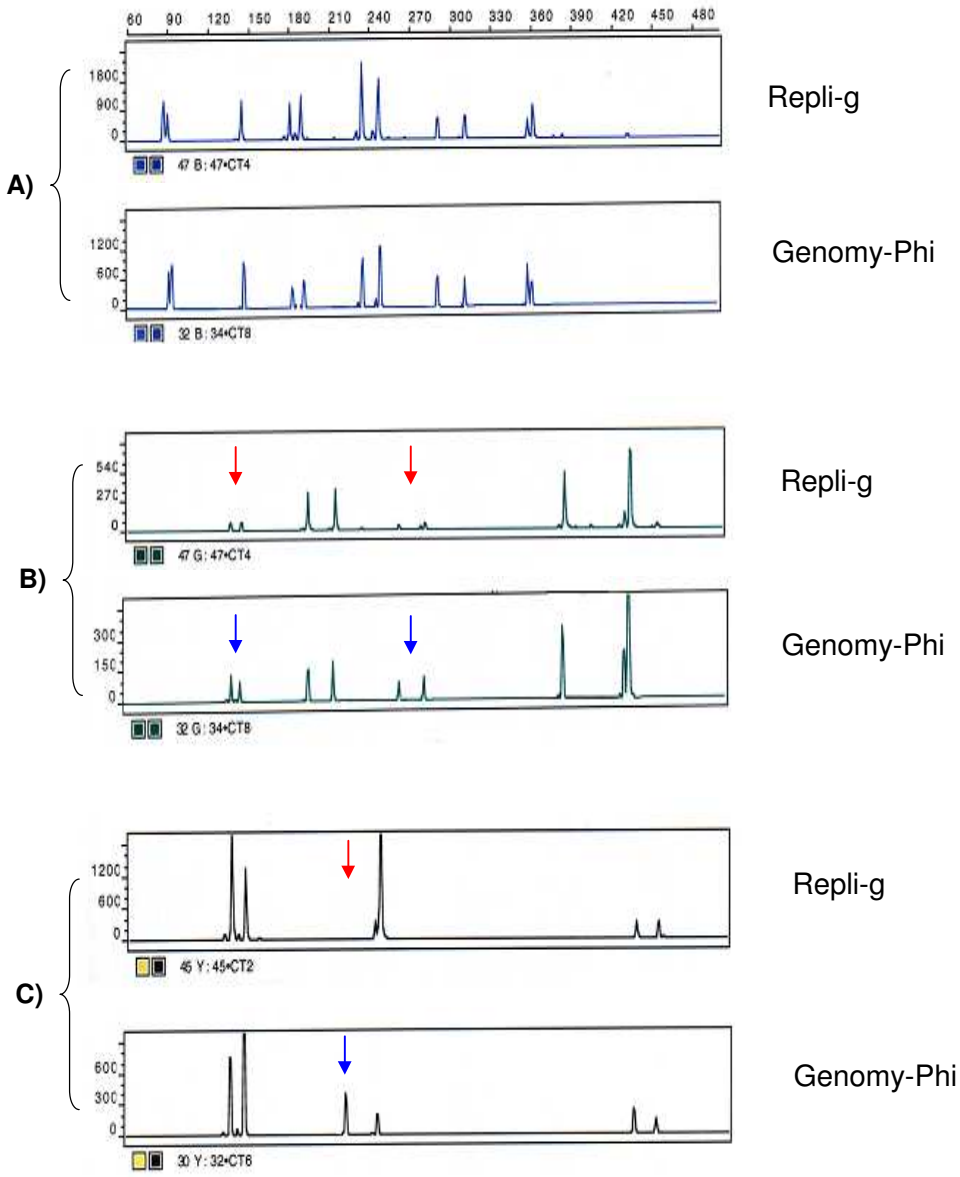

Fig.3.2 Comparison between Repli-g and Genomy-Phi using Humantype Chimera PCR Amplification kit.

This method is based on the amplification of 12 high-polymorphic loci. One of the primers is labelled with fluorescence dye. Of the x-axes are displayed: **A)** 6 loci - 6-FAM labelled; **B)** 4 loci - Hex labelled; **C)** 3 loci - NED labelled. DNA was isolated from 100000 cells (human control DNA), and for the whole genome preamplification 10 ng were used. After the amplification with Repli-g kit I found that some loci were lost (shown on the graph with the red arrows). I could improve the quality of the DNA using Genomy-Phi kit from Amersham so the missing loci could be detected (shown on the graph with the blue arrows).

Table 3.2 Mean value of the technical values after the hybridization.
The mean values of SNP Call and Signal Detection were calculated after the hybridisation of primary DNA and after the hybridization of amplificated DNA with Repli-g and Genomy-Phi kits.

DNA Preparation	SNP Call %	Signal Detection %
Primer	96,1	99,1
Repli-g Kit (Quiagen)	78,8	91,1
GenomyPhi Kit (Amersham)	92,8	98,1

3.2 Analyses of copy number changes in AML patients with normal karyotype

3.2.1 Copy number tool analyses

The copy number changes were analysed with the chromosome copy number analysis tool 4.0 (CNAT), which provides a graphical interface to facilitate identification of amplifications, deletions and UPD regions by chromosome for many sample types. Copy number changes and p-values were calculated based on SNP hybridization signal intensity data from the experimental sample relative to intensity distributions derived from a reference set containing over 100 ethnically diverse individuals (Huang *et al*. 2004). One typical case with LOH in chr. 11 is illustrated in Fig.3.3. In the upper panel, four graphs are displayed, showing from top to bottom: copy number estimation, p-value (or significance), Log2Ratio and LOH probability. The visible range of the y-axis for each graph is independently user adjustable. The physical coordinates on the chromosome are displayed along the bottom of the graphs. In the lower panel, a tabular view of the data along with the genotype calls and SNP ID, chromosome, and physical positions of each SNP are displayed.

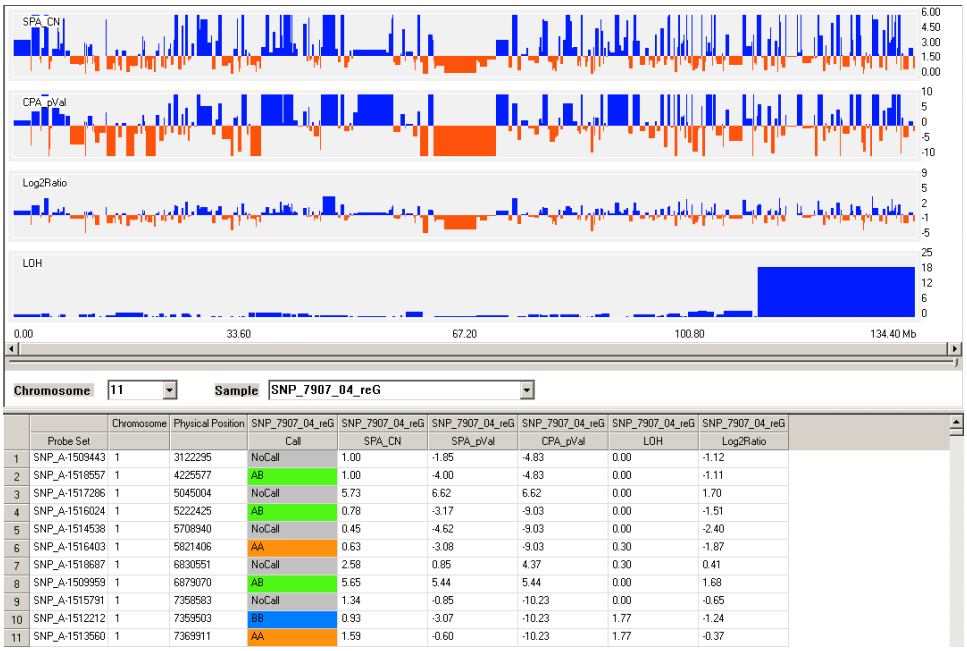

	Probe Set	Chromosome	Physical Position	SNP_7907_04_reG Call	SNP_7907_04_reG SPA_CN	SNP_7907_04_reG SPA_pVal	SNP_7907_04_reG CPA_pVal	SNP_7907_04_reG LOH	SNP_7907_04_reG Log2Ratio
1	SNP_A-1509443	1	3122295	NoCall	1.00	-1.85	-4.83	0.00	-1.12
2	SNP_A-1518557	1	4225577	AB	1.00	-4.00	-4.83	0.00	-1.11
3	SNP_A-1517286	1	5045004	NoCall	5.73	6.62	6.62	0.00	1.70
4	SNP_A-1516024	1	5222425	AB	0.78	-3.17	-9.03	0.00	-1.51
5	SNP_A-1514538	1	5708940	NoCall	0.45	-4.62	-9.03	0.00	-2.40
6	SNP_A-1516403	1	5821406	AA	0.63	-3.08	-9.03	0.30	-1.87
7	SNP_A-1518687	1	6830551	NoCall	2.58	0.85	4.37	0.30	0.41
8	SNP_A-1509959	1	6879070	AB	5.65	5.44	5.44	0.00	1.68
9	SNP_A-1515791	1	7358583	NoCall	1.34	-0.85	-10.23	0.00	-0.65
10	SNP_A-1512212	1	7359503	BB	0.93	-3.07	-10.23	1.77	-1.24
11	SNP_A-1513560	1	7369911	AA	1.59	-0.60	-10.23	1.77	-0.37

Fig.3.3 Copy Number Tools analyses in one case with LOH in chromosome 11q.

In the graph:

SPA_CN - Single point analysis of the copy number estimate.

SPA_pVal - Single point analysis of the copy number variation significance. When the value from the target cell line is higher than the reference mean, –log10(p-value) is used , which is a positive value, to represent the significance. When the value from the target cell line is lower than the reference mean, log10(p-value) is used, which is a negative value, to represent the significance.

CPA_pVal - Continuous point analysis of the significance value (meta analysis significance). CPA or meta analysis average the significance values over consecutive SNPs which display the same type of alteration (gain or loss). The higher the possibility values, the greater the chance the change is real. The average region is defined by a genomic region with a copy number above or below 2. When the value from the target cell lines is higher than the reference mean, -log10(p-value) is used, which is a positive value, to represent the significance. When the value from the target cell line is lower than the reference mean, log10(p-value) is used, which is a negative value, to represent the significance.

Log2Ratio - Smoothed Log2 ratio value.

LOH - the –log of the probability of continuous genomic region of homozygote calls.

In the LOH-graph, the value is higher than 20 of a large region which is an indication of LOH possibility.

In the first 15 patients, both the blasts and the T-cells were analysed for CNT-changes. The profiles of the blast and the T-cells in two patients with LOH in the second and in the thirteenth chromosome in Fig.3.4 are shown. In the LOH graph the ratio of the T-cells is lower than 5, but the ratio of the blasts in some regions is higher than 25, which is an indication of the LOH probability. In the remaining group of patients, only the blasts were analysed. In the cases with possible LOH regions the T- cells were also sorted and hybridized to the SNPs arrays to confirm the changes found in the blasts.

A. Chromosome 2

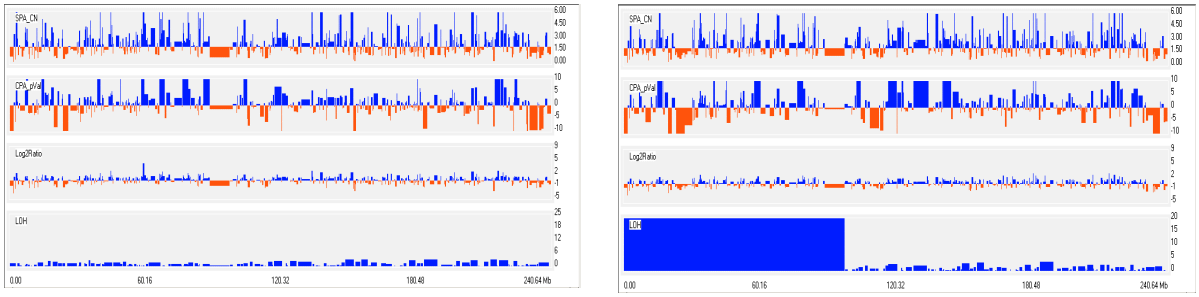

T-cells **Blasts**

B. Cromosome 13

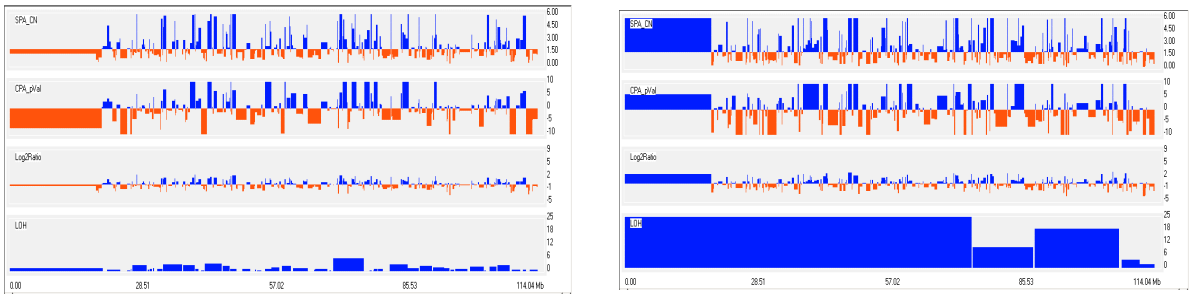

T-cells **Blasts**

Fig.3.4 CNT analyses in two patients with UPD.

A. The profile from the T-cells and the blasts from one patient with LOH in chromosome 2p. In the T-cells, the value is lower than four. In the blasts of a large region, the value is higher than 20, which is an indication of potential LOH.

B. The profile from the T-cells and the blasts from one patient with LOH in chromosome 13. The value in the T-cells is lower than six but in the blasts the value in almost the whole chromosome is higher than 20. This is an indication of Copy Number changes in the whole chromosome.

Very interesting was the detection of six cases with LOH in the blasts but I also found this phenomenon in the T-cells with unknown impact of the AML development (Fig.3.5).

A Chromosome 20

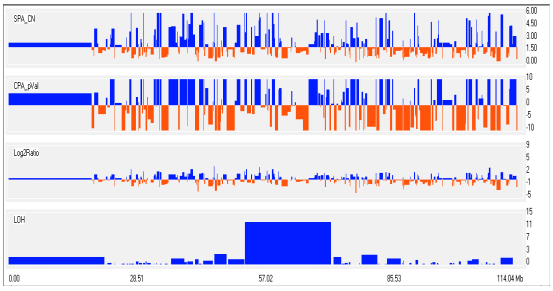

T-cells

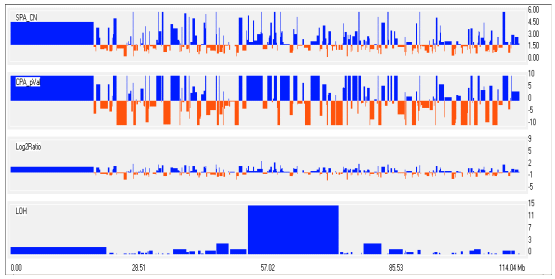

Blasts

B Chromosome 1

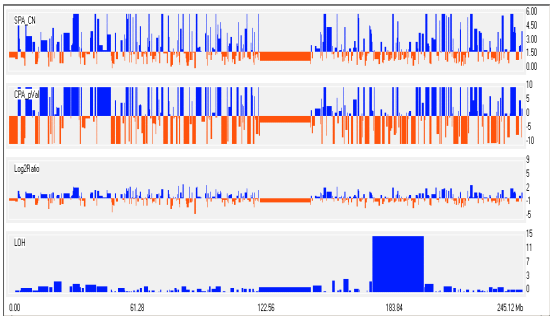

T-cells

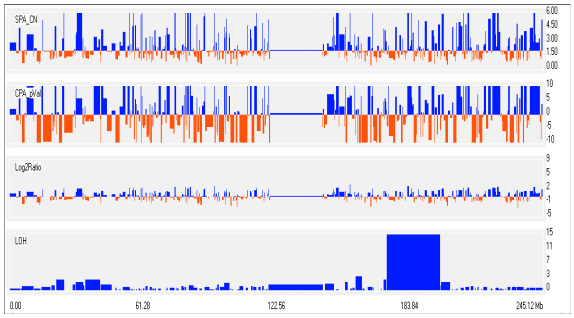

Blasts

Fig.3.5 CNT analyses in two patients with LOH in the blasts and in the T-cells.

A. T-cells and blasts in one case with LOH in chromosome 20.

B. T-cells and blasts in one case with LOH in chromosome 1.

Using Copy Number Analysis I could also identify some chromosome deletions or whole chromosome losses in patients classified with normal karyotype according to current methods. This was possible after the analyses of CAP_pVal value. (see explanation above (Fig.3.3)). I found two patients with loss of whole chromosome 7 and one patient with deletion in chromosome 10p (Fig.3.6).

A. Chromosome 7

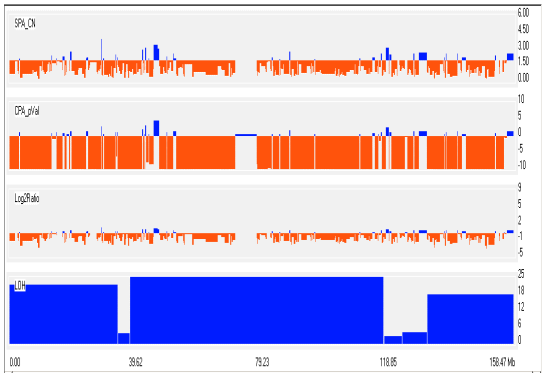

Blasts

B. Chromosome 10

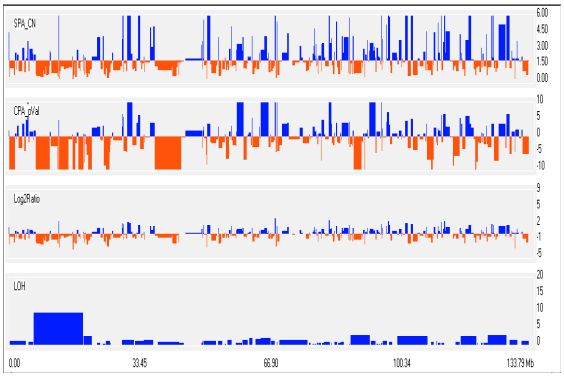

Blasts

Fig.3.6 CNT analyses in two patients with loss of genetic information.
After the analysis of CPA_pVal I was able to find deletion in chromosome 10p in one patient and loss of the whole chromosome 7 in two patients.

A. One of the two cases with loss of whole chromosome 7.

B. One case with deletion in chromosome 10p.

In this way all 146 patients were analysed and LOH in 30 cases was found. As described above, in 6 patients I confirmed this phenomenon in the blast as well as in the T-cells. Additionally I detected chromosome losses in 3 patients. I excluded these 9 cases from the UPD group so at the end I could confirm the UPD in 21 cases. The UPD-regions are located in different chromosomes where in almost all cases the telomere is also involved and covered between 11.5 and 88 Mb (Fig.3.7). Most commonly I found this aberration in the 2, 6, 7, 11, 13, and 21 chromosomes. Remarkably, in two patients, two chromosomes were affected at the same time: in the first case chromosome 21q and whole chromosome 7 and in the second case chromosomes 11p and 6p. In Table 3.3, the physical position of the LOH regions in each chromosome are presented.

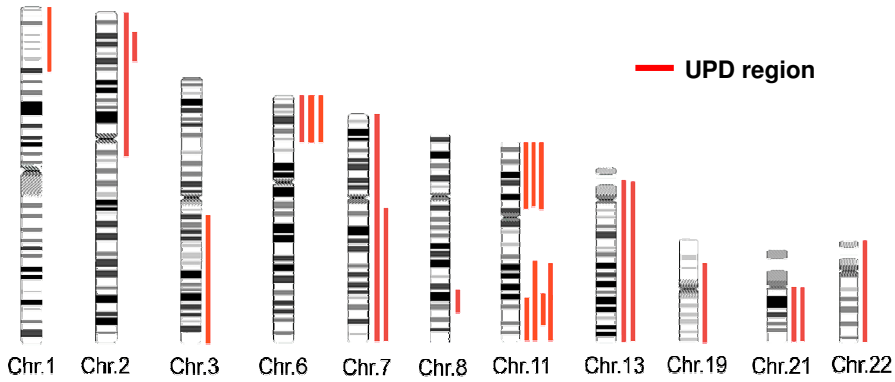

Fig.3.7 UPD regions found in 21 patients.

In two patients, two chromosomes with UPD were found: in the first case chr. 21q and 7; in the second case – 11p and 6p.

Table 3.3 Physical Positions of the UPD regions found from 146 patients in 21 cases.

Case number	Affected chromosome	Physical Position	
		start	end
1	LOH 2p	12078062	23603924
2	LOH 11q	111426718	134432350
3	LOH 2p	118345	98040934
4	LOH 11q	62639226	110235093
5	LOH 8q	108910464	122096140
6	LOH 13q	28927722	114040116
7	LOH 22	15685581	48881270
8	LOH 21	13520510	46782195
9	LOH 13	28927722	114040116
10	LOH 6p	150610	33112365
11	LOH 21q	26120971	46782195
	LOH 7	7264758	158466134
12	LOH 19q	35572679	63437743
13	LOH 11q	95822028	113791114
14	LOH 11p	2573106	45687359
	LOH 6p	150610	34589070
15	LOH 1p	3122295	54241547
16	LOH 11p	2573106	50096862
17	LOH 6p	150610	33112365
18	LOH 3q	103238428	199368514
19	LOH 7q	57299439	96038702
20	LOH 11q	96359849	116705080
21	LOH 11p	2573106	56371866

3.2.2 Short tandem repeat (STR) analyses

To confirm these results, a second method was used - Short tandem repeat analysis (STR). The method is based on the probability of different fragment lengths between heterozygosity alleles. Using the Mammalian Genotyping Service database I chose some STRs from the UPD regions with very high heterozygosity coefficient and analysed them for allele losses. In Fig.3.8 one example of LOH on chromosome 2 is presented. I analysed two STRs from Chromosome 2 in the T-cells and in the blasts. I found that in the blasts one allele was lost compared to the T-cells. In this way I confirmed the UPD in all 21 cases.

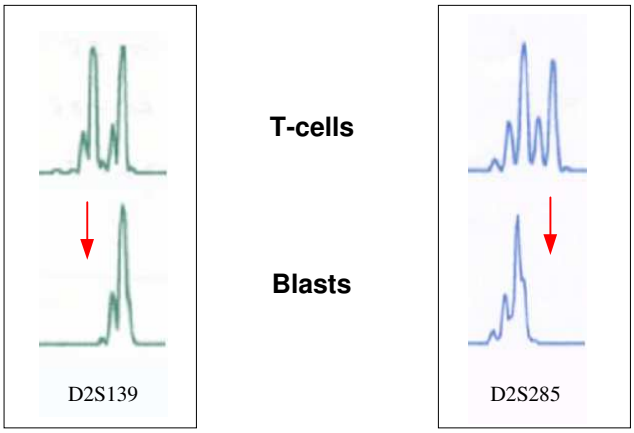

Fig.3.8 STR analyses in one case with UPD in chromosome 2.
In the UPD region, two STRs (D2S139 and D2S285) were analysed for loss of heterozygosity. In both of them one of the loci in the blasts is missing compared to the T-cells.

3.3 Relationship between UPD and AML

The next important question addressed was if there is any relationship between the UPD regions and AML. Currently, some genes in which mutations are directly connected with the development of AML have been described. So, I decided to look for the gene mutations important for the AML development in the different UPD region. For example, one of the most important haematopoietic transcription factors,

RUNX1 (runt-related transcription factor 1), located on the chromosome 21 (21q22.3), is often mutated in AML patients. In this study there were two cases with UPD on the 21q chromosome. Since aberrations in exons 3; 4; 5 from the RUNX1 gene were most often described, I sequenced these regions in both cases. I found point mutation in each case – in exon 3 and 4 (Fig.3.9). Moreover, the mutations of the WT1 (Wilms tumor) gene on chromosome 11p were reported to be relevant of the development of the AML. After sequencing of the exons 1, 6, 7, 8 and 9 from three patients with UPD in the chromosome 11p, I found a point mutation in the exon 7 in one of them (Fig.3.10). Additionally, one mutation was found in the CEBPA (CCAAT/enhancer binding protein) gene in one patient with UPD on chromosome 19 (sequenced by Marika Karger in our lab, data not shown). In this way it was possible to confirm the relationship between the UPD regions and AML.

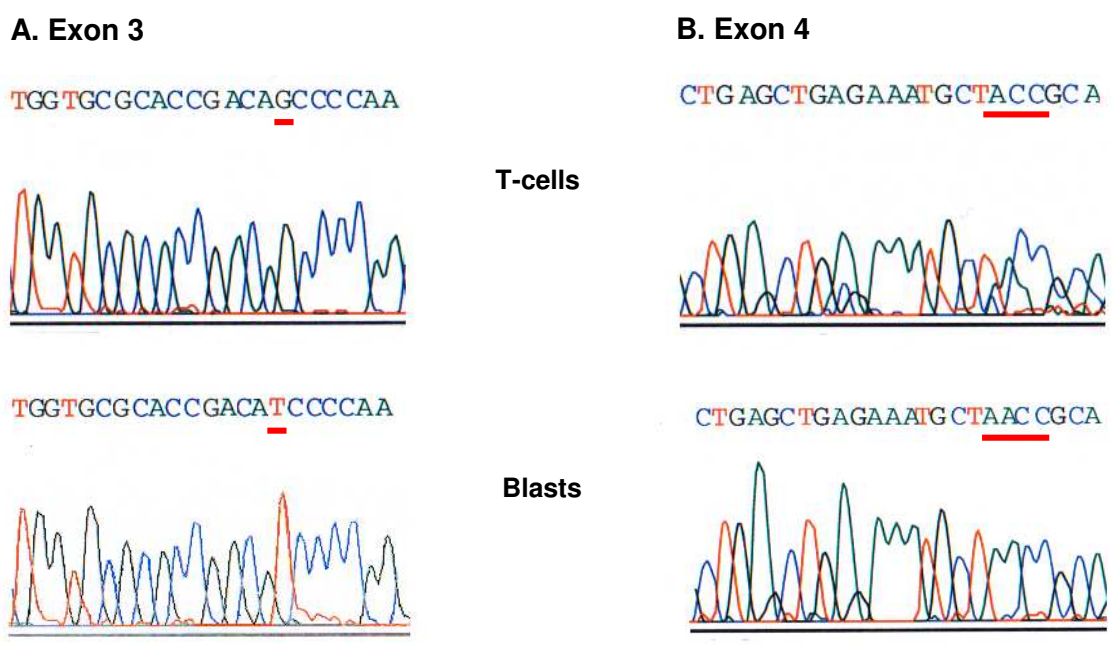

Fig.3.9 Mutations in RUNX1 gene in two cases with UPD in chromosome 21q.

The exons 3, 4 and 5 on chr. 21q were sequenced in two patients with UPD. At first, the cells were sorted and then the blasts were compared with the T-cells (negative control).

A. Point mutation in exon 3 in one of the patients.

B. Insertion in exon 4 in the second case.

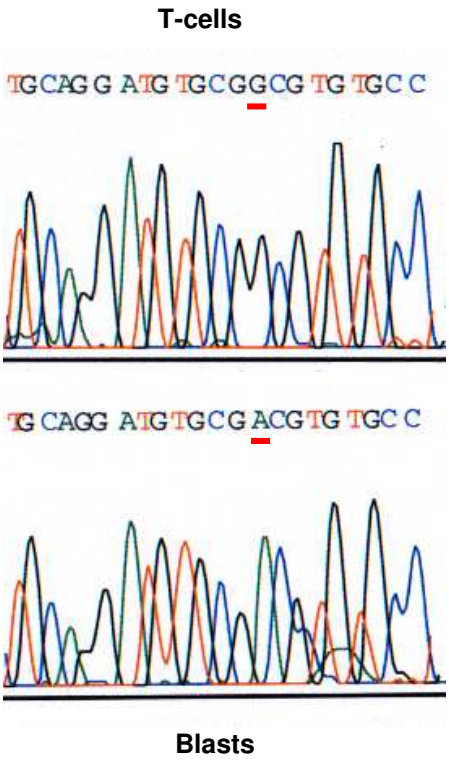

Fig.3.10 Point mutation in WT1 gene in one case of the UPD in chromosome 11p.

From 21 UPD positive patients, three cases with UPD in chromosome 11p were found. From these patients the cells were sorted and the blasts were compared with the T-cells (negative control). After sequencing of the WT1 gene (exons 1, 6, 7, 8 and 9) in these cases a point mutation in exon 7 was found in one of them.

3.4 Statistical analyses

Some statistical analyses were performed to discover if UPD has an impact on Overall Survival (OS), as well as if gender or AML subtype are related to this aberration. Kaplan-Meier method was used and the analyses were done together with Fr. Silke Soucek. I could not find any connection between age, WBC-counts (White Blood Cell counts) or sex and the UPD, but there was a clear correlation between the UPD and the AML subtype. The FAB M1 subtype was observed in 47.6% of the UPD positive patients, compared to only 19.2% of the UPD negative patients (P=0.04, n=146). Also I couldn't find any correlation between FLT3-ITD, MLL-PTD and NPM1 mutations in the UPD patients. They were present at the same rate in the UPD cases.

The rate of complete remission (CR) induction was 85.7% in the UPD positive cases and 76.8% in the UPD negative cases. Of the UPD positive patients in complete remission after induction chemotherapy, 60.0% relapsed within the first 6 months. In contrast, the rate of relapse in patients without UPD was only 38.2%, but these results were not significant (P=0.065).

Fig.3.11 shows the comparison of the OS between UPD positive patients UPD negative patients. Only the patients younger than 60 were analysed to exclude the impact of age on the results. After the induction chemotherapy the UPD positive patients showed clearly lower OS compared to the UPD negative cases.

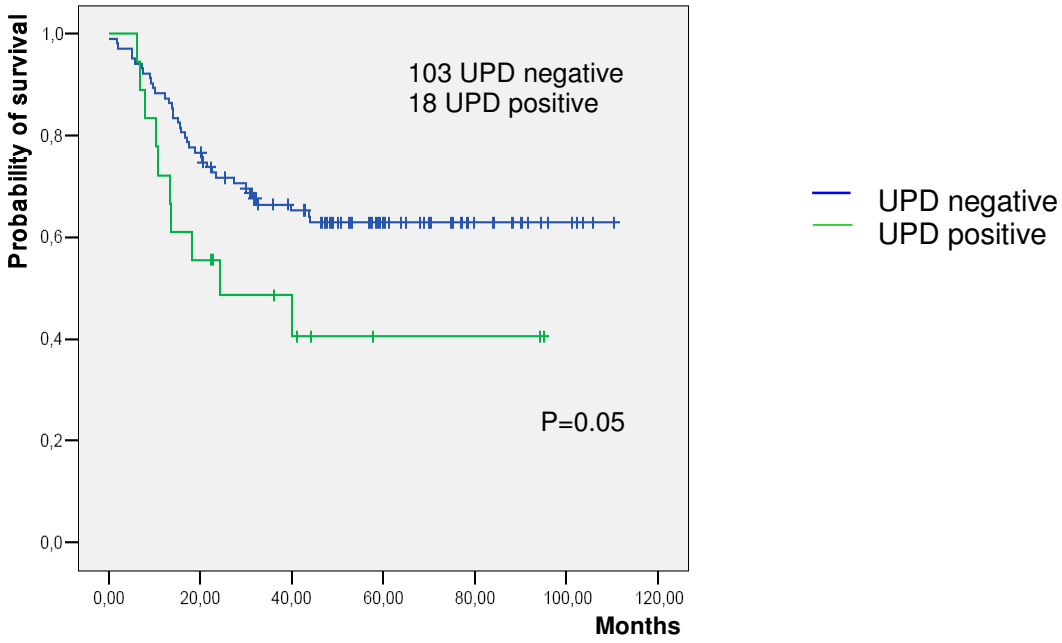

Fig.3.11 Kaplan-Meier analysis of the probability of OS in 121 patients with and without UPD.

Kaplan-Meier analysis of OS in AML patients with normal karyotype younger than 60 was done. UPD negative patients had a significantly higher probability of OS than UPD positive cases.

Furthermore, the patients with UPD on chr. 11 had the poorest outcome with a median OS of 13 months compared to the patients with UPD located on other chromosomes and UPD negative cases. In Fig.3.12, the patients with UPD on chr. 11 are presented separately from the remaining group of patients with UPD. All 146 patients were analysed.

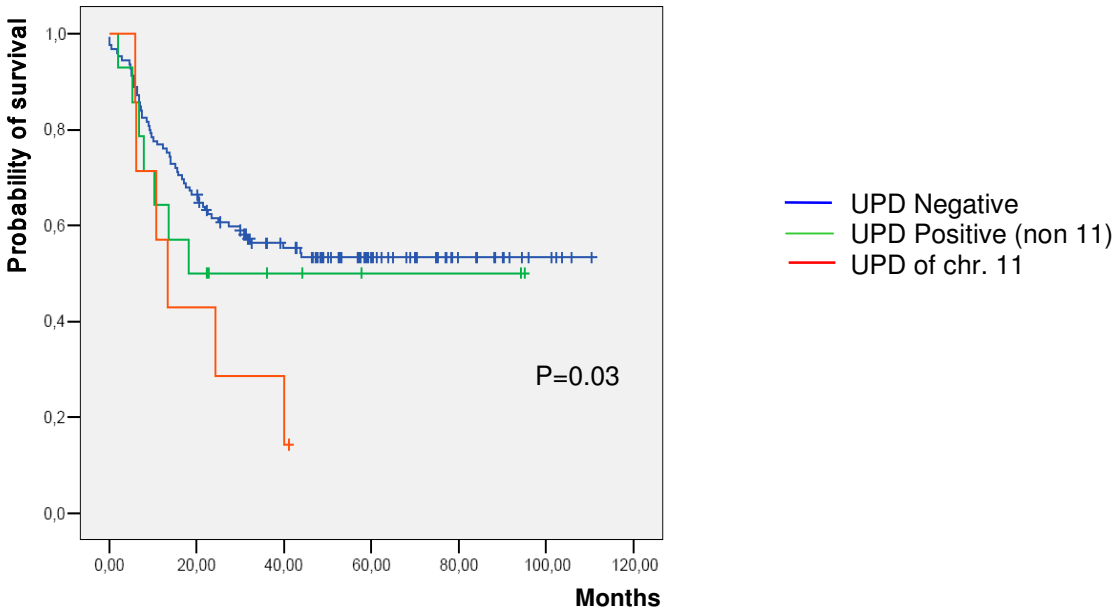

Fig.3.12 Kaplan-Meier analysis of the probability of OS in 146 patients with and without UPD.

The patients with UPD on chromosome 11 are presented separately. They show the poorest outcome compared to the remaining UPD positive cases and patients without UPD.

3.5 Gene expression analyses using Affymetrix array

Genome-wide gene expression profiling based on DNA microarrays represents one of the most powerful tools in the area of the current genomics. The utility and promise of the experimental use of DNA microarray technology to study human cancer has been demonstrated first by analysing acute leukaemia samples, which included cases of AML. Although known AML cases were predicted by using supervised data analysis approaches, new subtypes of AML have been identified with the aid of unsupervised analytic methodologies. In addition, the feasibility of gene expression-based outcome prediction in AML has been demonstrated, and DNA microarray technology has provided novel biological insights by its application to experimental models. To find out if patients with UPD could be classified in one group based on the similar gene expression profiling, expression analyses were performed using GeneChip Human Genome U133A arrays from Affymetrix. I started with five patients with UPD and compared them to five patients without UPD (the UPD negative cases

were hybridised by Dr. Christine Steudel). After the analysis with Gene Spring software, I found that the UPD positive patients and the UPD negative patients segregate into two different gene-expression cluster (Fig.3.13).

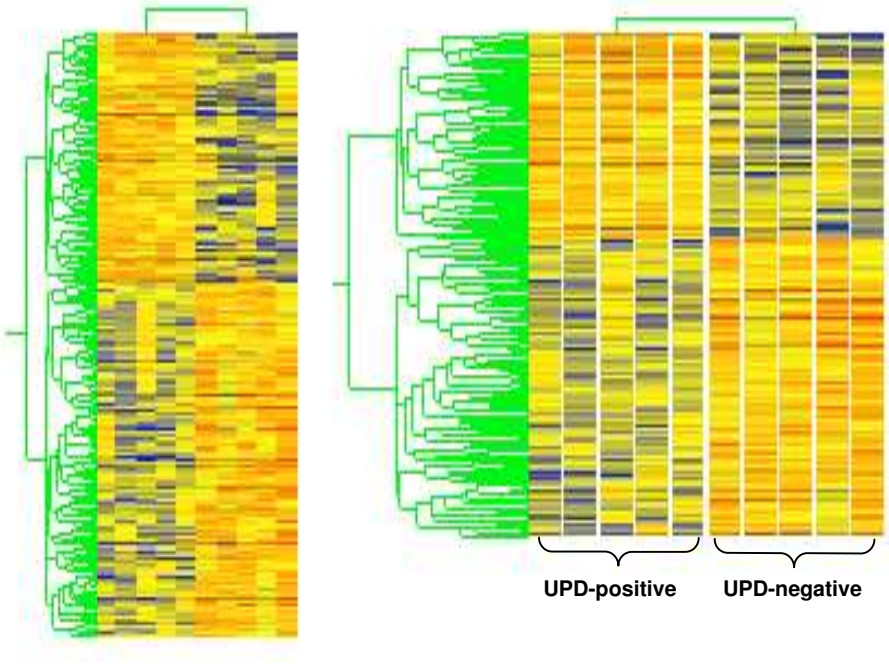

Fig.3.13 Gene expression analysis of patients with and without UPD using Gene Spring software.
Expression analysis were done in 5 UPD positive patients and 5 UPD negative patients using Affymetrix expression protocol and GeneChip Human Genome U133A arrays. 5µg of high quality RNA from each patient were used. The UPD positive patients clearly showed a different gene expression profile compared to the UPD negative patients. 1000 genes were analysed; $P \leq 0.05$.
Blue - low gene expression levels.
Red - high gene expression levels.

I continued this analysis with 14 UPD positive patients compared to 10 UPD negative cases (the UPD negative cases were hybridised by Dr. Christine Steudel). Also here I could validate different expression profiling between these two groups. For this analysis Array Assist software was used. In Fig.3.14 an example of a region with high gene expression in the patients with UPD compared to the patients without UPD is presented. Additionally I could identify some genes responsible for the repair process

in the human cells that were highly expressed in the UPD positive cases. This first analysis show that it is possible to separate the UPD positive patients from UPD negative cases according to the gene expression profile, which could be used for future research in this field.

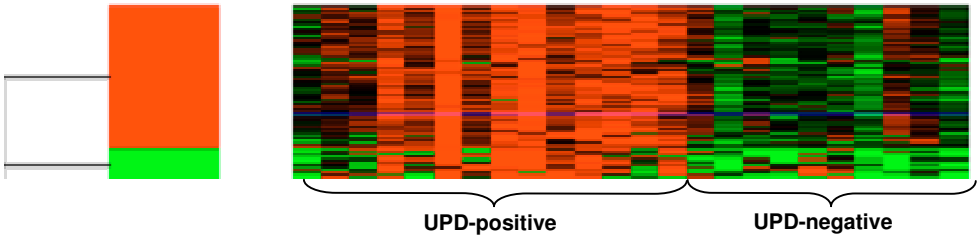

Fig.3.14 Gene expression analysis of patients with and without UPD using Array Assist software.

14 UPD positive patients were compared with 10 UPD negative patients using Affymetrix expression protocol and GeneChip Human Genome U133A arrays. 5 µg of high quality RNA were used. It was possible to generate clusters with different expression profiles in the UPD positive compared to the UPD negative patients. In the graph, one cluster with a high expression profile in the UPD positive cases is presented. 120 genes were analysed; P≤0.05

Green - low gene expression levels.

Red - high gene expression levels.

3.6 The effect of FLT3-ITD mutation on homologous recombination

3.6.1 Flow cytometry analysis of homologous recombination using the pmHPRT-DRGFP vector system

Internal tandem duplication (ITD) of the juxtamembrane region of the FLT3 receptor tyrosine kinase gene is one of the most common aberration in the AML patients. In this study six of the analysed 21 UPD positive patients, had a FLT3-ITD mutation. A previous study in our lab showed that the patients with an increased allelic ratio between mutated and wt FLT3 receptor have a significantly shorter overall and disease-free survival. The loss of the wt of FLT3 receptor was investigated and it was found that it resulted rather from a homologous recombination event in the leukaemic

cells then from an allelic deletion. Interestingly, one patient with UPD in chr. 13 was found without FLT3-ITD mutation, which was contrary to the possibility that FLT3-ITD mutation could be responsible for homologous recombination repair. Based on these results I wanted to find out if a FLT3-ITD mutation increased homologous recombination in cells and if the DNA -damaging agents used in the treatment of AML are limited by DNA repair pathways. For this, two vectors were used: pmHPRT-DRGFP and pCbASce. The first vector (pmHPRT-DRGFP) carries a intact but inactive GFP region, as well as a region with a mutated GFP with a restriction site – SceI. The second vector (pCbASce) encodes the I-SceI homing endonuclease (Fig.3.15).

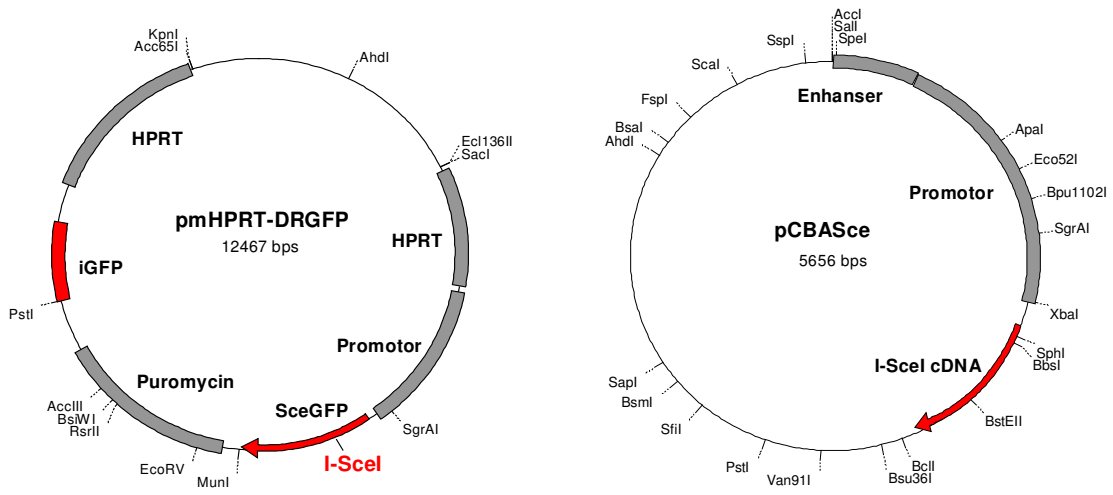

Fig.3.15 Vectors system used for HR analysis.

The pmHPRT-DRGFP vector contains two GFP regions. One of them is inactivated by one point mutation and I-SceI restriction size. The second GFP region is intact but inactive.

The pCbASce vector contains I-SceI endonuclease, which is able to generate double strands breaks in the SceI restriction size in pmHPRT-DRGFP vector.

The pmHPRT-DRGFP vector is used for assaying double-strand break (DSB)-mediated gene conversion in a mouse HPRT gene targeting complex. In this system, the GR-GFP reporter is the first gene targeted to the mouse HPRT locus in a quantifiable way. The cells successfully targeted with the reporter are transfected with pCbASce carrying the I-SceI homing endonuclease. The upstream GFP repeat (SceGFP) is nonfunctional owing to insertion of a recognition sequence for I-SceI;

hence, I-SceI expression will generate a DSB in this repeat. The break can then be repaired by several mechanisms including nonhomologous end joining (NHEJ), single-strand annealing (SSA), and gene conversion-homologous recombination (HR). HR results in repair of the DSB using the downstream internal fragment GFP repeat (iGFP) as a template. As a result, SceGFP becomes a constitutively expressed functional GFP+ gene and cells acquire green fluorescence easily quantifiable by flow cytometry (Fig.3.16).

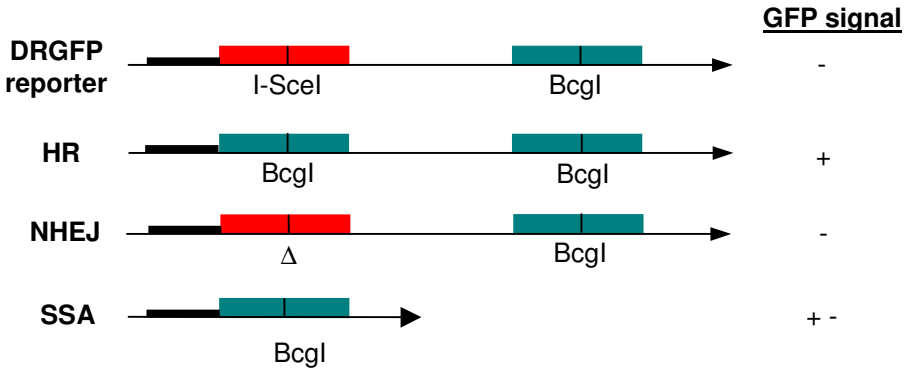

Fig.3.16 Different DSB repair products at the DRGFP locus.
HR, NHEJ and SSA are the possible DSB repair pathways but only HR results in GFP+ cells. All three DSB repair pathways result in I-SceI site loss; the homologous repair pathways HR and SSA additionally result in replacement of the I-SceI site with a BcgI restriction site.

When cells are supplied with an exogenous gene targeting construct, the construct can integrate either into the homologous locus (targeted) or into random loci (nontargeted). I used the nontargeted integration to investigate the repair mechanisms in some human cell lines. After transfection, the cells were selected with puromycin, whose resistance is carried by the vector. After the identification of cells that have successfully integrated the DRGFP reporter, DSB-induced gene conversion was quantified by assaying green fluorescence (GFP) after the transfection of these cells with the expression vector for the I-SceI endonuclease (pCbASce).

To determine whether the FLT3 mutation has a role in homologous recombination (HR) in human cells the following cell lines were transfected with the pmHPRT-DRGFP vector: MV4-11, Molm13, THP1 and K562, described in more detail in the materials and methods section. $MV_{4\text{-}11}$ expressed only FLT3-ITD but not FLT3wt - $MV_{4\text{-}11}$ (FLT3-ITD), while Molm13 expressed FLT3-ITD as well as FLT3wt - Molm13

(FLT3-IDT/wt) (Table 3.4). As a negative control THP1 (with expression of FLT3wt only) and K562 (without any detectable expression of FLT3) were used (Table 3.4).

Table 3.4 Cell lines used in this project and the expression status of FLT3wt and FLT3-ITD.

Cell lines	Lineage	FLT3-ITD status	FLT3wt status
MV_{4-11}	Myeloid	Yes	No
Molm13	Myeloid	Yes	Yes
K562	Myeloid	No	No
THP1	Myeloid	No	Yes

After the selection with puromycin for each cell line (the resistance level for each cell line is described in the materials and methods section (2.14.4)) a single clone was produced using FACSAria (Beckton Dickinson). I determined the single copies of the pmHPRT-DRGFP by Real Time quantitative PCR. ß-Globulin gene was used as a control. In Fig.3.17 the results from MV_{4-11} (FLT3-ITD) are shown. For example the MV4-11_64 and MV4-11_71 contain more then one copy of the pmHPRT-DRGFP vector. The remaining clones were with single copies of the vector. In the remaining cell lines the same procedure was performed (data not shown).

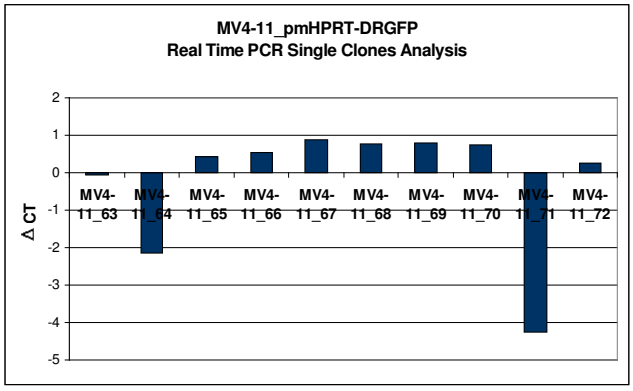

Fig.3.17 Single clone analysis using Real Time quantitative PCR.

The single clones from MV_{4-11} (FLT3-ITD), Molm13 (FLT3-ITD/wt), K562 and THP1 were selected and the clones with one copy of the pmHPRT-DRGFP cassette were detected using Real Time quantitative PCR. ΔCT value is calculated as a difference between the amplification of the GFP gene in the pmHPRT-DRGFP cassette and the ß-globulin gene. The graph presents the results from MV_{4-11} (FLT3-ITD). Two of the 10 clones (MV4-11_64 and MV4-11_71) have more then one copy of pmHPRT-DRGFP vector. The remaining clones have single copies of the vector.

Electroporation conditions were optimised before the transfection with the pCbASce vector (Fig.3.18.A). The optimal electroporation efficiency was achieved using the following electroporation conditions (Fig.3.18.B).

A. Electroporation efficiency

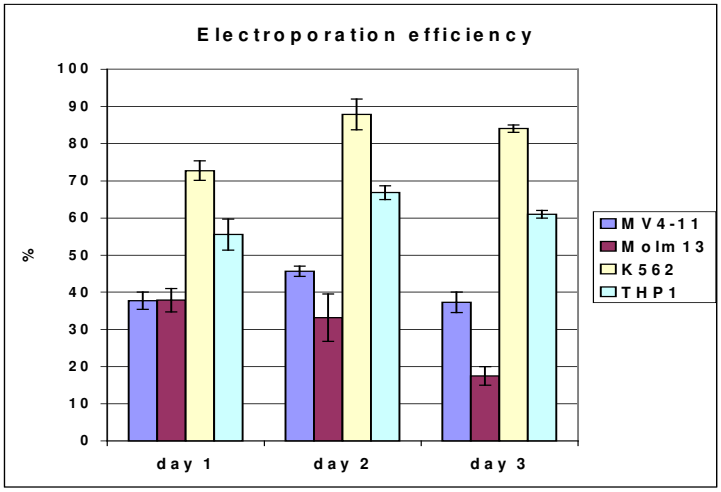

B. Electroporation conditions

Cell line	Voltage (V)	Time constant (ms)	Electroporation efficiency (%)
MV_{4-11}	300	7,5	45
Molm13	300	22,7	33,17
K562	300	6,6	87,85
THP1	250V	39,8	67

Fig.3.18 Electroporation efficiency and electroporation conditions in MV_{4-11} (FLT3-ITD), Molm13 (FLT3-ITD/wt), K562 and THP1 cell lines.

$2x10^7$ cells washed with RPMI medium were mixed with 40µg pmHPRT-DRGFP vector and after a 10 min ice-incubation were electroporated with BioRad (Gene Pulser II) under varying conditions.

A. The highest electroporation efficiency achieved in each cell line.

B. The electroporation conditions used in each cell line.

I chose one clone from each cell line with a single copy of pmHPRT-DRGFP vector and transient transfection with pCbASce was done to generate a DSB. Five days after transfection the GFP positive signal (caused by the repair of the DNA damage) was measured by flow cytrometry (Fig.3.19).

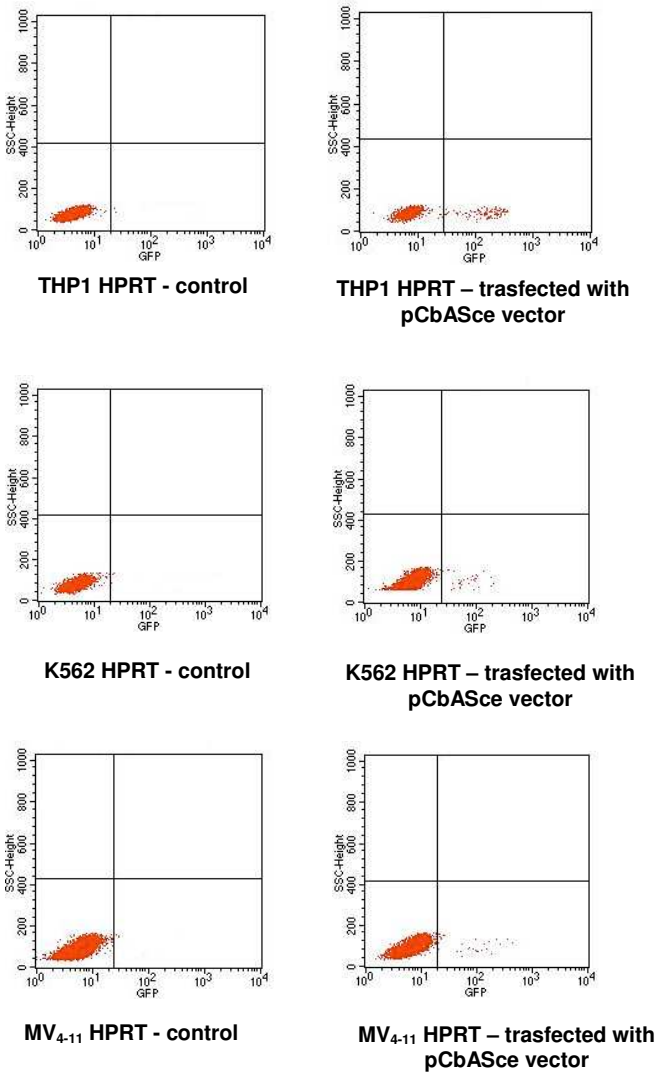

Fig.3.19 GFP positive signal measured by flow cytometry.
From each cell line a single clone containing one copy of pmHPRT-DRGFP vector was transfected with 40µg pCbASce vector using electroporation. Five days after transfection the GFP signal was measured.
In the left panels - as a control, MV4-11, K562 and THP1 transfected only with pmHPRT-DRGFP vector were used.
In the right panels - the GFP signal as a result of HR occurs after transfection with pCbASce vector.

To identify the homologous repair efficiency in the different cell lines, I related the % of GFP positive cells to the electroporation efficiency. Surprisingly THP1 showed very high HR efficiency compared to other cell lines. The HR capacity in K562 and MV_{4-11} (FLT3-ITD) was similar, but I couldn't identify any GFP positive signal in Molm13 (FLT3-ITD/wt) this could be an indication of lack of HR-repair. The results are shown in Fig.3.20.

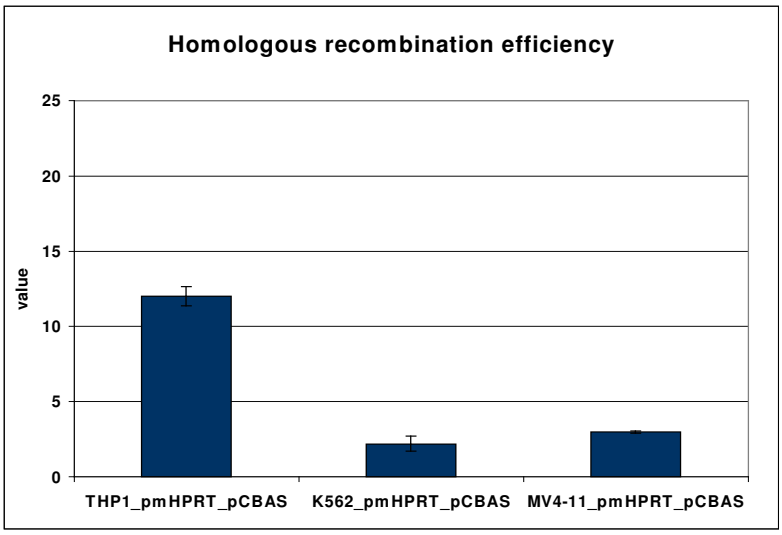

Fig.3.20 Homologous recombination (HR) efficiency measured by flow cytometry.
From each cell line one clone with a single copy of pmHPRT-DRGFP vector was additionally transfected with pCbASce to generate DSB. The result of the HR repair was a GFP positive signal. The % of GFP positive cells was related to the electroporation efficiency from each cell line. I couldn't identify any GFP positive signal in Molm13 (FLT3-ITD/wt).

3.6.2 Analysis of the repair possibilities using Short Tandem Repeat (STR)

3.6.2.1 Homologous recombination

I developed a system to confirm the HR and analysed the repair possibility based on STR analysis. I constructed one forward primer (Pr.1) at the end of the promoter before the mutated GFP fragment and one reverse primer (Pr.2 – Fam labelled) at the mutated position in the GFP fragment. The resulting fragment is 440bp long, is fam labelled and shows the primary state of the pmHPRT-DRGFP vector before any damage takes place. Also, as a second control I constructed the second pair of primers before the intact GFP fragment (Pr.3) and in the middle of the intact GFP (Pr.4 – Hex labelled). This fragment is 487bp long and it is Hex labelled. After HR the new fragment with pr.1 and pr.4 could be detected. This new fragment is hex labelled, 434 bp. long and it is a result of HR repair (Fig. 3.21.A/B and Fig.3.22).

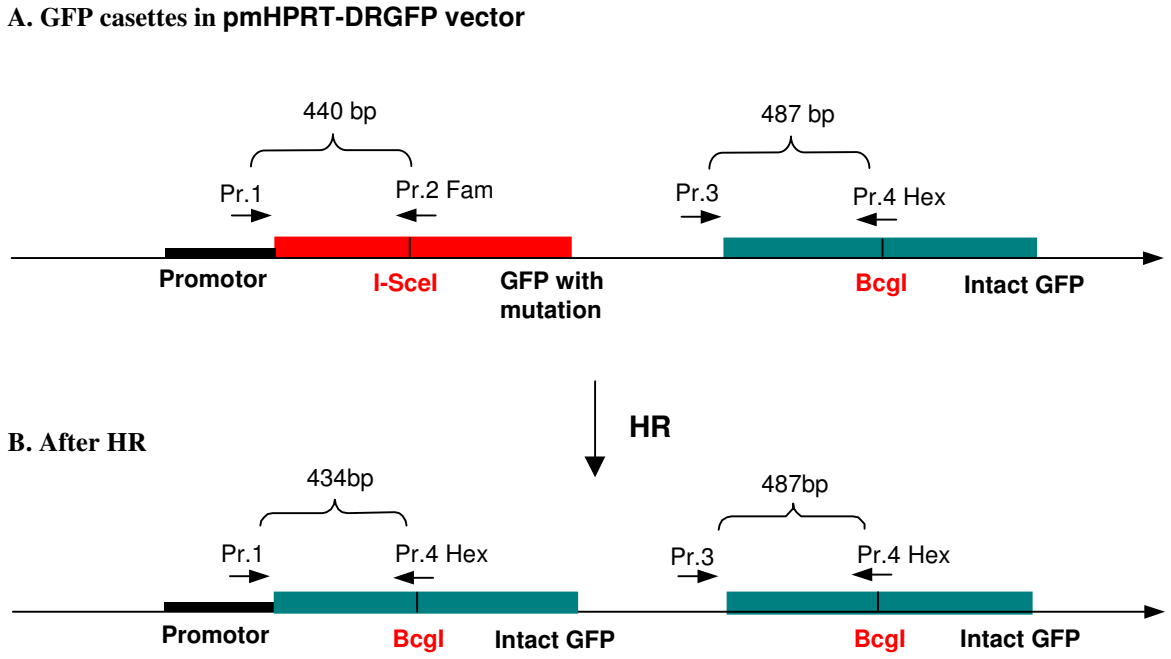

Fig.3.21 GFP system constructed to analyse the HR repair.

A. Primer state of the pmHPRT-DRGFP vector before any repair takes place. The mutated GFP region with I SceI restriction size is not active. After the generation of DSB with ISceI endonuclease in the mutated GFP region, the intact GFP region could be used as a template in the HR repair process. After the amplification reaction with primers 1 and 2 a fragment with 440 bp was produced. The fragment with primer 3 and 4 was 487 bp.

B. After HR the intact GFP fragment replaced the damaged GFP fragment. The resulting fragment with primer 1 and 4 is a consequence of HR and is 434bp.

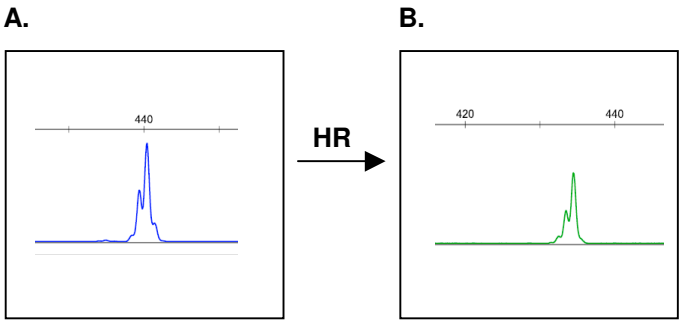

Fig.3.22 STR analyses of HR.

A. Before DSB occurred the primary fragment (with primers 1 and 2) was 440bp.

B. After the induction of DSB with SceI endonuclease HR took place and the new fragment 434bp (with primer 1 and 4) could be detected. HR was confirmed in THP1, K562 and $MV_{4\text{-}11}$.

The area of the HR – pick was different in the different cell lines, but it corresponded to the % of GFP cells measured by FACS (Fig.3.23). NPM1 was used as a single copy control. The value was calculated as a difference between the area of the NPM1 and the area of the HR pick. THP1 shows the highest value, while between MV_{4-11} (FLT3-ITD) and K562 there was no significant difference.

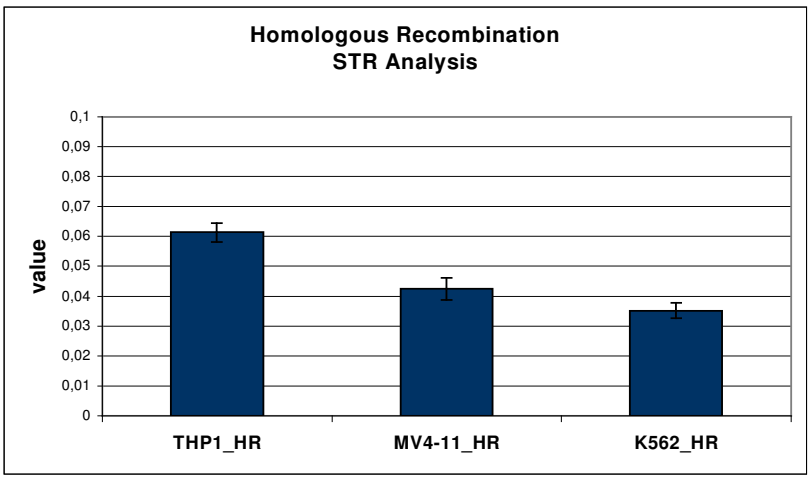

Fig.3.23 Homologous recombination (HR) efficiency measured by STR.
From each cell line a single clone containing one copy of pmHPRT-DRGFP vector was transfected with 40µg pCbASce vector using electroporation. Five days after transfection the efficiency of HR in the different cell lines measured by STR analysis was calculated as a value of the area of the HR picks and related to the NPM1 gene used as a control gene.

3.6.2.2 Nonhomologous end joining repair (NHEJ)

I used the same method based on STR analysis to find out the efficiency of NHER. This process occurs in a relatively simple end-splicing mechanism, but led to the loss of genetic information. I used two primers: the first one was primer 1 used above but Bo TMR labelled and located before the mutated GFP fragment, and the second – primer 5 was located after the cut place in the mutated GFP. The original fragment before the induction of DSB was 563bp long. I expected that after NHEJ repair it would be possible to identify fragments shorter than 563bp (Fig.3.24). After the

transfection of MV_{4-11} (FLT3-ITD); Molm13 (FLT3-ITD/wt); K562 and THP1 with pCbASce I proved the efficiency of NHER in all four cell lines, but I couldn't find any fragments shorter than 563bp. In Fig.3.25 the result of STR analysis in K562 is present.

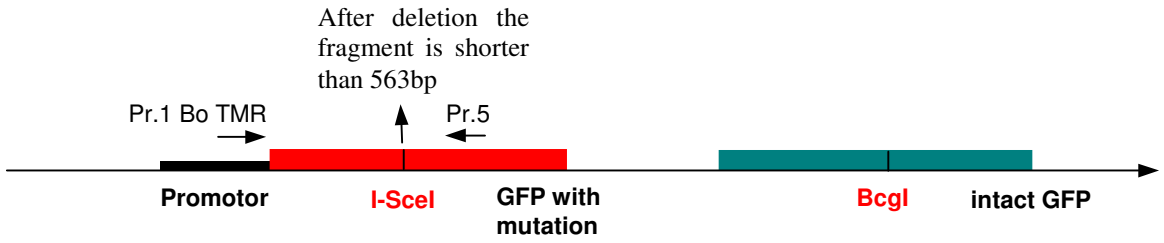

Fig.3.24 Primer system for detection of NHEJ repair.

Primer 1 Bo TMR and Primer 5 are constructed in the mutated GFP region in the pmHPRT-DRGFP vector. The result is a fragment 563bp long. After the deletion fragments shorter than 563bp should be identifiable.

Fig.3.25 Detection of NHEJ repair using STR analyses.

Primer 1 BoTMR and primer 5 were used to detect NHEJ repair in K562, MV_{4-11}, Molm13 and THP1 transfected with pmHPRT-DRGFP and pCbASce vectors. After the deletion fragments shorter than 563bp should be identifiable. In all four cell lines I couldn't found any NHEJ repair. On the graph the results from K562 are presented.

3.6.2.3 Single-strand annealing

The other DSB repair pathway using sequence homology is single-strand annealing (SSA). SSA is a highly efficient mechanism of DSB repair in mammalian cells involving direct repeats. Because a large portion of the mammalian genome consists of repeat sequences, SSA could potentially be an important alternative pathway of homologous repair. In the pmHPRT-DRGFP system the two GFP fragments are very close to each other so it makes this repair mechanism possible. The detection of SSA repair should also be possible with the STR analysis. Between the mutated GFP and the intact GFP the puromycin gene resistance is located. After SSA repair the mutated GFP and the puromycin resistance gene are replaced by the intact GFP gene. To detect this repair I used primer 1 Bo TMR and constructed an additional reverse primer for the region located after the intact GFP gene. The original fragment (before the repair took place) was 4440bp long and was not detectable with STR analysis. After the SSA, the fragment detected with primers 1 Bo TMR and 6 should be 850bp long and Bo TMR labelled (Fig.3.26). To make the detection of SSA repair possible the cells are incubated without puromycin, because the resistance should be lost after SSA repair. Unfortunately I couldn't detect any SSA repair with this system because of non-specific signals. I then used an indirect method to identify SSA in these cell lines based on the primer 3 and primer 4 (Hex labelled). As shown above (Fig.3.21) the resulting fragment obtained with these primers is 487bp. After SSA repair this fragment can not be identified anymore. I compared the areas of the resulting picks in all four cell lines after transfection with the pmHPRT-DRGFP vector and compared them with the picks areas after transfection with pCbASce vector. NPM1 was used as a control housekeeping gene. In $MV_{4\text{-}11}$ (FLT3-ITD), Molm13 (FLT3-ITD/wt) and THP1 I couldn't identify any SSA. In K562 I detected low level of SSA but it was not possible to quantify this repair.

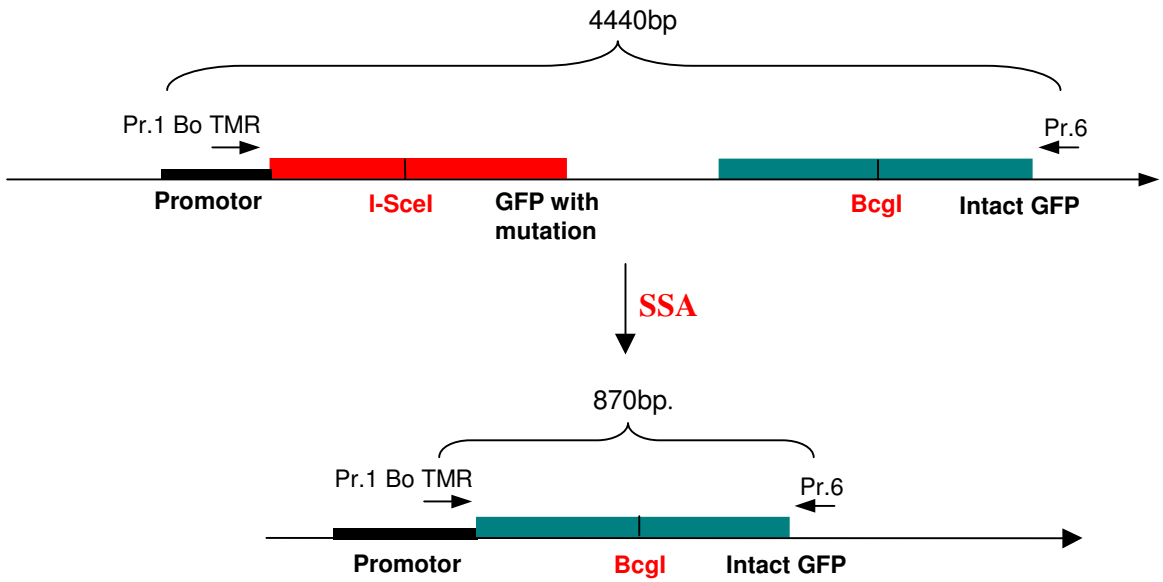

Fig.3.26 Primer system for detection of SSA.

The fragment produced after the amplification with primer 1 Bo TMR and primer 6 (before the induction of DSB with pCbASce) in pmHPRT-DRGFP vector is 4440bp long. After SSA the new fragment with primer 1 Bo TMR and 6 should be 870 bp long.

With the pmHPRT-DRGFP system I could show that in proliferating cells the homologous recombination repair predominates, as published by Hoeijmakers, 2001. However it was not possible to clearly conclude whether there is a difference between $MV_{4\text{-}11}$ (FLT3-ITD) and MOLM13 (FLT3-ITD/wt) in the repair efficiencies. Also I couldn't find any differences in the repair efficiencies between cell lines with FLT3 mutation ($MV_{4\text{-}11}$) and without FLT3 mutation (K562 and THP1). To clarify this uncertainty I chose another method based on the H2A.X phosphorylation which allowed me to directly measure the repair efficiency in the primary cell lines.

3.6.3 Repair analyses using γH2Ax assay

In the primary treatment of AML patients often combination chemotherapy is used. One of the currently using components is for example etoposide – DNA-damaging agents. Etoposide is a topoisomerase II inhibitor, and it induces double strand breaks

during DNA replication. DSBs induce a strong proapoptotic signal when damaged DNA is left unrepaired, since cell survival relies on the efficiency of DNA repair. One of the first enzymatic components to bind to the broken DNA ends is H2AX. H2AX is rapidly phosphorylated (yH2AX) in the chromatin micro-environment surrounding a DNA double-strand break (DSB). The measurement of the yH2AX provides information about the DSB-repair efficiency in different cell systems. yH2A.X phosphorylation assay was adopted to measure directly the repair efficiency in THP1, K562, MV_{4-11} (FLT3-ITD) and Molm13 (FLT3-ITD/wt)). I incubated the cells for one hour with etoposide to induce DSB and then, after three rinses in RPMI medium, the cells were returned to the incubator for 2h to allow time for repair to take place. Then cells were fixed and the yH2Ax phosphorylation was measured. The values from the chemiluminescence intensity after the incubation with etoposide and after 2h repair were compared and the difference defined the efficiency of repair calculated in %. Following treatment of THP1, K562 and MV_{4-11} (FLT3-ITD) with etoposide, there was a significant loss of yH2AX over 2 hours of repair, indicative of an active DSB repair pathway in these samples. However, the incubation of Molm13 (FLT3-ITD/wt) with etoposide demonstrated no loss of yH2AX after the same time period, indicative of a lack of repair of DSBs (Fig.3.27).

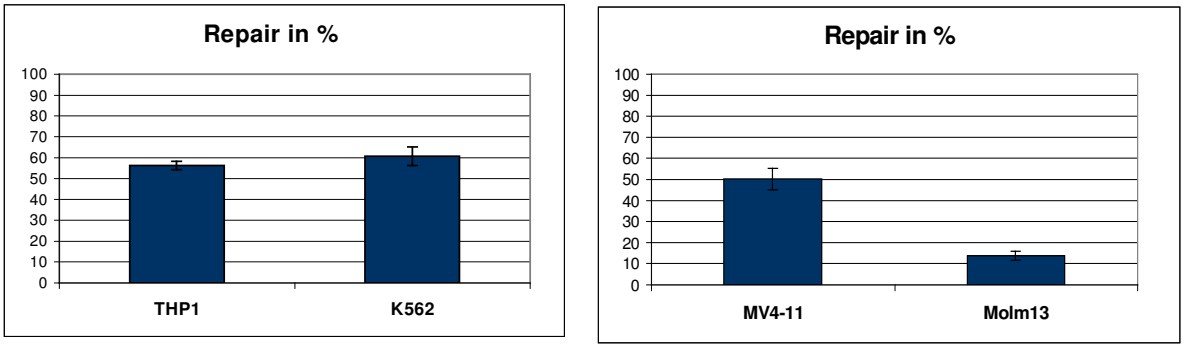

Fig.3.27 Repair efficiency measured by yHA2x assay.

The cells were cultivated with etoposide for one hour. After the wash with RPMI medium they were cultivated for an additional two hours in order for the repair to take place. The yH2Ax chemiluminescence was measured after the incubation with etoposide and after the repair time and the difference defined the efficiency of repair calculated in %.

Despite the absence of FLT3 expression in K562 the repair efficiency is very high and I couldn't determine any difference between K562 and MV_{4-11} (FLT3-ITD). K562 contains the BCR-ABL1 fusion gene (K562 (BCR-ABL1)) and following previous reports indicating the importance of the role of BCR-ABL fusion protein in the repair process, so this possibility was also tested in this project. The results are described below in the **chapter 1**. Additionally, to find out if the FLT3-ITD mutation has a direct impact on repair, I used a specific inhibitor for the FLT3 tyrosine kinase receptor – PKC412. The results are described below in **chapter 2**. Also the lower repair capacity in Molm13 (FLT3-ITD/FLT3wt) compared to MV_{4-11} (FLT3-ITD) could be explained by the effect of the heterozygosity state of FLT3 mutation in the cell repair process. To confirm this possibility I used MV_{4-11} (FLT3-ITD) transfected with vector containing the wt of FLT3 - MV4-11wt (provided by Dr. Sina Koch). The results are present below in **chapter 3**.

Chapter 1. The effect of BCR-ABL on the DNA-repair

The K562 cell lines contains the BCR-ABL1 b3-a2 fusion gene, which has a continuously active tyrosine kinase activity. The consequence is rapid proliferation of leukocytes in CML patients. BCR-ABL1 fusion protein could be responsible for the high repair efficiency published by Slupianek (Slupianek *et al.*, 2001). To confirm this I used Imatinib, which is a specific inhibitor of a number of tyrosine kinase enzymes including abl, c-kit and PDGF-R (Platelet-derived growth factor). Before the repair took place in the K562 (BCR/ABL), I first incubated the cells with Imatinib for four hours and then with etoposide for 1h to induce DSB. The values of chemiluminescence intensity after the incubation with etoposide and after a 2h repair were compared, and the difference defined the efficiency of repair calculated in %. As a control I used MV_{4-11} (FLT3-ITD) because it has no known inhibition effect from Imatinib on other tyrosine kinases like FLT3. In Fig.3.28 it can clearly be seen that the repair efficiency in K562 (BCR-ABL) incubated with Imatinib rapidly decreases compared to K562 (BCR-ABL) without imatinib, while the repair capacity in MV_{4-11} (FLT3-ITD) with Imatinib doesn't change compared to MV_{4-11} (FLT3-ITD) without Imatinib incubation.

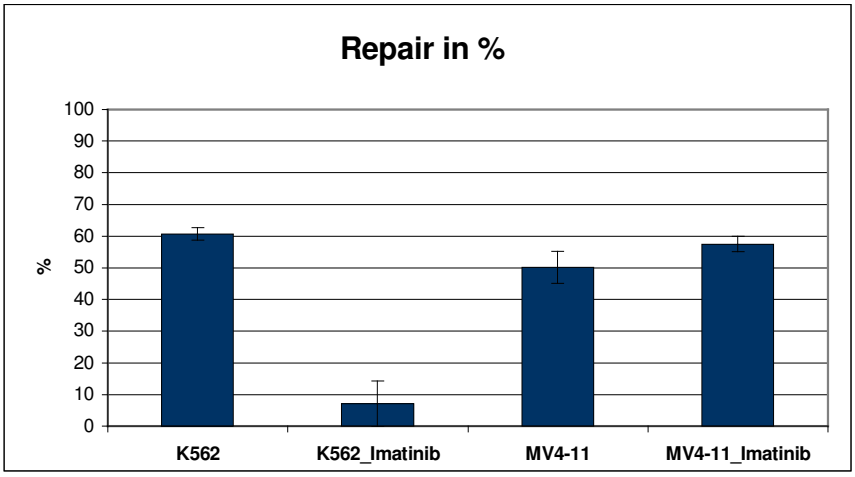

Fig.3.28 Repair efficiency after the Incubation of K562 (BCR-ABL) and MV_{4-11}(FLT3-ITD) with Imatinib.

The cells were incubated for four hours with Imatinib (specific inhibitor of Abl kinase) followed by incubation with etoposide and two hours repair time. The yH2Ax chemiluminescence was measured after the incubation with etoposide and after the repair time and the difference defined the efficiency of repair calculated in %.

Chapter 2. The effect of the FLT3-ITD mutation on the repair mechanism

To test if FLT3 mutation is responsible for a higher repair efficiency I used PKC412 (specific inhibitor of FLT3 kinase), which inhibits a number of class III tyrosine kinase receptors, including FLT3. I incubated MV_{4-11} (FLT3-ITD) with PKC412 for 4h before the incubation with etoposide. As a control I used K562 (BCR-ABL) because PKC412 has no inhibitory effect on BCR-ABL activity. In Fig.3.29 it is shown that PKC412 inhibits the repair efficiency in MV_{4-11} (FLT3-ITD), while there is no any effect in K562 (BCR-ABL) with and without PKC412 incubation.

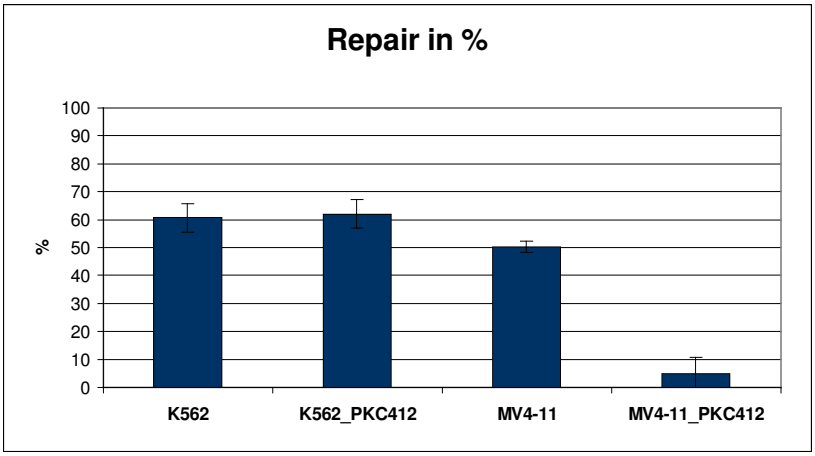

Fig.3.29 Repair efficiency after the incubation of K562(BCR-ABL) and MV_{4-11}(FLT3-ITD) with PKC412.

The cells were incubated for four hours with PKC412 (specific inhibitor of FLT3 kinase) followed by incubation with etoposide and two hours repair time. The yH2Ax chemiluminescence was measured after the incubation with etoposide and after the repair time and the difference defined the efficiency of repair calculated in %.

As was described above, the HR efficiency measured by flow cytometry in MV_{4-11} (FLT3-ITD) transfected with the pmHPRT-DRGFP vector was about 3% (Fig.3.20). I decided to confirm the inhibitory effect of PKC412 directly on HR as well. MV_{4-11} (FLT3-ITD) (transfected with pmHPRT-DRGFP and pCbASce vectors) was incubated with PKC412 for four hours. The cells were washed 3 times and further incubated for five days. As a control MV_{4-11} (FLT3-ITD) transfected with pmHPRT-DRGFP and pCbASce vectors was used. The GFP signal (resulting from HR) was measured using flow cytometry. I confirmed the HR of about 3% presented in Fig.3.20, but, as expected, I couldn't identify any GFP signal after PKC412 incubation (data not shown).

Chapter 3. Effect of the heterozygosity state of FLT3-ITD on the DNA repair

The next step in this project was to clarify if the missing of wt of FLT3 in MV_{4-11} (FLT3-ITD) increase the repair potential compared to Molm13 (FLT3-ITD/wt) (shown above on Fig.3.27). For this reason MV_{4-11} (FLT3-ITD) transfected with vector containing the wild type of FLT3 (MV4-11wt) was used for the measurement of the yH2Ax phosphorylation and for the determination of the repair efficiency. The results are shown in Fig.3.30. The repair efficiency decreased rapidly in MV_{4-11}wt compared to MV_{4-11} (FLT3-ITD). The level of the repair activity in MV_{4-11}wt was comparable with the level of repair in Molm13 (FLT3-ITD/wt). The very low level of repair in Molm13 measured with yH2Ax assays could be a possible explanation for the missing GFP signal observed after the transfection with pmHPRT-DRGFP and pCbASce vectors shown above.

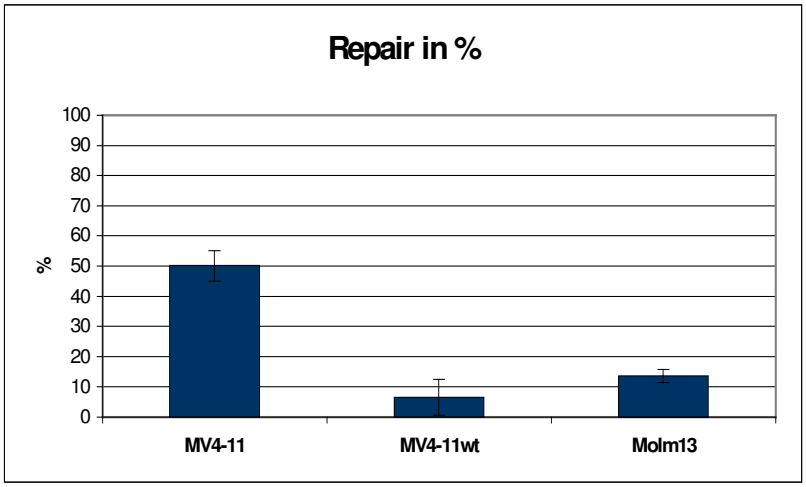

Fig.3.30 Repair efficiency in MV_{4-11} (FLT3-ITD), MV_{4-11}wt and Molm13 (FLT3-ITD/wt).
The cells were incubated for one hour with etoposide and after the wash procedure they were incubated for additionally two hours. The yH2Ax chemiluminescence was measured after the incubation with etoposide and after the repair time and the difference defined the efficiency of repair calculated in %.

3.7 Cell cycle analyses

Error-free, conservative HR repair involves strand invasion and requires a homologous DNA template. It is generally believed to occur preferentially in the late S, G2 and early M phases of the cell cycle, when the sister chromatid is available. Next, I attempted to clarify the effect of etoposide on the cell lines using cell cycle analysis. Additionally, the impact of the Imatinib and PKC412 followed by etoposide incubation on the cell cycle distribution was analysed. The results from the incubation of K562 (BCR/ABL), $MV_{4\text{-}11}$ (FLT3-ITD), $MV_{4\text{-}11}$wt (FLT3-ITD/wt) and Molm13 (FLT3-ITD/wt) with etoposide (1h) and after a 2h repair, as well as after the incubation with Imatinib and PKC412 (4h) followed by incubation with etoposide and a 2h repair are shown below. I could identify significant changes in the cell cycles in all four cell lines after the repair time. The 7h incubation of all four cell lines without inhibitors and induction of DSB didn't show any considerable changes and for this reason the results are not shown. In the K562 (BCR/ABL) (Fig.3.31/Table1 and Fig.3.32.A.) the fraction of the cells in the growth phases (S and G2/M phases) increased by 16.5% after the repair time. The impact of a 4h PKC412 incubation was the immediate 16.5% increase of the cell fraction in the growth phase. This is a known effect of PKC412 on leukaemic cells (Odgerel *et al*., 2007). This growth remained stable after the repair time. The movement of the cell fraction in the growth phase may correlate with the high repair efficiency measured after the incubation with etoposide as well as after the incubation with PKC412/Etoposide by yH2AX assay (Fig.3.29). No changes in the cell cycle in K562 (BCR/ABL) were observed after the incubation with Imatinib (ABL inhibitor) and etoposide, which may correlate with low repair efficiency measured by yH2AX assay (Fig.3.28).

I used the same procedure in measuring the cell cycle in $MV_{4\text{-}11}$ (FLT3-ITD). After the incubation with etoposide/repair time, the cells in the growth phase increased by 20.7% (Fig. 3.31/Table 2 and Fig. 3.32.B). Also a 12.8% increase of the cell fraction in the growth phase was measured after the incubation with Imatinib/Etoposide/repair. These results as well may correlate with the high repair efficiency measured after the incubation with etoposide as well as after the incubation with Imatinib/etoposide by yH2Ax assay (Fig.3.28). The impact of PKC412 on $MV_{4\text{-}11}$ (FLT3-ITD) is similar to K562: immediately after four hours of incubation with PKC412 (FLT3 inhibitor) the cell fraction increased by 20.5% in the growth

phase. However, unlike K562 the cell fraction in the growth phase decreased rapidly by 28.4% after the repair time, which is an indication of induction of apoptosis, as judged by an increase in the size of the sub-G_1 fraction (Fig.3.30/Table 2 and Fig.3.31.B). Again, these results may correlate with very low repair potential after the incubation with PKC412/etoposide measured by yH2Ax assay (Fig.3.29).

In contrast to K562 (BCR/ABL) and $MV_{4\text{-}11}$ (FLT3-ITD), $MV_{4\text{-}11}$wt (FLT3-ITD/wt) and Molm13 (FLT3-ITD/wt) cells were arrested in the G1 phase after etoposide incubation and 2h of repair, as well as after the incubation with Imatinib, PKC412 and etoposide (Fig.3.31/Table 3/4 and Fig.3.32.C/D). Apoptosis was barely observed in these cell lines up to 24 h after the repair time. These results may correlate with the very low repair efficiency measured in $MV_{4\text{-}11}$wt (FLT3-ITD/wt) and Molm13 (FLT3-ITD/wt) using yH2Ax assay (Fig.3.30).

Fig.3.31 Cell cycle distribution of K562 (BCR/ABL), $MV_{4\text{-}11}$ (FLT3-ITD), $MV_{4\text{-}11}$wt (FLT3-ITD/wt) and Molm13 (FLT3-ITD/wt).

Data are the means ± s.d. of n=3 independent experiments. Bold values indicate P<0.05. The proportion of cells in each phase of the cell cycle was calculated with the ModFitLT 2.0 program.

Table 1.

	K562 (BCR/ABL)				
	Control (%)	**Imatinib (%)**	**pV**	**PKC412 (%)**	**pV**
G0/G1	33.61 (±2.08)	34.64 (±0.72)	0,6	16.98 (±1.36)	**0.001**
S+G2/M	66.55 (±2.01)	65.36 (±0.72)	**0.5**	83.02 (±1.35)	**0.001**
1h etoposide					
G0/G1	46.94 (±4.08)	36.12 (±2.91)	0.11	16.18 (±2.08)	**0.004**
S+G2/M	53.06 (±4.08)	63.89 (±2.91)	0.11	85.48 (±0.84)	**0.01**
2h Repair					
G0/G1	16.94 (±0.42)	38.17 (±2,35)	**0,004**	17.19 (±2,24)	0.9
S+G2/M	83.06 (±0.42)	61.82 (±2.35)	**0.004**	82.42 (±1.88)	0.72

Table 2.

	MV_{4-11} (FLT3-ITD)				
	Control (%)	**Imatinib (%)**	**pV**	**PKC412 (%)**	**pV**
G0/G1	54.81(±0.72)	53.16 (±2.25)	0.35	34.32(±1.15)	**0.002**
S+G2/M	45.19 (±0.72)	46.84 (±2.25)	0.35	65.68 (±1.15)	**0.002**
1h etoposide					
G0/G1	48.67 (±0.5)	46.08(±3.6)	0.36	32.28 (±1.9)	**0.008**
S+G2/M	52.99 (±2.38)	53.91 (±3.61)	0.84	67.72 (±1.89)	**0.04**
2h Repair					
G0/G1	34.11(±1.23)	40.35(±2.96)	0.15	62.73(±0.35)	**0.001**
S+G2/M	65.89 (±1.23)	59.65 (±2.96)	0.15	37.27(±0.35)	**0.001**

Table 3.

	MV_{4-11}wt (FLT3-ITD/wt)				
	Control (%)	**Imatinib (%)**	**pV**	**PKC412 (%)**	**pV**
G0/G1	58,58(±1,97)	56,00(±2,86)	0.06	52,5(±2,15)	0.16
S+G2/M	41,42(±1,97)	44,00(±2,86)	0.06	47,48(±2,15)	0.16
1h etoposide					
G0/G1	63,17(±1.77)	62,37 (±3.35)	0.78	63,83 (±2.9)	0.85
S+G2/M	36.83(±1.77)	37.62 (±3.35)	0.78	36.16(±2.9)	0.85
2h Repair					
G0/G1	94.52 (±1.84)	89.77 (±3.96)	0.11	90.45 (±1.56)	0.08
S+G2/M	5.48 (±1.84)	10.23 (±3.96)	0.11	9.55 (±1.56)	0.08

Table 4.

	Molm13 (FLT3-ITD/wt)				
	Control (%)	**Imatinib (%)**	**pV**	**PKC412 (%)**	**pV**
G0/G1	63.79 (±2.92)	65.41 (±2.74)	0.46	46.56 (±0.79)	**0.02**
S+G2/M	36.21 (±2.92)	34.59 (±2.74)	0.46	53.44 (±0.79)	**0.02**
1h etoposide					
G0/G1	64.96 (±1.86)	63.92 (±1.97)	0.08	46.42 (±0.53)	**0.005**
S+G2/M	35.04 (±1.85)	36.08 (±1.97)	0.08	52.58 (±1.59)	**0.02**
2h Repair					
G0/G1	93.35 (±1.94)	91.55 (±2.01)	0.19	88.78 (±2.49)	0.14
S+G2/M	6.65 (±1.94)	8.45 (±2.01)	0.19	11.22 (±2.49)	0.14

Fig.3.32 Cell cycle changes in K562(BCR/ABL), MV_{4-11} (FLT3-ITD), MV_{4-11}wt (FLT3-ITD/wt) and Molm13 (FLT3-ITD/wt).

The cells were incubated with etoposide for one hour followed by further incubation for two hours for repair to take place. Additionally the cells were incubated with Imatinib or PKC412 for four hours before etoposide-incubation. Cells were harvested at the indicated time points, and stained with propidium iodide in preparation for cell cycle analysis. See Fig.3.31 for quantification and statistical analysis.

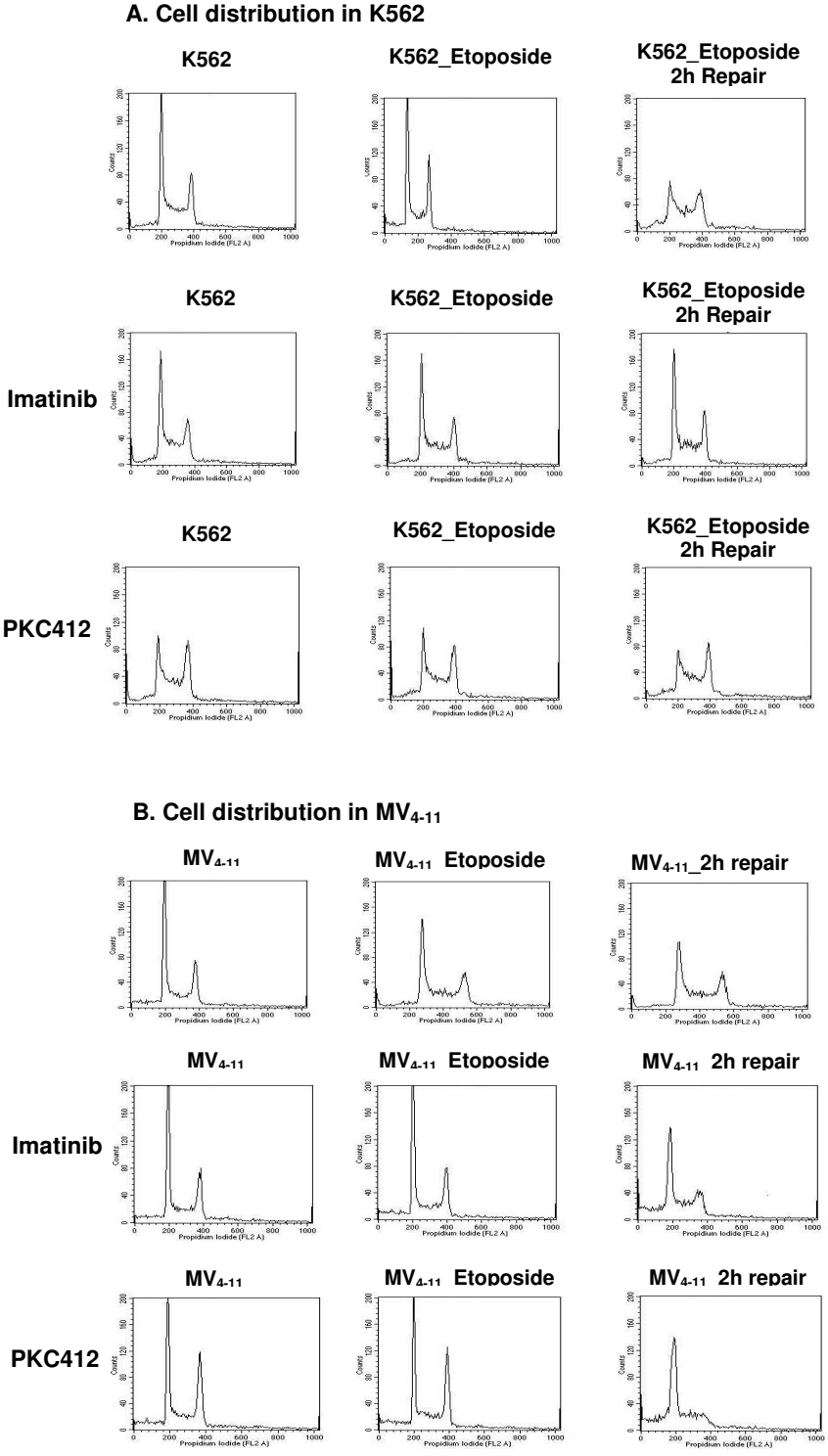

C. Cell distribution in MV_{4-11}wt

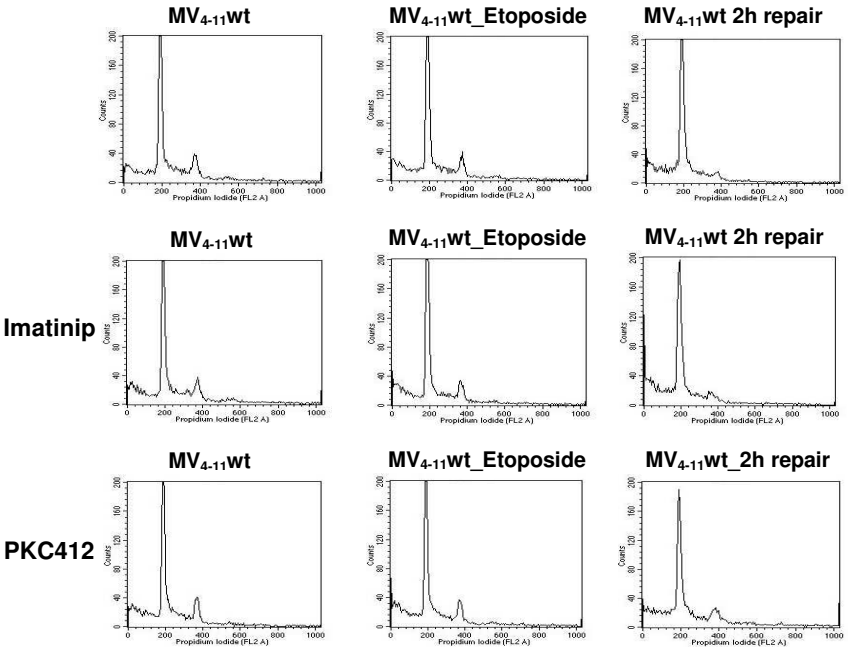

D. Cell distribution in Molm13

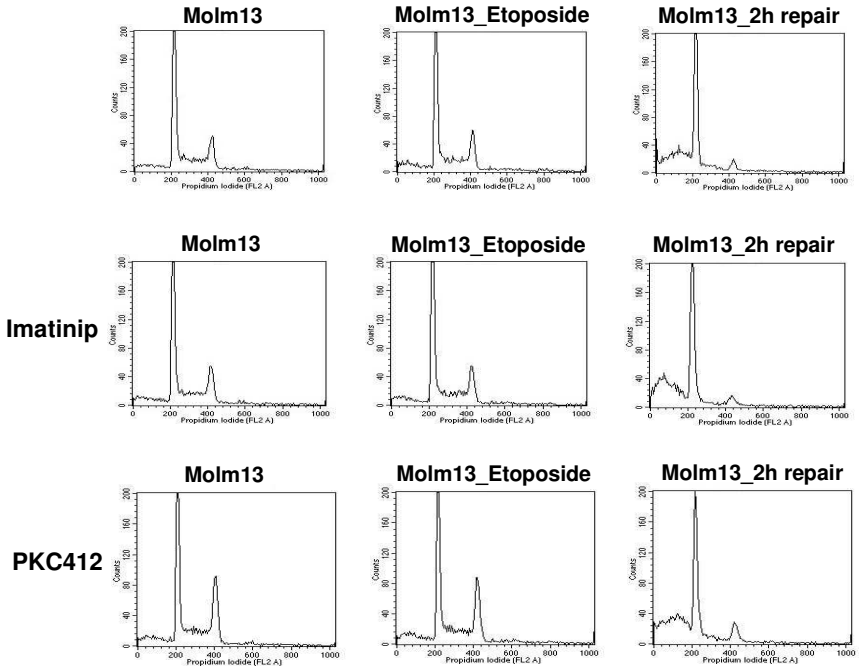

3.8 Expression of RAD51

The major enzymatic component of HHR in eukaryotic cells is RAD51, as cells deficient in RAD51 accumulate DSBs after replication or at stalled replication forks. I measured the expression of RAD51 in MV_{4-11} (FLT3-ITD), Molm13 (FLT3-ITD/wt) K562 (BCR/ABL) and THP1 using Real Time quantitative PCR. The results are presented in Fig.3.33. Despite the low repair efficiency in Molm13 measured by yH2Ax assay (Fig.3.27) the RAD51 expression levels in all 4 cell lines were very similar. I wanted to explain why despite the high expression of RAD51 in Molm13 the repair efficiency is very low.

The major HR proteins such as RAD51, RAD52, RAD54 etc., are re-localised within the nucleus in response to DNA damage to form distinct foci that can be visualised by immunofluorescent microscopy (Haaf *et al.,* 1995; Tan *et al.,* 1999; Liu & Maizels, 2000; Essers *et al*., 2002; Tarsounas *et al.,* 2004a). I next conducted an experiment based on immunofluorescence to test if any differences in the localisation of the RAD51 in the cells could be found. This could be a possible explanation of the different repair levels. Molm13 contains FLT3-ITD mutation as well as wt of FLT3 so I compared Molm13 (FLT3-ITD/wt) with MV_{4-11}wt (FLT3-ITD/wt), MV_{4-11} (FLT3-ITD) and K562 (BCR/ABL). I present here my preliminary experiments. The cells were incubated with etoposide for 1h to create a DSB. After this the cells were rinsed in RPMI medium and additionally incubated for 2h for repair to take place. RAD51 localisation was tested before the incubation with etoposide and after 2h repair. My preliminary results indicated that the RAD51 in K562 (BCR/ABL) (with high repair efficiency measured by yH2Ax assay) is mainly located in the cytoplasm before the incubation with etoposide. However, during the repair time a larger fraction of RAD51 could be detected in the nucleus (Fig.3.34). Similarly, in MV_{4-11} (FLT3-ITD) (with high repair efficiency measured by yH2Ax assay) RAD51 is mainly located in the cytoplasm, but could also be seen in the nucleus, at higher levels than in K562 (BCR/ABL). After the induction of double strand breaks, a small increase in RAD51 levels in the nucleus could be observed (Fig.3.34). This data indicate that in both cell lines the protein is imported into the nucleus during strand repair. In contrast, in Molm13 and MV_{4-11}wt (a cell line with low repair activity measured by yH2Ax assay) RAD51 is also detectable in the cytoplasm and nucleus before the incubation with etoposide, but after the repair time, the amount of RAD51 in the nucleus decreased

rapidly. In Fig. 3.34 the results from MV_{4-11}wt are presented. This is an indication that the protein was exported to the cytoplasm, and is, as expected, not part of the repair of DSB in the nucleus.

This data, although preliminary, indicate that in cell lines with different repair capacity RAD51 is probably involved in different signalling pathways contributing to its activation. Future experiments are necessary to prove if a direct association between FLT3-ITD and RAD51 exists as well as if this connection is relevant to the RAD51 activation and to establish if these results are statistically significant.

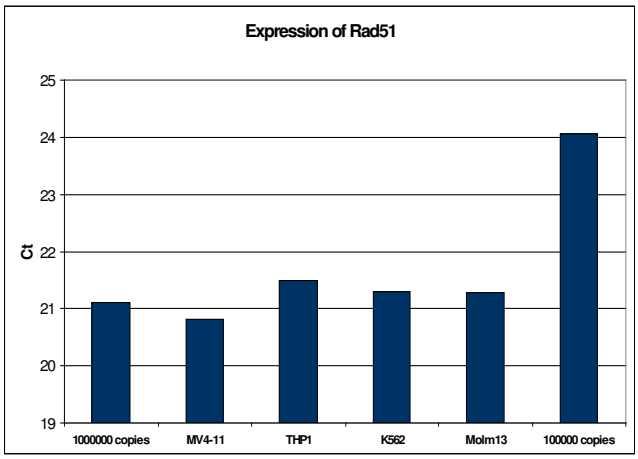

Fig.3.33 Expression level of RAD51 measured by Real Time quantitative PCR

The expression level in MV_{4-11}; Molm13; K562 and THP1 was measured by Real Time quantitative PCR using QuantiTect SYBR Green PCR Kit. All 4 cell lines showed simmilar level of RAD51 expression. These results don´t correlate with the different repair efficiency measured in these cell lines. GAPDH was used as a housekeeping gene.

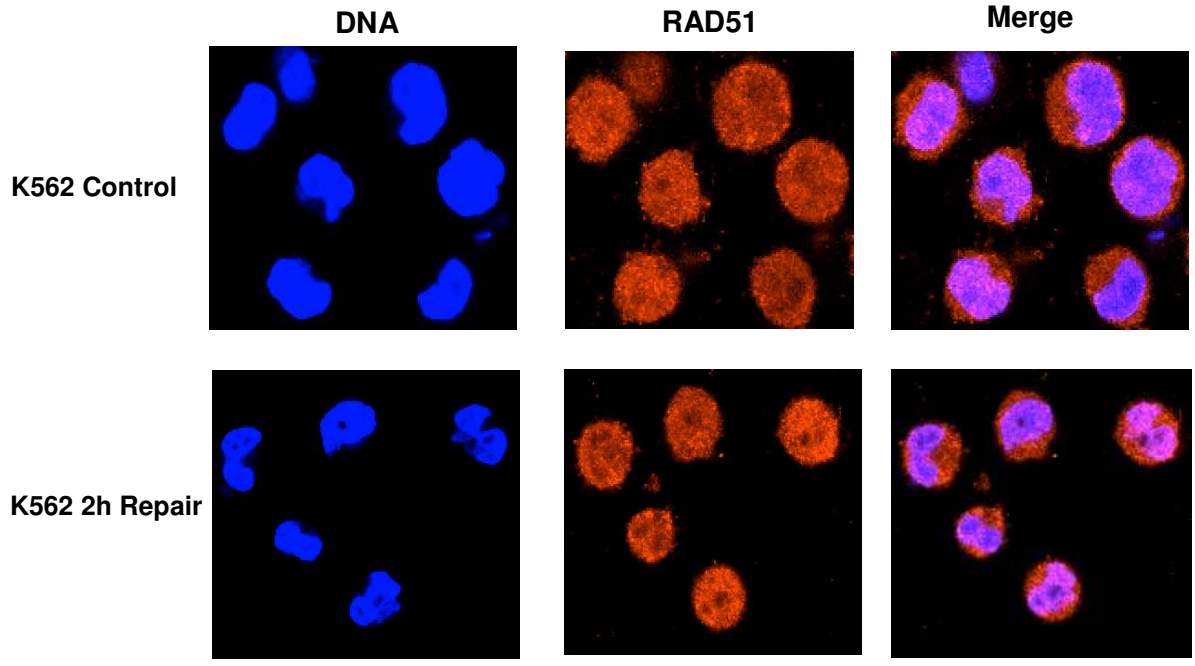

Fig.3.34; Page 92

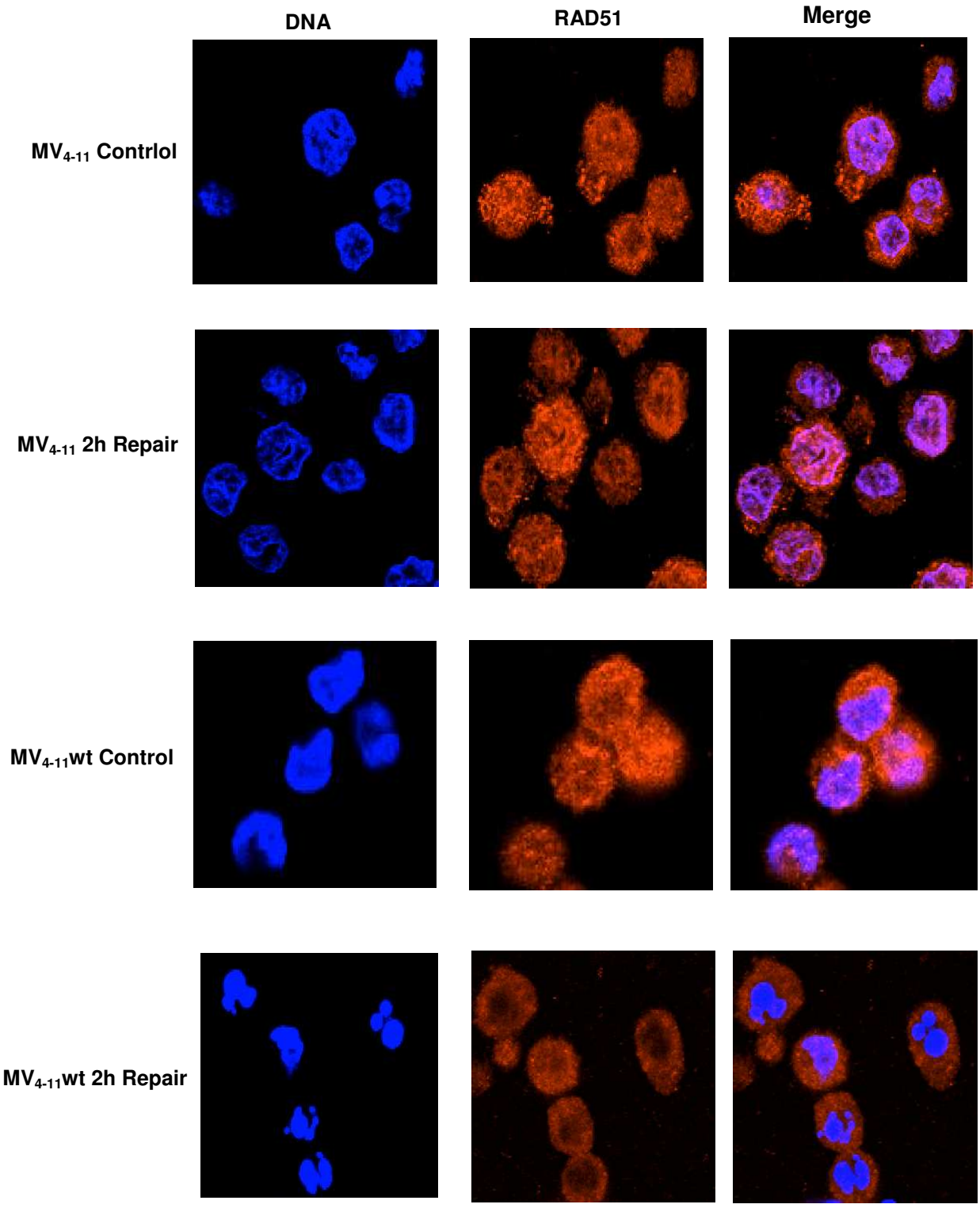

Fig.3.34 Confocal laser scanning microscopy of RAD51.

MV4-11, K562 and MV4-11wt cells were incubated with Etoposide followed by 2 hours further incubation (repair time). Immunofluorescence double-labelling was performed to identify the localisation of RAD51 in the cells before the etoposide incubation and after the repair time. DNA was stained with DAPI.

The scale bar is equal to 25 µm.

4. Discussion

4.1 Screening of AML patients for LOH using GeneChip Mapping 10K Array

Cytogenetics is considered one of the most valuable prognostic determinants in acute myeloid leukaemia (AML). The prognostic value of cytogenetic abnormalities identified by metaphase cytogenetic (MC) is well established in many malignancies. On the basis of response to induction treatment, relapse risk, and overall survival, the patients with detectable chromosome abnormalities could be classified in three prognostic groups – with favourable outcome, with poor prognosis and with intermediate prognosis. However, in a significant proportion of AML patients who show normal MC, this technique does not allow us further prognostic resolution. In all likelihood, clonal defects are present in patients, but their detection is precluded by low resolution of routine techniques. However some chromosomal aberrations were reported, like point mutations in the FLT3 gene, inactivated mutations in transcriptionfactor CEBPA and one of the most common mutations in the NPM1-gene. Raghavan also reported on uni-parental disomy (UPD) in connection with AML (Raghavan *et al.*, 2005).

Generally, development of cancer in human is a consequence of activation of protooncogenes and inactivation of tumorsupressor genes. Loss of genetic information through micro or macro deletions is a very common mechanism stimulating this process and transforming a normal cell into a cancer cell. The result is loss of one of the two alleles (loss of heterozygosity (LOH)) with a consequence - hemizygous genotype. The missing part can be duplicated from the remaining homologue chromosome known as UPD. In fact, UPD is a form of LOH where one allele is duplicated and a cell becomes a homologous genotype. When the duplicated region contains a tumorsupressor gene, that remaining allele is inactivated by point mutation, and the result is a complete loss of function in this gene, causing the development of cancer.

UPD was first described by Engel (Engel *et al.*,1980) who reported that it was likely to occur through meiotic error (i.e. constitutional UPD) (Shuman *et al.*, 2006 ; Smith *et al.*, 2007) and as a result of this germline event, all cells in the adult organism

carry the same UPD region. However, this event can also occur in somatic cells (i.e. acquired UPD) leading to development of cancer. Similar mechanisms of UPD have been shown to be important in the inactivation of tumorsuppressor genes or activation of oncogenes. One of these mechanisms occurs in the somatic cells during mitosis. This UPD might arise from a chromosomal segregation error, in which one allele is lost by anaphase lag and the remaining allele is then reduplicated, or it can stem from a non-disjunction error (Strachan *el al*., 2004). A second mechanisms, acquired segmental UPD can occur through mitotic recombination between pairs of high-identity, low-copy repeats (LCRs) in the S/G2 phase of the cell cycle (Stephens *et al*., 2006). Low-copy repeats (LCRs) can act as substrates for non-allelic homologous recombination (NAHR) and can result in deletions, duplications, translocations, or inversions of genomic segments located between the LCRs (Stankiewicz and Lupski 2002; Shaw and Lupski 2004). Another mechanism might be a double-strand break repair error, in which chromosomal breakage is followed by reduplication through homologous recombination to compensate for the loss of a segment.

Recently, UPD has been observed in different clonal haematologic disorders such as polycythaemia vera (Kralovics *et al*., 2002), childhood acute lymphoblastic leukaemia (ALL) (Rogan *et al*., 1995), hairy-cell leukaemia (HCL) (Forconi *et al*., 2008), chronic lymphocytic lymphoma (CLL) (Lehmann *et al*., 2008), myelodysplastic syndrome (MDS) (Wang *et al*. (2008), but also in solid tumors as breast cancer (Murthy *et al*., 2002), uveal melanoma (White et al., 1998), Wilm's tumors (Shearer *et al*., 1999), retinoblastoma (Hagstrom et al., 1999), tumors associated with Beckwith-Weidemann syndrome (Henry *at al*., 1991), glioblastoma (Lo *et al*., 2008) and meningioma (Krupp *et al*. 2008).

This project concentrated on the detection, classification and partially on the background of uni-parental disomy (UPD) in AML patients with normal karyotype. In fact, UPD might be a common but previously unrecognised mechanism in cancer development, because the karyotype appears 'normal' when examined by conventional cytogenetic analysis. Raghavan was the first to use Affymetrix technology to screen patients with AML for LOH changes, and to find that UPD occurring as a result of mitotic recombination could be found in about 20% of the AML patients with normal karyotype, but with unknown effect on AML development (Raghavan *et al*., 2005; Gorletta *et al*., 2005).

Within this work, in a group of 146 AML patients with normal karyotype and using 10K SNP arrays it was shown the utility of this technology platform to detect chromosomal abnormalities such as UPD. I showed that this aberration was present in 14% of the cases as either the sole abnormality or a concurrent defect (most commonly with FLT3-ITD or NPM1 mutations). This abnormality was present in various chromosomes starting from an undefined point and in almost all cases it also affected the telomere. Very interesting was the detection of UPD in the blasts as well as in the T-cells used as a disease free control in 6 patients. The possible mechanism is unknown, but if the event causing UPD happens during meiosis, no phenotypical anomalies occur, and this could be a possible explanation of UPD in the healthy material. Unfortunately, no remission material was available to prove the germline origin of the UPD in these 6 cases. Whether this event has an indirect impact on the disease progression is also unknown, but my data point out the necessity of analysing tumour-free material to confirm the somatic origin of the alteration. Certainly, the patients with LOH in the T-cells were excluded from the acquired UPD positive group.

In addition to the CN-neutral LOH, which cannot be detected by MC or fluorescence in situ hybridization, SNP arrays can also identify duplications and deletions. After screening 146 patients, I found three cases with losses of genetic information previously classified as having a normal karyotype according to conventional molecular diagnostics. Generally this technology improves the possibility of detecting a cryptic lesion in patients with normal karyotypes. Also by using SNP arrays it is possible to overcome several hurdles in cytogenetic analysis. First, the small DNA requirement (250 ng per array) allows rapid and exact molecular analysis even when very low cell numbers and small amounts of DNA are available. Second, the high resolution allows a more refined analysis, resulting in more accurate breakpoint determinations, detection of small deletions and amplifications, and identification of small segments of unbalanced translocations. Third, the SNP arrays provide information of chromosomal copy-number changes as well as single nucleotide polymorphism (SNP) genotypes, and this combination allows the detection of copy-neutral chromosomal aberrations such as UPD. However, SNP array technology can detect most but not all types of abnormalities such as balanced chromosome rearrangements - reciprocal translocations and inversions.

In this project Affymetrix 10K arrays were used, although arrays with much higher resolution are available from Affymetrix. The main reason for this is that this study was designed to identify large regions of UPD as a result of mitotic recombination, for which the 10K arrays are quite appropriate. However, higher-resolution arrays have the potential to identify much smaller recombinations of only a few thousand base pairs.

4.2 The impact of UPD on AML development

As was described above single gene mutations are an additional biological risk factor in AML. A possible mechanism for relapse is one in which a heterozygous mutation is followed by a mitotic recombination event or possibly by nondisjunction event (UPD) leading to homozygosity and clonal evolution. UPD might yield tumors that are homozygous for pre-existing mutations in genes, methylation of promoters of genes and focal deletion of genes. Raghavan reported that one AML patient with UPD in chr. 19q13.1 was homozygous for a CEBPA mutation (Raghavan *et al*., 2005). Additionally he found two patients with AML and UPD in chr. 11p. One case was with a homozygous methylated paternal H19 gene, whereas the other showed a homozygous non-methylated maternal pattern. H19 gene, located at 11p15.5, is normally methylated, and hence inactivated, in only the paternal allele. H19 is located in domain 1 of the 11p15.5 imprinted gene cluster. UPD in this region causes methylation or non-methylation of the H19 gene on both chromosomes which results either in biallelic silencing or biallelic activation of H19 respectively. Homozygous methylation was also identified in hepatoblastoma published by Suzuki (Suzuki. *et al*., 2008). All these results show that the UPD event in AML patients could have an important consequence in unmasking pre-existing mutations. Recently, some genes in which mutations are directly associated with the development of AML have been described. We sequenced some of the genes (RUNX1; WT1 and CEBPA) shown to be responsible for AML development that were located in the UPD regions. In one patient, with UPD in chr.19 we found an insertion in the CEBPA gene (CCAAT/enhancer binding protein). In AML, heterozygous as well as homozygous CEBPA mutations are well recognized (Lin LI *et al*., 2005). Although a biallelic mutation is not required for AML, it is important for the disease development. This

has been shown by Smith (Smith *et al.,* 2004) in cases in which a germ line CEBPA mutation is followed after a long latency by a second mutation leading to AML development and normally, these biallelic mutations are associated with acquired UPD of 19q (Wouters *et al*., 2007).

Another gene - RUNX1 (AML1), located in chr. 21, is the most frequent site of translocations in acute leukaemia such as t(8;21)(q22;q22) associated with AML-M2 and t(12;21)(p13;q22) associated with paediatric ALL (Look, 1997). The fusion onco-proteins resulting from these translocations, AML1-ETO and TEL-AML1, are well-known fusion oncogenes. Moreover, point mutations in RUNX1 have been observed in familial platelet disorder, a disease with predisposition to AML (Song *et al*., 1999; Buijs *et al*., 2001; Michaud *et al*., 2002). In addition, mutations, some of which were biallelic, have been observed in sporadic leukaemias (Osato *et al*., 1999; Preudhomme *et al*., 2000). Previous reports classified RUNX1 as a tumorsuppressor gene. In this study two patients with UPD in chr.21 were found and point mutations in RUNX1 gene were detected in both of them. Moreover, I sequenced the WT1 (Wilms' tumor) gene, also classified as a tumorsuppressor gene (Kim *et al*., 1998), in three patients with UPD in chr. 11, but a point mutation in only one of them was found. I proposed that more than one potential mutational target may be located in the UPD region, because relatively large regions of the genome are involved in this event. Also located in the long arm of chr. 11, the MLL and CBL genes are known to be responsible for leukaemia development. However, I found that these two genes were located in the aberrant region in 3 of 4 patients with UPD in chr. 11q. Which other genes from 11q could be additionally involved in disease progression is not clear. Recent reports have shown that aberrations in chr. 11 are generally correlated with intermediate to poor prognoses. My statistical analyses also show that the patients with UPD in chr. 11 have the poorest outcome compared with the remaining UPD positive cases and UPD negative patients. Moreover, I found that in patients with UPD who achieved complete remission after induction chemotherapy, 60.0% relapsed within the first 6 months. In contrast, the rate of relapse in patients without UPD was only 38.2% (P=0.065). Generally the OS in the patients with UPD was significantly lower compared with UPD negative cases.

Furthermore, I couldn't find any connection between age, WBC-counts or sex and UPD, but I found that the FAB M1 subtype was observed in 47.6% of the UPD positive patients, compared to only 19.2% of the UPD negative patients (P=0.04).

Again I found that UPD commonly correlated with FLT3-ITD, MLL-PTD or NPM1 mutations, but without significant differences.
The identification of new UPD regions in cancer might give us the opportunity to discover new cancer-related genes that are mutated, deleted, methylated or imprinted. This could have important implications for classifying cancers and might provide insight into their pathogenesis, prognosis and treatment options.

4.3 Gene expression profiling of the UPD positive and UPD negative cases

Gene expression profiling has been developed over the last years and has held promises to improve diagnosis, risk classification, and outcome prediction in acute leukaemias as well as in other human cancers. In fact, gene expression profiling in AML is becoming well established and has already been proven to be valuable in diagnosing different cytogenetic subtypes, discovering novel AML subclasses, and predicting clinical outcome. Recently, gene expression profiling studies in AML showed a remarkable level of concordance in findings that may ultimately lead to an increasingly refined molecular taxonomy (Golub *et al.,* 1999; Downing 2003). In the present study, 14% of the AML patients with normal karyotype were found to have UPD. The gene expression analyses could supply a valuable new approach to the classification of this subgroup of AML. Therefore, I used the Affymetrix gene expression system to compare some UPD positive patients with UPD negative patients. I could demonstrate clearly, that the UPD-positive group and the UPD negative group segregated in two different clusters based on different gene expression profiles. Also some subgroups could be identified, for example UPD in chr.11 together with UPD in chr.2. These results suggest that gene expression profiling might become useful as a powerful tool to identify novel cluster groups and potential targets for therapy. Furthermore, uniparental disomy may lead to alterations in the expression levels of imprinted genes. In addition, variation in expression between two alleles is common (Lo *et al.,* 2003). Therefore, if it is maintained after mitotic recombination, uniparental disomy could be associated with specific gene expression patterns. Taken together, this could be used to identify new tumor suppressor genes responsible for AML development. The detection and classification

of new genes involved in the development of AML is very important for future diagnostics and is significant in selecting the most appropiate therapies and determining the clinical outcome not only in AML, but also in other malignancies. Additionally, the identification of new lesions could allow for further stratification within prognostic groups defined by the WHO.

4.4 The impact of FLT3-ITD on repair efficiency

In this study UPD was often diagnosed as a dual aberration with FLT3 or NPM1 mutations. FLT3 is a class III receptor tyrosine kinase (RTK) structurally related to the receptors for platelet derived growth factor (PDGF), colony stimulating factor 1 (CSF1), and stem cell factor receptor (c-KIT). These RTK contain extracellular domain composed of five immunoglobulin-like domains, one transmembrane region, and a cytoplasmic kinase domain split into two parts by a kinase-insert domain. FLT3 receptor is activated by binding of the fms-related tyrosine kinase 3 ligand (FL) to the extracellular domain, which induces homodimer formation in the plasma membrane leading to autophosphorylation of the receptor and subsequent signalling through posphorylation of multiple cytoplasmatic proteins with important functions in the survival, proliferation and differentiation of primitive hemopoietic progenitor cells. FLT3 mutations consist of two major types: internal tandem duplication (ITD) mutations of 3-400 bp (always in-frame) that map to the juxtamembrane region (25-30% of AML patients); point mutations that most frequently involve aspartic acid 835 of the kinase domain (KD) but have also been found less frequently in several other sites (5–12% of AML patients). The mutations mapping to the juxtamembrane region (frequently insertions, but also point mutations) are sometimes referred to as length mutations (LM) in the literature. Both types of mutations result in autophosphorylation as well as phosphorylation of a number of proteins, either directly or indirectly. Previous studies on diagnostic material have shown that FLT3-ITD is a marker of a poor prognosis (Thiede *et al.*, 2002; Whitman *et al.*, 2001) and increases the risk of relapse (Gale *et al.,* 2005). Additionally, FLT3-ITD patients (without FLT3wt) have a significantly shortened survival compared with FLT3wt and/or FLT3-ITD/wt patients. More recently, reports have shown that the most important prognostic factor is not the FLT3 mutations alone, but the allelic ratio of FLT-ITD/wt. Patients with a high

mutant/wildtype ratio of the FLT3 receptor have a significantly shorter OS (Steudel et al., 2003). The loss of the wt of FLT3 receptor in AML patients with FLT3-ITD mutation is a consequence of deletions in chr.13. Cells with only one copy of the mutated tyrosine kinase receptor (FLT3-ITD/-) have hemizygous genotypes - $FLT3^{ITD/-}$. Recently it was shown that in patients with normal karyotype the missing part is duplicated by homologous recombination (Thiede *et al.,* 2002). Numerous signalling pathways are disturbed in the AML patients with FLT3-ITD mutation, but generally they have a higher rate of treatment failure. An enhanced ability to survive genotoxic assimilation might explain this clinical observation, leading us to focus on the DNA repair process in FLT3-ITD positive patients. I identified 6 patients with FLT3-ITD mutation and UPD in different chromosomes but not in chromosome 13. Additionally, it was interesting to find one case with UPD in chromosome 13 but without FLT3-ITD mutation. I proposed to investigate the impact of the FLT3-ITD mutation on homologous recombination using pmHPRT-DRGFP/pCbASce vectors-system and yHA2x assay. As expected, the homologous recombination measured with pmHPRT-DRGFP/pCbASce vectors-system was the predominant repair mechanism in haematopoetic cell lines, but I couldn't find any difference between FLT3-ITD positive and FLT3-ITD negative cells. Also the identification of SSA was difficult with this vector system. The pmHPRT-DRGFP vector carries a gene conferring resistance to puromycin. Puromycin is used only in cell biology as a selective agent in cell culture systems, but it is toxic to prokaryotic and eukaryotic cells. It is possible that in some aspects this toxicity has a negative effect on the repair mechanism in the haematopoetic cell lines. To overcome this effect I next used HA2x assay to measure the repair efficiency directly in the cells. With this assay and using PKC412 (specific inhibitor of FLT3-ITD) I was able to confirm the impact of FLT3-ITD on the repair process. The results after incubation with PKC412 of FLT3-ITD cells was reduction of DNA repair; in contrast, no difference in the repair capacity was observed in cells without FLT3 expression. Also Seedhouse demonstrated that FLT3-ITD cells repair DSBs in DNA more efficiently than FLT3wt cells. Incubation with PKC412 resulted in a reduction of DNA repair in FLT3-ITD cells but not in FLT3wt cells. They also proposed that increased DNA repair in FLT3-ITD cells contributes to the risk of disease relapse by allowing damaged leukaemia cells to repair their genome, survive and mediate relapse (Seedhouse *et al.,* 2006).

Furthermore, in this project clear difference was shown in the repair efficiency between the cells only with FLT3-ITD mutation and heterozygous (FLT3-ITD/wt) cells; the FLT3-ITD cells rapidly enhanced the repair process while in heterozygous (FLT3-ITD/wt) cells, the repair efficiency was very low. These results were confirmed using cells with FLT3-ITD mutation (without FLT3wt expression) transfecting with a vector containing FLT3wt. After the transfection a rapid decrease in the repair capacity in the cells with FLT3-ITD/wt compared with the primary (FLT3-ITD) cells was observed. Moreover, I showed that different mutations could be responsible for the enhanced DNA repair, for example BCR-ABL translocation. Slupianek published that the BCR-ABL1 fusion protein could be responsible for the high repair efficiency (Slupianek *et al.*, 2001). After incubation with imatinib (specific inhibitor of bcr-abl) the repair efficiency rapidly decreased in the cells containing this aberration. No changes in the repair capacity were found in the bcr-abl negative cells after incubation with Imatinib. These results might also explain the high homologous repair efficiency measured in the cell lines with FLT3-ITD mutation and cell lines without FLT3-ITD mutation but with BCR-ABL translocation using pmHPRT-DRGFP/pCbASce vectors system.

Error-free, conservative HR repair involves strand invasion and requires a homologous DNA template. It is generally believed to occur preferentially in the late S, G2 and early M phases of the cell cycle, when the sister chromatid is available. Cell cycle analyses of the cell lines used in this work revealed a clear correlation between the repair efficiency and cell cycle changes. The high repair efficiency is related to the movement of the cell fraction in the growth phases (S and G2/M phases). This conclusion was confirmed after the incubation with specific inhibitors like imatinib and PKC412. PKC412 is a specific inhibitor for FLT3-ITD and induces G2 arrest but not apoptosis in AML cell lines without aberrant FLT3 activation. In contrast, PKC412- induces massive apoptosis without markedly affecting cell cycle patterns in AML cell lines harbouring FLT3 mutations. After the incubation of FLT3-ITD cells with PKC412 the repair potential decreased rapidly, correlating with the arrest of the cell fraction in the G1 sub-phase. In contrast, after the incubation with PKC412, high repair efficiency was observed in cells without FLT3 expression; this was correlated with the increase of the cell fraction in the growth phases (S and G2/M phases). Furthermore, after the incubation with imatinib, the repair efficiency in cells containing BCR-ABL aberration rapidly decreased, an event associated with the

arrest of the cell fraction in the G1 sub-phase. The cells without this aberration maintained a high repair capacity aligned with the increase of the cell fraction in the growth phases (S and G2/M phases). The very low repair efficiency of the heterozygous (FLT3-ITD/wt) cells correlate with the arrest of the cell fraction in G1 sub-phase and induction of apoptosis.

All these results show clearly that the enhancement of the repair efficiency in cells with FLT3-ITD mutation is correlated with the lag of the wt of the FLT3 receptor. Probably in patients with FLT3-ITD/wt genotype and UPD in other chromosomes the repair capacity is not increased which was speculated at the start of these experiments. Generally, the development of leukaemia is correlated with the co-operation of a minimum of two mutations - “two hit” model (described in chapter 1.3.4). Recently, in mice models it was shown that FLT3-ITD mutation alone is not enough for the development of AML disease phenotype. I suggest that the existence of FLT3-ITD mutation could be responsible for the duplication of mutations in tumorsupressor genes as a second event in the pathogenesis of AML. This correlates with the detection of some mutations in genes in some of the UPD regions described as important for AML development shown above (4.2).

4.5 Expression of RAD51

Aberrant signalling in FLT3-ITD cells occurs via a number of pathways, including signal transducers and activator of transcription 5 (STAT5), mitogen-activated protein (MAP) kinase and phosphatidylinositol 3 (PI3) kinase pathways (Hayakawa *et al.*, 2000; Mizuki *et al*,. 2000). STAT5 regulates the expression of a variety of proteins, among them Bcl-x(L) and RAD51, by direct transcriptional activation. Bcl-x(L) belongs to the family of Bcl-2 proteins and plays an essential role in resistance to apoptotic cell death by preventing membrane hyperpolarization and mitochondrial swelling in response to death stimuli (Heiden *et al.*, 1997). Bcl-x(L) is overexpressed in a high percentage of AML patients and confers a poor prognosis in these patients (Schaich *et al*,. 2001).

RAD51 plays a central role in homologous recombinational (HR) repair of DNA double-strand breaks (DSBs) (Daboussi *et al.*, 2002). Elevated transcription of RAD51 was shown to be dependent on STAT5 expression in BCR/ABL-transformed

cells (Slupianek *et al*., 2001). The role of RAD51 in drug resistance appears to be specific for drugs that induce DSBs, for example, etoposide as was published by Lundin *et al*., who observed fewer DSBs and faster HR of DNA lesions in RAD51-overexpressing cells after etoposide treatment compared to control cells (Lundin *et al*., 2003). In addition, RAD51 plays a dual role in both HR of DSBs and telomere protection from attrition and fusion (Tarsounas *et al*., 2004b).

Following previous reports indicating the importance of the role of RAD51 in leukaemic cells, the expression level of this protein in cell lines without FLT3-ITD mutation as well as with FLT3-ITD/- and FLT3-ITD/wt genotypes was investigated using Real Time quantitative PCR. I couldn't identify any correlation between the expression level in the cells with and without FLT3-ITD as well as with FLT3-ITD/wt. This result was in contrast to the very low repair efficiency measured in the FLT3-ITD/wt cells. The major HR proteins such as RAD51, RAD52 and RAD54, are re-localised within the nucleus in response to DNA damage to form distinct foci. To investigate if this process was not disturbed in cells with low repair efficiency I performed the visualisation of the location of RAD51 using imunofluorescence. My previous results show that even though RAD51 could be found in the nucleus, it is mainly present in the cytoplasm in all the cell lines I analysed. After the induction of DSB, the nuclear amount of the RAD51 rapidly increased in cells with high repair efficiency. In contrast, in the cells with very low repair efficiency the nuclear level of RAD51 rapidly decreased. These data indicate that in cells with very high repair potential this protein is imported into the nucleus during strand repair. In contrast, in cells with low repair capacity the protein was exported to the cytoplasm, and is, as expected, not part of the repair of DSB in the nucleus.

AML is a very heterogeneous disease and different signalling pathways are dysregulated. Although it is possible that, in parallel to the STAT5 upregulation of RAD51, other activating mutations and signalling pathways contribute to RAD51 activation. These data, although preliminary, indicate that in cell lines with wt FLT3, different regulatory mechanisms are responsible for RAD51 expression. Future experiments are necessary to clarify the association between FLT3-ITD or the wt of FLT3 and RAD51, as well as the signalling background of the RAD51 regulation in AML patients.

5. Summary

Acute myeloid leukaemia represents a heterogeneous group of early stem cell disorders. characterised by an uncontrolled expansion of malignant cells (“blasts”) blocked at certain stages of myeloid differentiation. AML is the most common acute leukaemia affecting adults with median age of 65 to 70 years. This disease is genetically very heterogeneous and is associated with diverse cytogenetic abnormalities such as chromosomal deletions, translocations and duplications. The outcome for patients with AML depends greatly on the age of the patient and leukaemic cell karyotype. For this reason the diagnosis of the karyotype is one of the most important factors to determine patient outcome. The development of new methods of diagnosis and the classification of different genetic aberrations present in leukaemia is very important for the treatment of this disease.

This study focused on the detection, classification and partially on the background of uniparental disomy (UPD) in adult patients with AML. The following results were obtained:

1. Using Affymetrix technology 14% UPD was identified in one group of 146 patients with normal karyotype. In 6 patients this aberration was found in the blast as well as in the T-cells, with unknown impact. Additionally deletions in three patients previously classified with normal karyotype according to conventional molecular diagnostics were detected. Generally this technology improves thus the possibility of detecting a cryptic lesion in patients with normal karyotypes.
2. The relationship between UPD and AML was confirmed with the detection of specific gene aberrations in some UPD regions. Furthermore, the obtained data indicate that patients with UPD have a higher rate of treatment failure and this might be used as a prognostic marker in the future.
3. It was demonstrated that the UPD positive group and the UPD negative group segregate in two different clusters based on different gene expression profiles. These preliminary results suggest that gene expression profiling might become useful as a powerful tool to identify novel cluster groups and potential targets for therapy.
4. Furthermore, the available results demonstrated that FLT3-ITD mutation increased the DSB repair by homologous recombination rapidly. It was shown

also that PKC412 inhibits the DSB repair in FLT3-ITD positive cells. In contrast, in cells without FLT3 expression after the incubation with PKC412, no changes in the repair efficiency were observed. Also differences were found in the repair efficiencies between FLT3-ITD cells and FLT3-ITD/wt cells. The heterozygous cells clearly showed low repair efficiency compared to the FLT3-ITD cells. This was confirmed by transfection of homozygous FLT3-ITD cells with FLT3wt vector. After the transfection the repair efficiency in FLT3-ITD/wt cells decreased rapidly compared to the primary FLT3-ITD cells. Additionally, It was demonstrated that also another mutation, BCR-ABL, increased the HR repair. After the inhibition of the BCR-ABL activity using Imatinib (bcr-abl inhibitor) the repair efficiency decreased rapidly.

5. The preliminary results suggest that not only the expression of RAD51, but mainly its localisation, is important for its HR repair capacity. Moreover, RAD51 supposedly is involved in different signalling pathways in FLT3-ITD cells and FLT3-ITD/wt cells as well as in the FLT3wt cells.

On the basis of these data and data from literature I can conclude that UPD is a common aberration in AML patients with normal karyotype. I suggest that this aberration constitute a „second hit“ event in leukaemia development and different tumor supressor genes could be involved in this process. The event of HR is associated with the high DSB repair capacity resulting in the impact of different mutations such as FLT3-ITD or BCR-ABL. Moreover, I found that the wt of FLT3 is able to eliminate the high repair capacity of the FLT3-ITD mutation. This correlates with of the finding that the patients with DLT3-ITD/wt have better prognosis compared to the patients with very high FLT3-ITD ratio. The high DSB repair capacity enhances the ability to survive genotoxic assimilation by chemotherapy drugs, and it may at the same time contribute to the high incidence of relapse. These results imply that downregulation of RAD51 (for example by FLT3 inhibition) would be valuable before DNA damage occurs through the genotoxic agent in order to reduce the relapse risk of AML.

6. References

Ailles LE, Gerhard B, Hogge DE. (1997) "Detection and characterization of primitive malignant and normal progenitors in patients with acute myelogenous leukemia using long-term coculture with supportive feeder layers and cytokines." *Blood;* 90(7):2555-64.

Akashi K, Traver D, Miyamoto T, Weissman IL. (2000) "A clonogenic common myeloid progenitor that gives rise to all myeloid lineages." *Nature;* 404(6774):193-7.

Albala JS, Thelen MP, Prange C, Fan W, Christensen M, Thompson LH, Lennon GG. (1997) "Identification of a novel human RAD51 homolog, RAD51B." *Genomics;* 46, 476--479.

Batty, D.P. and Wood, R.D. (2000) "Damage recognition in nucleotide excision repair of DANN." *Gene;* 241,193-204.

Benhamou, S. and Sarasin, A. (2000) "Variability in nucleotide excision repair and cancer risk: a review." *Mutat Res;* 462,149-58.

Bennett JM, Catovsky D, Daniel MT, Flandrin G, Galton DA, Gralnick HR, Sultan C. (1976) "Proposals for the classification of the acute leukaemias. French-American-British (FAB) co-operative group." *Br J Haematol.;* 33(4):451-8.

Beran M, Luthra R, Kantarjian H, Estey E. (2004) " FLT3 mutation and response to intensive chemotherapy in young adult and elderly patients with normal karyotype*." Leukemia Research;* 28(6):547-50.

Bloomfield CD, Goldman A, Hassfeld D, de la Chapelle A. (984) "Fourth International Workshop on Chromosomes in Leukemia, 1982: Clinical significance of chromosomal abnormalities in Acute myeloid leukaemia" *Can. Genetics and Cytogen.;* 11, 332-350.

Bloomfield CD, Herzig GP, Caligiuri MA. (1997) "Introduction: acute leukemia: recent advances." *Semin Oncol;* 24(1):1-2.

Blume-Jensen, P. and Hunter, T. (2001) "Oncogenic kinase signalling." *Nature;* 411(6835):355-65.

Braybrooke JP, Spink KG, Thacker J, Hickson ID. (2000) "The RAD51 family member, RAD51L3, is a DNA-stimulated ATPase that forms a complex with XRCC2." *J. Biol. Chem.*; 275, 29100--29106.

Brenneman MA, Wagener BM, Miller CA, Allen C, Nickoloff JA.Brenneman MA, Wagener BM, Miller CA, Allen C, Nickoloff JA. (2002) "XRCC3 controls the fidelity of homologous recombination: roles for XRCC3 in late stages of recombination." *Mol Cell*; 10(2):387-95.

Buijs A, Poddighe P, van Wijk R, van Solinge W, Borst E, Verdonck L, Hagenbeek A, Pearson P, Lokhorst H. (2001) "A novel CBFA2 single-nucleotide mutation in familial platelet disorder with propensity to develop myeloid malignancies." *Blood;* 98(9):2856-8.

Byrd JC, Mrózek K, Dodge RK, Carroll AJ, Edwards CG, Arthur DC, Pettenati MJ, Patil SR, Rao KW, Watson MS, Koduru PR, Moore JO, Stone RM, Mayer RJ, Feldman EJ, Davey FR, Schiffer CA, Larson RA, Bloomfield CD; Cancer and Leukemia Group B (CALGB 8461). (2002) "Pretreatment cytogenetic abnormalities are predictive of induction success, cumulative incidence of relapse, and overall survival in adult patients with de novo acute myeloid leukemia: results from Cancer and Leukemia Group B (CALGB 8461)." *Blood;* 100(13):4325-36.

Caligiuri MA, Strout MP, Lawrence D, Arthur DC, Baer MR, Yu F, Knuutila S, Mrózek K, Oberkircher AR, Marcucci G, de la Chapelle A, Elonen E, Block AW, Rao PN, Herzig GP, Powell BL,

Ruutu T, Schiffer CA, Bloomfield CD. (1998) “Rearrangement of ALL1 (MLL) in acute myeloid leukemia with normal cytogenetics” *Cancer Research;* 58, 55-59.

Care RS, Valk PJ, Goodeve AC, Abu-Duhier FM, Geertsma-Kleinekoort WM, Wilson GA, Gari MA, Peake IR, Löwenberg B, Reilly JT. 2003 “ Incidence and prognosis of c-KIT and FLT3 mutations in core binding factor (CBF) acute myeloid leukaemias.“ *Br J Haematol.;* 121(5):775-7.

Carow CE, Levenstein M, Kaufmann SH, Chen J, Amin S, Rockwell P, Witte L, Borowitz MJ, Civin CI, Small D. (1996) “Expression of the hematopoietic growth factor receptor FLT3 (STK-1/Flk2) in human leukemias.” *Blood;* 87(3):1089-96.

Cartwright R, Tambini CE, Simpson PJ, Thacker J.Cartwright,R. (1998) “The XRCC2 DNA repair gene from human and mouse encodes a novel member of the recA/RAD51 family.” *Nucleic Acids Res.;* 26, 3084--3089.

Cary RB, Peterson SR, Wang J, Bear DG, Bradbury EM, Chen DJ. (1997) “DNA looping by Ku and the DNA-dependent protein kinase.” *Proc Natl Acad Sci U S A.*; 94: 4267–72.*Cell.*; 91:627-637.

Champion MD., Hawley RS. (2002) “Playing for half the deck: the molecular biology of meiosis.” *Nat Cell Biol; 4(Suppl):* s50-s56.

Chu G. (1997) “Double-strand break repair.” *J Biol Chem.*; 272: 24097–100.

Cleaver, J.E.. (2005) “Cancer in xeroderma pigmentosum and related disorders of DANN repair.“ *Nat Rev Cancer;* 5,564-73.

Colaia´covo, M. P., F. Paˆques, and J. E. Haber. (1999) “Removal of one nonhomologous DNA end during gene conversion by a RAD1- and MSH2- independent pathway.” *Genetics* 151:1409–1423.

Costa RM, Chigançcas V, Galhardo Rda S, Carvalho H, Menck CF. (2003) ”The eukaryotic nucleotide excision repair pathway.” *Biochimie;* 85,1083-99.

Crane MM, Strom SS, Halabi S, Berman EL, Fueger JJ, Spitz MR, Keating MJ. (1996) “Correlation between selected environmental exposures and karyotipe in acute myelocytic leukemia.“ *Cancer Epidemiol. Biomarkers Prev.*; 5, 639-644.

Critchlow SE, Bowater RP, Jackson SP. (1997) “Mammalian DNA double-strand break repair protein XRCC4 interacts with DNA ligase IV.” *Curr Biol.*; 7: 588–98.

Critchlow SE, Jackson SP. (1998) “DNA end-joining: from yeast to man.” *Trends Biochem Sci.*; 23: 394–8.

Daboussi F, Dumay A, Delacote F, Lopez BS. (2002) “DNA double-strand break repair signalling: the case of RAD51 post-translational regulation.” *Cell Signal.;*14:969-975.

de Laat WL, Jaspers NG, Hoeijmakers JH. (1999) “Molecular mechanism of nucleotide excision repair.” *Genes Dev;* 13(7),768-85.

Deschler B, Lübbert M. (2006) „Acute myeloid leukemia: epidemiology and etiology.“ Cancer; 107(9):2099-107.

Döhner K, Tobis K, Ulrich R, Fröhling S, Benner A, Schlenk RF, Döhner H. (2002) “Prognostic significance of partial tandem duplications of the MLL gene in adult patients 16 to 60 years old with acute myeloid leukemia and normal cytogenetics: a study of the Acute Myeloid Leukemia Study Group Ulm.“ *Journal of Clinical Oncology;* 20(15):3254-61.

Dosanjh MK, Collins DW, Fan W, Lennon GG, Albala JS, Shen Z, Schild D.Dosanjh,M.K. (1998) "Isolation and characterization of RAD51C, a new human member of the RAD51 family of related genes." *Nucleic Acids Res.;* 26, 1179--1184.

Downing JR. (2003) " Acute leukemia: subtype discovery and prediction of outcome by gene expression profiling." Verh Dtsch Ges Pathol.; 87:66-71.

Drexler, H. G. (1996) "Expression of FLT3 receptor and response to FLT3 ligand by leukemic cells." *Leukemia*; 10(4): 588-99.

Drexler, HG. (1996) "Expression of FLT3 receptor and response to FLT3 ligand by leukemic cells." *Leukemia;*10(4):588-99. Review.

Dzierzak E. (2005) "The emergence of definitive hematopoietic stem cells in the mammal." *Curr Opin Hematol;* 12(3):197-202.

Engel, E. (1980) "A new genetic concept: uniparental disomy and its potential effect, isodisomy." *Am. J. Med. Genet.*; 6, 137–143.

Essers J, Houtsmuller AB, van Veelen L, Paulusma C, Nigg AL, Pastink A, Vermeulen W, Hoeijmakers JH, Kanaar R. (2002) "Nuclear dynamics of RAD52 group homologous recombination proteins in response to DNA damage." *EMBO J;* 15;21(8):2030-7.

Estay, E. and Döhner, H (2006) "Acute myeloid leukaemia" *Lancet;* 306, 1894-1907.

Farag SS, Archer KJ, Mrózek K, Ruppert AS, Carroll AJ, Vardiman JW, Pettenati MJ, Baer MR, Qumsiyeh MB, Koduru PR, Ning Y, Mayer RJ, Stone RM, Larson RA, Bloomfield CD. (2006) " Pretreatment cytogenetics add to other prognostic factors predicting complete remission and long-term outcome in patients 60 years of age or older with acute myeloid leukemia: results from Cancer and Leukemia Group B 8461." *Blood;* 108(1):63-73.

Farag SS, Ruppert AS, Mrózek K, Mayer RJ, Stone RM, Carroll AJ, Powell BL, Moore JO, Pettenati MJ, Koduru PR, Stamberg J, Baer MR, Block AW, Vardiman JW, Kolitz JE, Schiffer CA, Larson RA, Bloomfield CD. (2005) "Outcome of induction and postremission therapy in younger adults with acute myeloid leukemia with normal karyotype: a cancer and leukemia group B study." *Journal of Clinical Oncology;* 23(3):482-93.

Feldmann E, Schmiemann V, Goedecke W, Reichenberger S, Pfeiffer P. (2000) "DNA double-strand break repair in cellfree extracts from Ku80-deficient cells: implications for Ku serving as an alignment factor in non-homologous DNA end joining." *Nucleic Acids Res.*; 28: 2585–96.

Fenske TS, Pengue G, Mathews V, Hanson PT, Hamm SE, Riaz N, Graubert TA. (2004) "Stem cell expression of the AML1/ETO fusion protein induces a myeloproliferative disorder in mice". *Proc Natl Acad Sci U S A;* 101, 15184-15189.

Fenske TS, Pengue G, Mathews V, Hanson PT, Hamm SE, Riaz N, Graubert TA. (2005) "Genetic polymorphisms in the base excision repair pathway and cancer risk: a HuGE review." *Am J Epidemiol;* 162, 925-42.

Fishman-Lobell, J., and J. E. Haber. (1992) "Removal of nonhomologous DNA ends in double-strand break recombination: the role of the yeast ultraviolet repair gene RAD1." *Science;* 258:480–484.

Forconi F, Poretti G, Kwee I, Sozzi E, Rossi D, Rancoita PM, Capello D, Rinaldi A, Zucca E, Raspadori D, Spina V, Lauria F, Gaidano G, Bertoni F. (2008) "High density genome-wide DNA profiling reveals a remarkably stable profile in hairy cell leukaemia." *Br J Haematol.*; 141, 622–630.

Fortini P, Pascucci B, Parlanti E, D'Errico M, Simonelli V, Dogliotti E. (2003) "The base excision repair: mechanisms and ist relevance for cancer susceptibility" *Biochimie;* 85(11):1053-71.

French CA, Masson JY, Griffin CS, O'Regan P, West SC, Thacker J. (2002) “Role of mammalian RAD51L2 (RAD51C) in recombination and genetic stability.” *J. Biol. Chem;* 277, 19322--19330.

Friedberg, E.C. (2001) “How nucleotideexcision repair protects against cancer.” *Nat Rev Cancer;* 1,22-33.

Fröhling S, Schlenk RF, Stolze I, Bihlmayr J, Benner A, Kreitmeier S, Tobis K, Döhner H, Döhner K. (2002) ”CEBPA mutations in younger adults with acute myeloid leukemia and normal cytogenetics: prognostic relevance and analysis of cooperating mutations.“ *J Clin Oncol*; 22(4):624-33

Gabbianelli M, Pelosi E, Montesoro E, Valtieri M, Luchetti L, Samoggia P, Vitelli L, Barberi T, Testa U, Lyman S. (1995) ”Multi-level effects of flt3 ligand on human hematopoiesis: expansion of putative stem cells and proliferation of granulomonocytic progenitors/monocytic precursors.“ *Blood;* 86(5):1661-70.

Gale RE, Hills R, Kottaridis PD, Srirangan S, Wheatley K, Burnett AK, Linch DC. (2005) „No evidence that FLT3 status should be considered as an indicator for transplantation in acute myeloid leukemia (AML): an analysis of 1135 patients, excluding acute promyelocytic leukemia, from the UK MRC AML10 and 12 trials.“ *Blood;* 106(10):3658-65.

Gilliland and Griffin 2002a “The roles of FLT3 in hematopoiesis and leukemia.“ *Blood*; 100(5):1532-42.

Gilliland and Griffin 2002b “Role of FLT3 in leukemia.“ *Curr Opin Hematol;* 9(4):274-81.

Golub TR, Slonim DK, Tamayo P, Huard C, Gaasenbeek M, Mesirov JP, Coller H, Loh ML, Downing JR, Caligiuri MA, Bloomfield CD, Lander ES. (1999) ” Molecular Classification of Cancer: Class Discovery and Class Prediction by Gene Expression Monitoring.“ Science.; 286(5439):531-7.

Goger M, Gupta V, Kim WY, Shigesada K, Ito Y, Werner MH. (1999) “Molecular insights into PEBP2/CBF beta-SMMHC associated acute leukemia revealed from the structure of PEBP2/CBF beta.“ *Nat Struct Biol;* 6(7):620-3.

Gorletta TA, Gasparini P, D’Elios M, Trubia M, Giuseppe Pelicci P and Paolo Di Fiore P. (2005) “Frequent Loss of Heterozygosity without Loss of Genetic Material in Acute Myeloid Leukemia with a Normal Karyotype.“ GENES, CHROMOSOMES & CANCER 44:334–337.

Grawunder U, Wilm M, Wu XT, Kulesza P, Wilson TE, Mann M, Lieber MR. (1997) “Activity of DNA ligase IV stimulated by complex formation with XRCC4 protein in mammalian cells.” *Nature*.; 388: 492–5.

Grawunder U, Zimmer D, Fugmann S, Schwarz K, Lieber MR. (1998) “DNA ligase-IV is essential for V(D)J recombination and DNA double-strand break repair in human precursor lymphocytes.” *Mol Cell*.; 2: 477–84.

Grimwade D, Walker H, Harrison G, Oliver F, Chatters S, Harrison CJ, Wheatley K, Burnett AK, Goldstone AH; Medical Research Council Adult Leukemia Working Party. (2001) “The predictive value of hierarchical cytogenetic classification in older adults with acute myeloid leukemia (AML): analysis of 1065 patients entered into the United Kingdom Medical Research Council AML11 trial.“ *Blood;* 98(5):1312-20.

Grimwade D, Walker H, Oliver F, Wheatley K, Harrison C, Harrison G, Rees J, Hann I, Stevens R, Burnett A, Goldstone A. (1998) “The importance of diagnostic cytogenetics on outcome in AML: analysis of 1,612 patients entered into the MRC AML 10 trial. The Medical Research Council Adult and Children's Leukaemia Working Parties.“ *Blood;* 92(7):2322-33.

Gu YS, Jin SF, Gao YJ, Weaver DT, Alt FW. (1997) “Ku70-deficient embryonic stem cells have increased ionizing radiosensitivity, defective DNA end-binding activity and inability to support V(D)J recombination.” *Proc Natl Acad Sci U S A*.; 94: 8076–81.

Haaf T, Golub EI, Reddy G, Radding CM, Ward DC.(1995) "Nuclear foci of mammalian Rad51 recombination protein in somatic cells after DNA damage and its localization in synaptonemal complexes." *Proc Natl Acad Sci U S A;* 92(6):2298-302.

Haase D, Feuring-Buske M, Könemann S, Fonatsch C, Troff C, Verbeek W, Pekrun A, Hiddemann W, Wörmann B. (1995) "Evidence for malignant transformation in acute myeloid leukemia at the level of early hematopoietic stem cells by cytogenetic analysis of CD34+ subpopulations." *Blood;* 86(8):2906-12.

Haferlach, T. and Schoch, C. (2002) "Modern techniques in leukemia diagnosis*". Internist (Berl)*; 43, 1190, 1193-1196, 1199-1202.

Hagstrom SA, Dryja TP. (1999) "Mitotic recombination map of 13cen-13q14 derived from an investigation of loss of heterozygosity in retinoblastomas." *Proc Natl Acad Sci USA*;96:2952-7.

Harris NL, Jaffe ES, Diebold J, Flandrin G, Muller-Hermelink HK, Vardiman J, Lister TA, Bloomfield CD. (1999). "The World Health Organization classification of neoplastic diseases of the hematopoietic and lymphoid tissues. Report of the Clinical Advisory Committee meeting, Airlie House, Virginia, November, 1997". *Ann Oncol;* 10, 1419-1432.

Hayakawa F, Towatari M, Kiyoi H, Tanimoto M, Kitamura T, Saito H. (2000) "Tandem-duplicated FLT3 constitutively activates STAT5 and MAP kinase and introduces autonomous cell growth in IL-3- dependent cell lines." *Oncogene*; 2000; 19: 624–631.

Heiden M, Chandel N, Williamson E, Schumacker P, Thompson C. (1997) "Bcl-xL regulates the membrane potential and volume homeostasis of mitochondria." *Cell.*; 91:627-637.

Henry I, Bonaiti-Pellie C, Chehensse V, *et al*. (1991) "Uniparental paternal disomy in a genetic cancerpredisposing syndrome." *Nature*; 351:665–7.

Henry-Mowatt J, Jackson D, Masson JY, Johnson PA, Clements PM, Benson FE, Thompson LH, Takeda S, West SC, Caldecott KW. (2003) "XRCC3 and Rad51 modulate replication fork progression on damaged vertebrate chromosomes*." Moll Cel*; 11(4):1109-17.

Hjertson M, Sundström C, Lyman SD, Nilsson K, Nilsson G. (1996) "Stem cell factor, but not flt3 ligand, induces differentiation and activation of human mast cells." *Exp Hemat;* 24(6):748-54.

Hoeijmakers JH. 2001 "Genome maintenance mechanisms for preventing cancer." *Nature*; 411:366-74

Huang J, Wei W, Zhang J, Liu G, Bignell GR, Stratton MR, Futreal PA, Wooster R, Jones KW, Shapero MH. (2004) "Whole genome DNA copy number changes identified by high density oligonucleotide arrays." *Human Genomics;* 1(4):287-99

Hung RJ, Brennan P, Canzian F, Szeszenia-Dabrowska N, Zaridze D, Lissowska J, Rudnai P, Fabianova E, Mates D, Foretova L, Janout V, Bencko V, Chabrier A, Borel S, Hall J, Boffetta P. (2005) "Large-scale investigation of base excision repair genetic polymorphism and lung canser risk in a multicenter study." J Nat Cancer Inst; 97,567-76.

Jackson S. P. (2001) "Detecting, signalling and repairing DNA double-strand breaks." Biochem Soc Trans.: 655-61.

Jackson S. P. (2002) " Sensing and repairing DNA double-strand breaks." Carcinogenesis.: 687-96.

Jascur, T. and Boland, C.R. (2006) "Structure and function of the components of the human DNA mismatch repair system." *Int J Cancer;* 119(9):2030-5.

Jasin, M., (2002) “Homologous repair of DNA damage and tumorigenesis: the BRCA connection.” *Oncogene;* 21(58):8981-93.

Jeggo PA, Tesmer J, Chen DJ. (1991) “Genetic-analysis of ionizing-radiation sensitive mutants of cultured mammalian-cell lines.” *Mutat Res.*; 254: 125–33.

Jeggo PA. *(*1998) “Identification of genes involved in repair of DNA double-strand breaks in mammalian cells.“ *Radiat Res.;* 150: S80–91.

Junop MS, Modesti M, Guarne A, Ghirlando R, Gellert M, Yang W. (2000) “Crystal structure of the Xrcc4 DNA repair protein and implications for end joining.” *EMBO J.*; 19: 5962–70.

Kainz B, Heintel D, Marculescu R, Schwarzinger I, Sperr W, Le T, Weltermann A, Fonatsch C, Haas OA, Mannhalter C, Lechner K, Jaeger U. (2002) ”Variable prognostic value of FLT3 internal tandem duplications in patients with de novo AML and a normal karyotype, t(15;17), t(8;21) or inv(16).“ *Hematology Journal;* 3,283-289.

Karran P, Offman J, Bignami M. (2003) Human mismatch repair, druginduced DANN damage,and secondary.“ *Biochimie;* 85,1149-60.

Kelly LM, Liu Q, Kutok JL, Williams IR, Boulton CL, Gilliland DG. (2002) “FLT3 internal tandem duplication mutations associated with human acute myeloid leukemias induce myeloproliferative disease in a murine bone marrow transplant model.“ *Blood;* 99, 310-318.

Khanna KK, Jackson SP. (2001) “DNA double-strand breaks: signaling, repair and the cancer connection.” *Nat Genet.*; 27: 247–54.

Kiyoi H, Naoe T, Nakano Y, Yokota S, Minami S, Miyawaki S, Asou N, Kuriyama K, Jinnai I, Shimazaki C, Akiyama H, Saito K, Oh H, Motoji T, Omoto E, Saito H, Ohno R, Ueda R. (1999) “Prognostic implication of FLT3 and N-RAS gene mutations in acute myeloid leukemia.“ Blood; 93(9):3074-80.

Kiyoi H, Towatari M, Yokota S, Hamaguchi M, Ohno R, Saito H, Naoe T. (1998) “Internal tandem duplication of the *FLT3* gene is a novel modality of elongation mutation which causes constitutive activation of the product.” *Leukemi; 12:* 1333– 1337.

Knudson, A.G. (2001) “Two genetic hits (more or less) to cancer.” *Nat. Rev. Cancer;* 1,157–170

Kobayashi J, Antoccia A, Tauchi H, Matsuura S, Komatsu K. (2004) “NBS1 and its functional role in the DNA damage response.“ *DNA Repair;* 3: 855-861

Kondo M, Weissman IL, Akashi K. (1997) “Identification of clonogenic common lymphoid progenitors in mouse bone marrow.“ *Cell;* 28;91(5):661-72.

Kottaridis PD, Gale RE, Frew ME, Harrison G, Langabeer SE, Belton AA, Walker H, Wheatley K, Bowen DT, Burnett AK, Goldstone AH, Linch DC. (2001) ”The presence of a FLT3 internal tandem duplication in patients with acute myeloid leukemia (AML) adds important prognostic information to cytogenetic risk group and response to the first cycle of chemotherapy: analysis of 854 patients from the United Kingdom Medical Research Council AML 10 and 12 trials.“ *Blood;* 98(6):1752-9.

Kottaridis PD, Gale RE, Linch DC. (2003) “Flt3 mutations and leukaemia.” *Br. J. Haematol.*; 122,523–538.

Kralovics R, Guan Y, Prchal JT. (2002) “Acquired uniparental disomy of chromosome 9p is a frequent stem cell defect in polycythemia vera.“ *Exp. Hematol.*; 30, 229–236.

Kristoffer Valerie and Lawrence F Povirk (2003) “ Regulation and mechanisms of mammalian double-strand break repair.“ Oncogene; 22**,** 5792–5812.

Krogh BO, Symington LS. (2004) “Recombination proteins in yeast.“ Annu Rev Genet.; 38:233-71.

Kruglyak and Nickerson 2001 ”Variation is the spice of life.“ *Nat Genet;* 27(3):234-6.

Krupp, W. et al. (2008) “Genome-wide genetic characterization of an atypical meningioma by single-nucleotide polymorphism array-based mapping and classical cytogenetics.“ *Cancer Genet. Cytogenet.*; 184, 87– 93.

Kurumizaka H, Ikawa S, Nakada M, Eda K, Kagawa W, Takata M, Takeda S, Yokoyama S, Shibata T. (2001) “Homologous-pairing activity of the human DNA-repair proteins Xrcc3.Rad51C.” *Proc Natl Acad Sci U S A;* 98(10):5538-43.

Lee KJ, Huang J, Takeda Y, Dynan WS. (2000) “DNA ligase IV and XRCC4 form a stable mixed tetramer that functions synergistically with other repair factors in a cell-free end-joining system.” *J Biol Chem.*; 275: 34787–96.

Lees-Miller SP, Godbout R, Chan DW, Weinfeld M, Day RS, Barron GM, Allalunis-Turner J. (1995) “Absence of p350 subunit of DNA-activated protein kinase from a radiosensitive human cell line.” *Science.*; 267: 1183–5.

Lehmann S, Ogawa S, Raynaud SD, Sanada M, Nannya Y, Ticchioni M, Bastard C, Kawamata N, Koeffler HP. (2008) “Molecular allelokaryotyping of early-stage, untreated chronic lymphocytic leukemia.“ *Cancer* ; 112, 1296–1305.

Lemischka, I. (2001) “Stem cell dogmas in the genomics era.“ *Rev Clin Exp Hematol;* 5(1):15-25.

Lin LI, Chen CY, Lin DT, Tsay W, Tang JL, Yeh YC, Shen HL, Su FH, Yao M, Huang SY, Tien HF. (2005) ”Characterization of CEBPA mutations in acute myeloid leukemia: most patients with CEBPA mutations have biallelic mutations and show a distinct immunophenotype of the leukemic cells.“ *Clin Cancer Res.*; 11:1372-1379.

Liu & Maizels, (2000) “Coordinated response of mammalian Rad51 and Rad52 to DNA damage.“ *EMBO Rep;* 1(1):85-90.

Liu N, Lamerdin JE, Tebbs RS, Schild D, Tucker JD, Shen MR, Brookman KW, Siciliano MJ, Walter CA, Fan W, Narayana LS, Zhou ZQ, Adamson AW, Sorensen KJ, Chen DJ, Jones NJ, Thompson LH. (1998) “XRCC2 and XRCC3, new human Rad51-family members, promote chromosome stability and protect against DNA crosslinks and other damages.” *Mol. Cell;* 1, 783--793.

Liu Y, Masson JY, Shah R, O'Regan P, West SC. (2004) “RAD51C is required for Holliday junction processing in mammalian cells.” *Science;* 303, 243--246.

Lo HS, Wang Z, Hu Y, Yang HH, Gere S, Buetow KH, Lee MP. (2003) “Allelic variation in gene expression is common in the human genome.” *Genome Res.;* 13:1855–62.

Lo KC, Bailey D, Burkhardt T, Gardina P, Turpaz Y, Cowell JK. (2008) “Comprehensive analysis of loss of heterozygosity events in glioblastoma using the 100K SNP mapping arrays and comparison with copy number abnormalities defined by BAC array comparative genomic hybridization.“ *Genes Chromosomes Cancer*; 47, 221–237.

Look, AT. (1997) “ALL E2A-HLF chimeric transcription factors in pro-B cell acute lymphoblastic leukemia.“ *Curr Top Microbiol Immunol.;* 220:45-53.

Lundin C, Schultz N, Arnaudeau C, Mohindra A, Hansen L, Helleday T. (2003) “RAD51 is involved in repair of damage associated with DNA replication in mammalian cells.” *J Mol Biol.;* 328:521-535.

Mahajan KN, Nick McElhinny SA, Mitchell BS, Ramsden DA. (2002) “Association of DNA polymerase mikro (pol mikro) with Ku and ligase IV: role for pol mikro in end-joining double-strand break repair.” *Mol Cell Biol.*; 22: 5194–202.

Mazin AV, Alexeev AA, Kowalczykowski SC. (2003) “A novel function of Rad54 protein. Stabilization of the Rad51 nucleoprotein filament.” *J. Biol. Chem;* 278: 14029–14036.

Mehrotra B, George TI, Kavanau K, Avet-Loiseau H, Moore D 2nd, Willman CL, Slovak ML, Atwater S, Head DR, Pallavicini MG. (1995) “Cytogenetically aberrant cells in the stem cell compartment (CD34+lin-) in acute myeloid leukemia.“ *Blood;* 86(3):1139-47.

Melnick A, Licht JD.Melnick A. (1999) “Deconstructing a disease: RARalpha, its fusion partners, and their roles in the pathogenesis of acute promyelocytic leukemia.“ *Blood;* 93(10):3167-215.

Michaud J, Wu F, Osato M, Cottles GM, Yanagida M, Asou N, Shigesada K, Ito Y, Benson KF, Raskind WH, Rossier C, Antonarakis SE, Israels S, McNicol A, Weiss H, Horwitz M, Scott HS. (2002) ”In vitro analyses of known and novel RUNX1/AML1 mutations in dominant familial platelet disorder with predisposition to acute myelogenous leukemia: implications for mechanisms of pathogenesis.“ *Blood;* 99(4):1364-72.

Mitelman F, Nilsson PG, Brandt L, Alimena G, Gastaldi R, Dallapiccola B. (1981) “Chromosome pattern, occupation and clinical feature in patients with acute nonlymphocytic leukemia.“ *Cancer Genet. Cytogenet,;* 4, 197-214.

Mizuki M, Fenski R, Halfter H, Matsumura I, Schmidt R, Müller C, Grüning W, Kratz-Albers K, Serve S, Steur C, Büchner T, Kienast J, Kanakura Y, Berdel WE, Serve H. 2000 ”Flt3 mutations from patients with acute myeloid leukemia induce transformation of 32D cells mediated by the Ras and STAT5 pathways.“ *Blood;* 96(12):3907-14.

Moorman AV, Roman E, Willett EV, Dovey GJ, Cartwright RA, Morgan GJ. (2001) “Karyotype and age in acute myeloid leukemia. Are they linked?“ *Cancer Genet Cytogenet;* 126(2):155-61.

Mortensen UH, Bendixen C, Sunjevaric I, Rothstein R. (1996) “DNA strand annealing is promoted by the yeast Rad52 protein.” *Proc. Natl. Acad. Sci. USA*; 93:10729–10734.

Mrózek K, Döhner H, Bloomfield CD. (2007) “ Influence of new molecular prognostic markers in patients with karyotypically normal acute myeloid leukemia: recent advances*.“ Curr Opin Hematol.;*14(2):106-14.

Mrózek K, Heerema NA, Bloomfield CD. (2004) “Cytogenetics in acute leukemia.“ *Blood Rev.* 18(2):115-36.

Mrózek K, Heinonen K, Bloomfield CD. (2001) “Clinical importance of cytogenetics in acute myeloid leukaemia.” *Best Pr. and Research Clinical Haemat.;* 14, 19-47

Mrózek K, Heinonen K, de la Chapelle A, Bloomfield CD. (1997) “Clinical significance of cytogenetics in acute myeloid leukemia.“ *Semin Oncol;* 24(1):17-31.

Muñoz L, Nomdedéu JF, Villamor N, Guardia R, Colomer D, Ribera JM, Torres JP, Berlanga JJ, Fernández C, Llorente A, Queipo de Llano MP, Sánchez JM, Brunet S, Sierra J; Spanish CETLAM Group. (2003) “Acute myeloid leukemia with MLL rearrangements: clinicobiological features, prognostic impact and value of flow cytometry in the detection of residual leukemic cells.” *Leukemia;* 17, 76-82.

Murthy SK, DiFrancesco LM, Ogilvie RT, Demetrick DJ. (2002) “Loss of heterozygosity associated with uniparental disomy in breast carcinoma.“ *Mod Pathol*; 15: 1241–50.

Nakao M, Yokota S, Iwai T, Kaneko H, Horiike S, Kashima K, Sonoda Y, Fujimoto T, Misawa S. (1996) “Internal tandem duplication of the flt3 gene found in acute myeloid leukemia.” *Leukemia;* 10, 1911-1918

Neubauer A, Dodge RK, George SL, Davey FR, Silver RT, Schiffer CA, Mayer RJ, Ball ED, Wurster-Hill D, Bloomfield CD. (1994) “ Prognostic importance of mutations in the ras proto-oncogenes in de novo acute myeloid leukemia.“ *Blood;* 83(6):1603-11.

Nickoloff JA. 2002 “Recombination: mechanisms and roles in tumorigenesis.” *In: Bertino JR, ed. Encyclopedia of Cancer. 2nd Edition. San Diego, USA: Elsevier Science*; 49-59.

Odgerel T, Kikuchi J, Wada T, Shimizu R, Futaki K, Kano Y, Furukawa Y. 2007 „The FLT3 inhibitor PKC412 exerts differential cell cycle effects on leukemic cells depending on the presence of FLT3 mutations“ *Oncogene*; 1–9.

Osato M, Asou N, Abdalla E, Hoshino K, Yamasaki H, Okubo T, Suzushima H, Takatsuki K, Kanno T, Shigesada K, Ito Y. (1999) “Biallelic and heterozygous point mutations in the runt domain of the AML1/PEBP2alphaB gene associated with myeloblastic leukemias.“ *Blood;* 93(6):1817-24.

Paˆques, F., and J. E. Haber. (1997) “Two pathways for removal of nonhomologous DNA ends during double-strand break repair in Saccharomyces cerevisiae.” *Mol. Cell. Biol.;* 17:6765–6771

Pabst T, Mueller BU, Zhang P, Radomska HS, Narravula S, Schnittger S, Behre G, Hiddemann W, Tenen DG. (2001) “Dominant-negative mutations of CEBPA, encoding CCAAT/enhancer binding protein-α (C/EBPα), in acute myeloid leukemia.” *Nature Genetics;* 27, 263-270.

Pang D, Yoo S, Dynan WS, Jung M, Dritschilo A. (1997) “Ku proteins join DNA fragments as shown by atomic force microscopy.” *Cancer Res.*; 57: 1412–5.

Paull TT, Gellert M. (1998) “The 3'-5' exonuclease activity of Mre11 facilitates repair of DNA double strand breaks.” *Mol Cell.*; 1: 969–79.

Pedersen-Bjergaard J, Pedersen M, Roulston D, Philip P. (1995) “Different genetic pathwasy in leukemogenesis for patients presenting with therapy-related myelodisplasia and therapy-related acute myeloid leukemia.“ *Blood;* 86, 3542-3552.

Pittman DL, Weinberg LR, Schimenti JC. (1998) “Identification, characterization, and genetic mapping of Rad51d, a new mouse and human RAD51/RecA-related gene.” *Genomics;* 49, 103--111.

Preudhomme C, Sagot C, Boissel N, Cayuela JM, Tigaud I, de Botton S, Thomas X, Raffoux E, Lamandin C, Castaigne S, Fenaux P, Dombret H; ALFA Group. (2002) “Favorable prognosic significance of CEBPA mutations in patients with de novo acute myeloid leukemia: a study from the Acute Leukemia French Association (ALFA).” *Blood;* 100(8):2717-23.

Preudhomme C, Warot-Loze D, Roumier C, Grardel-Duflos N, Garand R, Lai JL, Dastugue N, Macintyre E, Denis C, Bauters F, Kerckaert JP, Cosson A, Fenaux P. (2000) “High incidence of biallelic point mutations in the Runt domain of the AML1/PEBP2 alpha B gene in Mo acute myeloid leukemia and in myeloid malignancies with acquired trisomy 21.“ *Blood;* 96(8):2862-9.

Rabbitts, T.H. (1994) “Chromosomal translocations in human cancer.” *Nature*; 372, 143–149.

Raghavan M, Lillington DM, Skoulakis S, Debernardi S, Chaplin T, Foot NJ, Lister TA, Young BD. 2005 „Genome-wide single nucleotide polymorphism analysis reveals frequent partial uniparental disomy due to somatic recombination in acute myeloid leukemias.“ *Cancer Res.*; 65(2):375-8.

Rasko JE, Metcalf D, Rossner MT, Begley CG, Nicola NA. (1995) ”The flt3/flk-2 ligand: receptor distribution and action on murine haemopoietic cell survival and proliferation.“ *Leukemia;* 9(12):2058-66.

Ratajczak MZ, Ratajczak J, Ford J, Kregenow R, Marlicz W, Gewirtz AM. (1996) ”FLT3/FLK-2 (STK-1) Ligand does not stimulate human megakaryopoiesis in vitro.“ Stem Cells; 14(1):146-50.

Reya T, Morrison SJ, Clarke MF, Weissman IL. (2001) “Stem cells, cancer, and cancer stem cells.“ *Nature;* 414(6859):105-11.

Riballo E, Critchlow SE, Teo SH, Doherty AJ, Priestley A, Broughton B, Kysela B, Beamish H, Plowman N, Arlett CF, Lehmann AR, Jackson SP, Jeggo PA. (1999) “Identification of a defect in DNA ligase IV in a radiosensitive leukaemia patient.” *Curr Biol.*; 9: 699–702.

Rice MC, Smith ST, Bullrich F, Havre P, Kmiec EB. (1997) “Isolation of human and mouse genes based on homology to REC2, a recombinational repair gene from the fungus Ustilago maydis.” *Proc. Natl Acad. Sci. USA;* 94, 7417--7422.

Rogan PK, Close P, Blouin JL, *et al*. (1995) “Duplication and loss of chromosome 21 in two children with Down syndrome and acute leukemia.“ *Am J Med Genet*; 59:174–81.

Rosnet O, Bühring HJ, Marchetto S, Rappold I, Lavagna C, Sainty D, Arnoulet C, Chabannon C, Kanz L, Hannum C, Birnbaum D. (1996) “Human FLT3/FLK2 receptor tyrosine kinase is expressed at the surface of normal and malignant hematopoietic cells.“ *Leukemia;* 10(2):238-48.

Rosnet O, Schiff C, Pébusque MJ, Marchetto S, Tonnelle C, Toiron Y, Birg F, Birnbaum D. (1993) “Human FLT3/FLK2 gene: cDNA cloning and expression in hematopoietic cells.“ *Blood;* 82,1110–1119.

Sanger F, Nicklen S, Coulson AR. (1977) “DNA sequencing with chain-terminating inhibitors. 1977.“ *Biotechnology.* 1992;24:104-8.

Schaich M, Illmer T, Seitz G. (2001) “The prognostic value of Bcl-XL gene expression for remission induction is influenced by cytogenetics in adult acute myeloid leukemia.” *Haematologica;* 86:470-477.

Shaw CJ, Lupski JR. (2004) “Implications of human genome architecture for rearrangement-based disorders: the genomic basis of disease.” *Hum Mol Genet*; 13:57R–64R.3,6.

Shearer PD, Valentine MB, Grundy P, *et al*. (1999) “Hemizygous deletions of chromosome and 16q24 in Wilms tumor: detection by fluorescence in situ hybridization.“ *Cancer Genet Cytogenet*; 115: 100–5.

Schichman SA, Caligiuri MA, Strout MP, Carter SL, Gu Y, Canaani E, Bloomfield CD, Croce CM. (1994) “ ALL tandem duplication in acute myeloid leukemia with a normal karyotype involves homologous recombination between *Alu* elements” *Cancer Research;* 54, 4277-4280

Schnittger S, Kinkelin U, Schoch C, Heinecke A, Haase D, Haferlach T, Büchner T, Wörmann B, Hiddemann W, Griesinger F. (2000) “Screening for MLL tandem duplication in 387 unselected patients with AML identify a prognostically unfavorable subset of AML.“ *Leukemia;* 14(5):796-804.

Schnittger S, Schoch C, Dugas M, Kern W, Staib P, Wuchter C, Löffler H, Sauerland CM, Serve H, Büchner T, Haferlach T, Hiddemann W. (2002) ”Analysis of FLT3 length mutations in 1003 patients with acute myeloid leukemia: correlation to cytogenetics, FAB subtype, and prognosis in the AMLCG study and usefulness as a marker for the detection of minimal residual disease.“ *Blood;* 100(1):59-66

Schoch C, Haferlach T. (2002); “ Cytogenetics in acute myeloid leukemia.“ *Curr Oncology Reports;* 4(5):390-7.

Schoch C, Kern W, Krawitz P, Dugas M, Schnittger S, Haferlach T, Hiddemann W. (2001) ”Dependence of age-specific incidence of acute myeloid leukemia on karyotype.“ *Blood;* 98(12):3500.

Schoch C, Kern W, Schnittger S, Hiddemann W, Haferlach T. (2004) “ Karyotype is an independent prognostic parameter in therapy-related acute myeloid leukemia (t-AML): an analysis of 93 patients with t-AML in comparison to 1091 patients with de novo AML.“ *Leukemia;* 18(1):120-5.

Schoch C, Schnittger S, Klaus M, Kern W, Hiddemann W, Haferlach T. (2003) “AML with 11q23/MLL abnormalities as defined by the WHO classification: incidence, partner chromosomes, FAB subtype, age distribution, and prognostic impact in an unselected series of 1897 cytogenetically analyzed AML cases.“ *Blood;* 102(7):2395-402.

Seedhouse CH, Hunter HM, Lloyd-Lewis B, Massip A-M, Pallis M, Carter GI, Grundy M, Shang S and Russell NH. (2006) " DNA repair contributes to the drug-resistant phenotype of primary acute myeloid leukaemia cells with FLT3 internal tandem duplications and is reversed by the FLT3 inhibitor PKC412" Leukemia; 20, 2130–2136.

Shuman, C, Shuman C, Smith AC, Steele L, Ray PN, Clericuzio C, Zackai E, Parisi MA, et al. (2006) " Constitutional UPD for chromosome 11p15 in individuals with isolated hemihyperplasia is associated with high tumor risk and occurs following assisted reproductive technologies." *Am. J. Med. Genet. A.*; 140, 1497–1503.

Shiah HS, Kuo YY, Tang JL, Huang SY, Yao M, Tsay W, Chen YC, Wang CH, Shen MC, Lin DT, Lin KH, Tien HF. (2002) "Clinical and biological implications of partial tandem duplication of the MLL gene in acute myeloid leukemia without chromosomal abnormalities at 11q23." *Leukemia;* 16(2):196-202.

Shinohara A, Shinohara M, Ohta T, Matsuda S, Ogawa T. (1998) "Rad52 forms ring structures and co-operates with RPA in single-strand DNA annealing." *Genes Cells;* 3:145–156.

Sibanda BL, Critchlow SE, Begun J, Pei XY, Jackson SP, Blundell TL, Pellegrini L. (2001) "Crystal structure of an Xrcc4-DNA ligase complex." *Nat Struct Biol*.; 8: 1015–9.

Sigurdsson S, Van Komen S, Bussen W, Schild D, Albala JS, Sung P. (2001) "Mediator function of the human Rad51B-Rad51C complex in Rad51/RPA-catalyzed DNA strand exchange." *Genes Dev;*15(24):3308-18.

Sigurdsson S, Van Komen S, Petukhova G, Sung P. (2002) "Homologous DNA pairing by human recombination factors Rad51 and Rad54." *J. Biol. Chem.;* 277: 42790–42794.

Slovak ML, Kopecky KJ, Cassileth PA, Harrington DH, Theil KS, Mohamed A, Paietta E, Willman CL, Head DR, Rowe JM, Forman SJ, Appelbaum FR. (2000) "Karyotypic analysis predicts outcome of preremission and postremission therapy in adult acute myeloid leukemia: a Southwest Oncology Group/Eastern Cooperative Oncology Group Study." *Blood;* 96(13):4075-83

Slupianek A, Schmutte C, Tombline G, Nieborowska-Skorska M, Hoser G, Nowicki MO, Pierce AJ, Fishel R, Skorski T. (2001) "BCR/ABL regulates mammalian RecA homologs, resulting in drug resistence." *Mol Cell*; 8: 795-806.

Small D, Levenstein M, Kim E, Carow C, Amin S, Rockwell P, Witte L, Burrow C, Ratajczak MZ, Gewirtz AM, (1994) "STK-1, the human homolog of Flk-2/Flt-3, is selectively expressed in CD34+ human bone marrow cells and is involved in the proliferation of early progenitor/stem cells." *Proc. Natl. Acad. Sci. U. S. A;* 91, 459–463.

Smith AC, Shuman C, Chitayat D, Steele L, Ray PN, Bourgeois J, Weksberg R. (2007) "Severe presentation of Beckwith-Wiedemann syndrome associated with high levels of constitutional paternal uniparental disomy for chromosome 11p15." *Am. J. Med. Genet. A.*; 143A, 3010–3015.

Smith ML, Cavenagh JD, Lister TA, Fitzgibbon J. (2004) " Mutation of CEBPA in familial acute myeloid leukemia." N Engl J Med.; 351(23):2403-7.

Song WJ, Sullivan MG, Legare RD, Hutchings S, Tan X, Kufrin D, Ratajczak J, Resende IC, Haworth C, Hock R, Loh M, Felix C, Roy DC, Busque L, Kurnit D, Willman C, Gewirtz AM, Speck NA, Bushweller JH, Li FP, Gardiner K, Poncz M, Maris JM, Gilliland DG. (1999) "Haploinsufficiency of CBFA2 causes familial thrombocytopenia with propensity to develop acute myelogenous leukaemia."*Nat Genet.;* 23(2):166-75.

Speck and Gilliland (2002) "Core-binding factors in haematopoiesis and leukaemia." *Nat Rev Cancer*; 2(7):502-13

Stankiewicz P, Lupski JR. (2002) "Genome architecture, rearrangements and genomic disorders." *Trends Genet*; 18:74–82.

Stephens K, Weaver M, Leppig KA, Maruyama K, Emanuel PD, Le Beau MM, Shannon KM. (2006) "Interstitial uniparental isodisomy at clustered breakpoint intervals is a frequent mechanism of NF1 inactivation in myeloid malignancies." *Blood*; 108, 1684–1689.

Steudel C, Wermke M, Schaich M, Schäkel U, Illmer T, Ehninger G, Thiede C. (2003) "Comparative analysis of MLL partial tandem duplication and FLT3 internal tandem duplication mutations in 956 adult patients with acute myeloid leukemia." *Genes Chromosomes Cancer*.; Jul;37(3):237-51.

Stirewalt D.L. and Radich, J.P. (2003) "The role of FLT3 in haematopoietic malignancies." *Nat. Rev. Cancer;* 3,650–665.

Strachan, T. and Read, A (1996) "Mutability and instability of human DNA*" Human molecular genetics. BIOS Scientific Publishers Ltd, New York.*

Strachan, T. and Read, A.P., eds (2004) Human Molecular Genetics, Garland Science Publishers Inc.

Sugawara N, Pâques F, Colaiácovo M, Haber JE. (1997) "Role of Saccharomyces cerevisiae Msh2 and Msh3 repair proteins in double-strand break-induced recombination*." Proc. Natl. Acad. Sci. USA*.; 94:9214–9219.

Suzuki M, Kato M, Yuyan C, Takita J, Sanada M, Nannya Y, Yamamoto G, Takahashi A, Ikeda H, Kuwano H, Ogawa S, Hayashi Y. (2008) " Whole-genome profiling of chromosomal aberrations in hepatoblastoma using high-density single-nucleotide polymorphism genotyping microarrays." *Cancer Sci.*; 99, 564–570.

Swansbury GJ, Lawler SD, Alimena G, Arthur D, Berger R, Van den Berghe H, Bloomfield CD, de la Chappelle A, Dewald G, Garson OM. (1994)."Long-term survival in acute myelogenous leukemia: a second follow-up of the Fourth International Workshop on Chromosomes in Leukemia." *Cancer Genet Cytogenet*; 73(1):1-7

Tan TL, Essers J, Citterio E, Swagemakers SM, de Wit J, Benson FE, Hoeijmakers JH, Kanaar R. (1999) "Mouse Rad54 affects DNA conformation and DNA-damage-induced Rad51 foci formation." *Curr Biol;* 9(6):325-8.

Tarsounas M (2004a) „RAD51 localization and activation following DNA damage." *Philos Trans R Soc Lond B Biol Sci.;* 359(1441):87-93.

Tarsounas M, Munoz P, Claas A. (2004b) "Telomere maintenance requires the RAD51D recombination/repair protein." *Cell.*; 117:337-347.

Tenen DG. (2003) "Disruption of differentiation in human cancer: AML shows the way." Nat *Rey Cancer;* 3(2):89-101.

Thiede C, Steudel C, Mohr B, Schaich M, Schäkel U, Platzbecker U, Wermke M, Bornhäuser M, Ritter M, Neubauer A, Ehninger G, Illmer T. 2002 "Analysis of FLT3-activating mutations in 979 patients with acute myelogenous leukemia: association with FAB subtypes and identification of subgroups with poor prognosis." *Blood;* 99(12):4326-35.

Till JE and McCulloch EA (1961) "A direct measurement of the radiation sensitivity of normal mouse bone marrow cells." *Radiat Res;* 14:213-22.

van der Geer P, Hunter T, Lindberg RA. (1994)."Receptor protein-tyrosine kinases and their signal transduction pathways." *Annu Rey Cell Biol;* 10:251-337.

Vardiman JW, Harris NL, Brunning RD.James W. (2002) "The World Health Organization (WHO) classification of the myeloid neoplasms" *Blood;* 100(7):2292-302.

Wang L, Fidler C, Nadig N, Giagounidis A, Della Porta MG, Malcovati L, Killick S, Gattermann N, Aul C, Boultwood J, Wainscoat JS. (2008) "Genome-wide analysis of copy number changes and

loss of heterozygosity in myelodysplastic syndrome with del(5q) using high-density single nucleotide polymorphism arrays.“ *Haematologica*; 93, 994–1000.

Weaver DT. (1996) “Regulation and repair of double-strand DNA breaks.” *Crit Rev Eukaryot Gene Expr.*; 6: 345–75.

Weissman IL. (2000) “Translating Stem and Progenitor Cell Biology to the Clinic: Barriers and Opportunities.“ *Cell*; 287(5457):1442-6

White VA, McNeil BK, Horsman DE. (1998) “Acquired homozygosity (isodisomy) of chromosome 3 in uveal melanoma.“ *Cancer Genet Cytogenet*; 102:40–5.

Whitman SP, Archer KJ, Feng L, Baldus C, Becknell B, Carlson BD, Carroll AJ, Mrózek K, Vardiman JW, George SL, Kolitz JE, Larson RA, Bloomfield CD, Caligiuri MA. (2001) „Absence of the wild-type allele predicts poor prognosis in adult de novo acute myeloid leukemia with normal cytogenetics and the internal tandem duplication of FLT3: a cancer and leukemia group B study.“ *Cancer Res.*; 61(19):7233-9.

Wouters BJ, Sanders MA, Lugthart S, Geertsma-Kleinekoort WM, van Drunen E, Beverloo HB, Löwenberg B, Valk PJ, Delwel R. (2007) “Segmental uniparental disomy as a recurrent mechanism for homozygous CEBPA mutations in acute myeloid leukemia.“ *Leukemia;* 21:2382-2384

Yaneva M, Kowalewski T, Lieber MR. (1997) “Interaction of DNA-dependent protein kinase with DNA and with Ku: biochemical and atomic-force microscopy studies.” *EMBO J.*; 16: 5098–112.

Yokoyama H, Kurumizaka H, Ikawa S, Yokoyama S, Shibata T. (2003) “Holliday junction binding activity of the human Rad51B protein.” *J Biol Chem;* 278(4):2767-72.

Yuan Y, Zhou L, Miyamoto T, Iwasaki H, Harakawa N, Hetherington CJ, Burel SA, Lagasse E, Weissman IL, Akashi K, Zhang DE. (2001) “AML1-ETO expression is directly involved in the development of acute myeloid leukemia in the presence of additional mutations.“ Proc Natl Acad Sci U S A; *98*, 10398-10403.

Zhang S, Fukuda S, Lee Y, Hangoc G, Cooper S, Spolski R, Leonard WJ, Broxmeyer HE. (2000) “Essential role of signal transducer and activator of transcription (Stat)5a but not Stat5b for Flt3-dependent signaling.“ *J. Exp. Med.;* 192,719–28.

7. Appendix

Acknowledgements

The work of this thesis was performed at the Department of Haematology and Oncology University Hospital Dresden. Many people have directly and indirectly made this thesis possible and I would like to thank especially:

Prof. Dr. med. Ehninger for the opportunity to work in the Department of Haematology and Oncology and especially my supervisor Prof. Dr. med. Christian Thiede for giving me the opportunity to perform this work, for going through and giving valuable comments to all my manuscripts and for supporting me in becoming an independent scientist.

Dr. Christine Schteudel for teaching me the Affimetrix Array methods and for suporting my Affymetrix analyses.

All the members of the Laboratory of Molecular Diagnostic, especially: Coni, Manuela, Ulrike, Marika, Marita, Peggy, Sandra and Karina for teaching me different methods, for all the fun we had together, our nice chats and for always knowing where to find everything in the lab.

Dr. Uta Oelschlägel for teaching me the Facs method and for always being there for my questions.

Dr. Marianne Größe for her generous support and for the help with the Affymetrix machines and methods.

The members of the Laboratory of Haematology for always keeping cool when I came to count my cells and specially for shearing the work taking the cells from the big containers.

Dr. Brigitte Mohr for helping with the cytological diagnostic.

Dr. Anastassiadis for the opportunity to measure the chaemylumenescense in his lab.

Special thanks to Prof. Dr. Gerold Barth for his generous support from the start and for the good advice which he has given me all these years.

Special thanks to my colleague and friend Dr. Mihaela Anitei for all the discussions and support in my work and for teaching me the immunofluorescence method. Thanks also for the nice time together in the cinema and in the pubs in Dresden and all the fun we have had together.

I would like to thank especially Dr. Irina Parschina for all the time we have had together (more then 10 years) and specially for believing in me and giving me encouragement when I had doubts. Thank you for all the conversation we have had together, for the nice lunches and for the wonderful and carefree time during the long nights on the Dresden streets.

Thank you Emma - the best friend in my life. With you I decided to study biology when I was 12 years old.

Thanks to all my friends in Dresden for making Germany my home country!

My family-in-law for being such interesting people and specially my mother-in-law for preparing all celebrations. With you it is never boring!

Specially I thank my friend Svetla for always being close to me, for always having time to listen my problems, my breakdowns and successes, for keeping me on the ground and giving me the best suggestions. Thanks also to you, your husband Simeon and Airin for the amazing night parties we have had together with a lot of fun and laughter.

I'm incredibly appreciative to Dorina Near, a really good friend to me and a great babysitter for my children even when they were sick. You have given me amazing support in my life! Without you, this thesis wouldn´t have been possible!!! Thanks to your big family for giving me the feeling that I also have relatives here in Dresden. For always being happy and cheerful and always taking the opportunity to celebrate together every family event. Your support is always important to me!

My parents and sister Elitza for all your incredible support and for believing and loving me because of me. Thank you for the feeling that I always have a second choice in my life and that you are always close to me.

To my husband Georgi. Thank you for your love, all your support, all your help, kindness and for your efforts to understand what I am doing in the lab all the time. And to my children Gabi and Alex for being the most wonderful children in the world and the best thing in my life.

Selbständigkeitserklärung

Ich erkläre, daß ich die vorliegende Arbeit selbständig und nur unter Verwendung der angegebenen Hilfsmittel und Literatur angefertigt habe.

Dresden, den 15.07.2009 Sofia Traikov

Erklärung zur Bewerbung

Hiermit erkläre ich, daß ich mich mit der vorliegenden Arbeit an keiner anderen Hochschule um den akademischen Grad Doctor rerum naturalium beworben habe und daß ich weder früher noch gegenwärtig die Eröffnung eines Verfahrens zum Erwerb des oben genannten akademischen Grades an einer anderen Hochschule beantragt habe. Die Promotionsordnung der Fakultät Mathematik und Naturwissenschaften der Technische Universität Dresden (TUD) ist mir bekannt.

Dresden, den 15.07.2009 Sofia Traikov